Structural Characterisation and Response Modelling of Paraffin-Based Hybrid Rocket Motor Fuel Grains

by

Kirsty Lynn Veale

Doctoral thesis by manuscript submitted in fulfilment of the requirements for the degree of Doctor of Philosophy

in Mechanical Engineering

College of Agriculture, Engineering and Science

University of KwaZulu-Natal

Durban

South Africa

October 2020

PREFACE

The research contained in this thesis was completed by the candidate while based in the Discipline of Mechanical Engineering, School of Engineering, of the College of Agriculture, Engineering and Science, University of KwaZulu-Natal, Howard College Campus, South Africa. The research was financially supported by the NRF Thuthuka Grant.

The contents of this work have not been submitted in any form to another university and, except where the work of others is acknowledged in the text, the results reported are due to investigations by the candidate.

_____

Signed: Professor Sarp Adali

Date: October 2020

_____

Signed: Dr Jean Pitot de la Beaujardiere

Date: October 2020

_____

Signed: Dr Clinton Bemont

Date: October 2020

DECLARATION 1: PLAGIARISM

I, Kirsty Lynn Veale, declare that:

      (i)   the research reported in this dissertation, except where otherwise indicated or acknowledged, is my original work;

      (ii)   this dissertation has not been submitted in full or in part for any degree or examination to any other university;

      (iii)   this dissertation does not contain other persons' data, pictures, graphs or other information, unless specifically acknowledged as being sourced from other persons;

      (iv)   this dissertation does not contain other persons' writing, unless specifically acknowledged as being sourced from other researchers. Where other written sources have been quoted, then:

          a)   their words have been re-written but the general information attributed to them has been referenced;

          b)   where their exact words have been used, their writing has been placed inside quotation marks, and referenced;

      (v)   where I have used material for which publications followed, I have indicated in detail my role in the work;

      (vi)   this dissertation is primarily a collection of material, prepared by myself, published as journal articles or presented as a poster and oral presentations at conferences. In some cases, additional material has been included;

      (vii)   this dissertation does not contain text, graphics or tables copied and pasted from the Internet, unless specifically acknowledged, and the source being detailed in the dissertation and in the References sections.

_____

Signed: Kirsty Lynn Veale

Date: October 2020

DECLARATION 2: PUBLICATIONS

My role in each paper and presentation is indicated. The * indicates corresponding author.

Publications

The dissertation is made up of three original papers published (or under review) in peer-reviewed journals. The development and writing of the papers (published and unpublished) was the principal responsibility of myself. The research content was developed by me and presented carefully in a series of follow-on publications. I conducted all experimental, design, simulation and data analysis work, and wrote all the publications with editing assistance and guidance offered by the co-authors.

Chapter 2

***Veale, K.L**., Adali, S., Pitot, J. and Brooks, M., "A review of the performance and structural considerations of paraffin wax hybrid rocket fuels with additives", Acta Astronautica, Volume 141, Pages 196 – 208, 2017

Chapter 3

***Veale, K.L**., Adali, S., Pitot, J. and Bemont, C., "The structural properties of paraffin wax based hybrid rocket fuels with aluminium particles", Acta Astronautica, Volume 151, Pages 864 – 873, 2018

Chapter 4

***Veale, K.L**., Adali, S., Pitot, J. and Bemont, C., "Explicit modelling of the ignition transient structural response of a paraffin wax hybrid rocket motor fuel grain", Journal of Aerospace Technology and Management, Under review, 2020

Other research outputs

Other research outputs emanating from this study are listed below. The contributions of these publications are either directly or indirectly related to the research outputs, and thus require noting, even though they do not make up chapters in the thesis. My contributions are detailed for each paper group.

The research reported in the below publication shows preliminary structural tests on paraffin wax as well as initial structural simulations of fuel grains of various sizes. The results indicated a need for development in this field, thus creating the basis of the study presented here. I conducted the simulations and experimental tests, analysed the data, wrote the publication with editing assistance and guidance offered by the co-authors. Furthermore, I presented the work.

***Veale, K.L.**, Brooks, M.J. and Pitot de la Beaujardiere, J.P., "Structural performance of large scale paraffin wax based fuel grains", Proceedings of the 51st AIAA/ASME/SAE/ASEE Joint Propulsion Conference & Exhibit, 2015, Orlando, Florida

The research presented in the next group of publications details the development of a 100 km apogee large scale hybrid sounding rocket, and the effects that various design parameters can have on flight performance. I assisted with conducting preliminary structural simulations on the conceptualised fuel grains as well as assistance with interpreting the simulated case studies and with writing the publications.

*Leverone, F.K., Brooks, M., Pitot, J. and **Veale, K.L.**, "Performance sensitivity study on a blowdown nitrous oxide paraffin wax hybrid sounding rocket", Acta Astronautica, Volume 160, Pages 230 – 239, 2019

*Leverone, F.K., **Veale, K.L.**, Brooks, M.J., Pitot de la Beaujardiere, J.P., and Roberts, L.W. "Performance modeling of the Phoenix-2A hybrid sounding rocket using the HYROPS software", Proceedings of the 49th AIAA/ASME/SAE/ASEE Joint Propulsion Conference & Exhibit, 2013, San Jose, California

The published work listed below was achieved as a result of two MSc students with me as their principal supervisor. I conceptualised the research ideas to compliment my primary research goals. My contributions included co-developing one of the experimental systems, some design aspects and assisting with publication writing.

*Theba, R., **Veale, K.L.** and Bemont, C.P., "Development of a combustion visualisation hybrid rocket motor", R&D Journal of the South African Institute of Mechanical Engineers, Volume 33, Pages 97 – 104, 2017

*Maharaj, C., **Veale, K.L.**, Pitot de la Beaujardiere, J.P. and Bemont, C.P., "Characterisation of aluminium additives in paraffin wax hybrid rocket fuels", Paper ready for submission, 2019

*Theba, R., **Veale, K.L**. and Bemont, C.P., "Development of a hybrid rocket slab motor", Proceedings of the 52nd AIAA/ASME/SAE/ASEE Joint Propulsion Conference & Exhibit, 2016, Salt Lake City, Utah

*Maharaj, C., **Veale, K.L**., Pitot de la Beaujardiere, J.P. and Bemont, C.P., "Development of a 75 mm hybrid rocket motor to test metal additives", Proceedings of the 52nd AIAA/ASME/SAE/ASEE Joint Propulsion Conference & Exhibit, 2016, Salt Lake City, Utah

Finally, the next group of published work detailed the development of ASReG's hybrid sounding rocket program, and the subsequent launch and design of two vehicles. The effort required technical input from all members listed on the authorship list. My contribution included the provision of technical assistance, co-supervision of one of the listed postgraduate students, assistance with grain manufacturing technique development, as well as guidance with writing the publications.

*Genevieve, B., Pitot de la Beaujardiere, J.P., Brooks, M.J., Chowdhury, S.M., **Veale, K.L**., Leverone, F.K., Balmogim, U. and Mawbey, R. "Flight test of the Phoenix-1A hybrid Rocket", Proceedings of the 51st AIAA/ASME/SAE/ASEE Joint Propulsion Conference & Exhibit, 2015, Orlando, Florida

*Balmogim, U., Brooks, M.J., Pitot de la Beaujardiere, J.P., **Veale, K.L**., Roberts, L.W., Genevieve, B., "Preliminary design of the Phoenix-1B hybrid rocket", Proceedings of the 51st AIAA/ASME/SAE/ASEE Joint Propulsion Conference & Exhibit, 2015, Orlando, Florida

*Pitot de la Beaujardiere, J.P., Brooks, M.J., Chowdhury, S.M., Genevieve, B., **Veale, K.L**. and. Roberts, L.W. "The Phoenix Hybrid Sounding Rocket Program: A progress report 2012", Proceedings of the 48th AIAA/ASME/SAE/ASEE Joint Propulsion Conference & Exhibit, 2012, Atlanta, Georgia

_____

Signed: Kirsty Lynn Veale

Date: October 2020

ABSTRACT

Often, the focus of research into paraffin wax as a hybrid rocket motor fuel is based on its combustion and regression rate performance, while very little focus is given to the structural performance of paraffin wax as a solid fuel grain during in-flight loading conditions. An in-depth review of the existing use cases and testing techniques applied to paraffin wax as a hybrid rocket motor fuel was conducted as the first objective of this thesis, highlighting the significant potential in its application while indicating areas which could benefit from further development. Much of the literature was found to be focused on combustion and regression rate performance, while very little focus was given to the structural performance of paraffin wax as a solid fuel grain during in-flight loading conditions. To adequately describe the state of development, the review assessed the progress made in paraffin wax combustion testing and the effects that different measurement techniques and geometries had on the combustion properties. The differences in results between sources highlight that aspects often overlooked, such as the grade of paraffin wax or the casting techniques used, yield different performance results. Additionally, the approach to regression rate measurement and the nature of the grain geometry affect the quantification of these performance metrics.

The clear deficiency in structural performance data led to an objective of developing a structural testing regime aimed at addressing the complex nature of paraffin wax material structural performance during flight. The thesis investigates the material characterisation of SASOL 0907 microcrystalline paraffin wax, with and without a 40 wt% aluminium powder additive. The thermal conductivity of paraffin wax containing the aluminium additive was found to be approximately three times higher than that of pure wax, creating some concerns regarding the extent of thermal penetration during combustion. Structural testing was conducted in the form of tensile and compression tests, at three different strain-rates and for three different temperatures. The structural test results indicated a strong strain-rate dependency and temperature dependency. The stress-strain curves for paraffin wax with the aluminium additive showed similar trends to that of pure paraffin wax, but with higher ultimate tensile strength values and lower allowable strain. It is also clear that the strain-rate dependency of the material, while still evident, is less at higher temperatures.

The material characterisation results indicated that complex computational modelling would be required for analysing the structural performance of a paraffin wax fuel grain. Specifically, a

model which could adequately capture the strain-rate and temperature dependency of the material was required. The use of the Johnson-Cook material constitutive model and the Johnson-Cook failure model was found to be appropriate in approximating the material response within the tested range. The model is defined by material constants extracted from the mechanical testing data. Verification of the model's validity was achieved by modelling the tensile tests and plotting simulated stress-strain curves against the experimental data. The verification yielded close agreement between the simulated and actual responses, and on this basis, the study proceeded onto detailed fuel grain response modelling.

The grain modelling exercise considered only the ignition pressurisation transient, which is considered the worst-case loading condition in a hybrid rocket motor for the purposes of this study. The inclusion of theoretical ignition pressure spikes, or hard starts, resulted in a predicted failure. The extent of the resultant stresses is highly dependent on the aspect ratio and outer diameter of the fuel grain. The results of these simulations indicated that the pressure profiles expected in these motors are nearing the limit of the grains' ability to endure the ignition pressurisation.

ACKNOWLEDGEMENTS

I would like to express my sincerest gratitude to my PhD supervisors, Professor Sarp Adali, Dr Jean Pitot and Dr Clinton Bemont, for their guidance and support. Their vast knowledge and encouragement kept me on track throughout this adventure. Finding the time to do a PhD part-time is difficult, but with the encouragement of my CERN manager, Dr Martin Jäkel, it was possible

I would also like to thank the staff and students of ASReG, notably Dr Mike Brooks, for creating a firm base from which I could pursue my research goals. Our research group is driven to greatness through excellence, teamwork, and sheer dedication. Any single achievement is not possible without this camaraderie.

I would like to acknowledge the members of the hybrid community who I met along the way, but specifically Professor Cantwell for his willingness to offer technical guidance whenever needed. I would like to express my gratitude to the 'Hybrid Rocket Ladies' for their motivational spirit. I made it!

This would not have been possible without the kindness and support of my friends, but especially Avern, who was always there for me with a cup of coffee and an open mind. Recognition should also be given to 'the A-team'. Without the welcome distraction and hours of endless entertainment that this group brought me, I would never have achieved what I have.

Finally, I would like to extend a special thank you to my family. To my wife, Fiona, for her endless guidance, both scientifically and emotionally, throughout these years. To my brother, Dr Veale, for just being himself. To my mother, Lesley, for her constant love and support, and to the rest of the family for never giving up on me.

This thesis is dedicated to my mother, Lesley Veale.

You encouraged me to always pursue my dreams. Without you, I would not be who I am today.

"What it all comes down to is that everything's gonna be fine fine fine"

- Alanis Morissette

TABLE OF CONTENTS

LIST OF TABLES

LIST OF FIGURES

CHAPTER 1: INTRODUCTION

1.1 Background

The need for rockets, and thus rocket propulsion has steadily increased due to our reliance on advances such as satellite technology for telecommunications, as well as our drive for understanding in fields such as space-based research and space exploration.

In general, chemical propulsion has, over the years, dominated the field of rocket propulsion (Sutton and Biblarz, 2001). There are three types of chemical propulsion methods which are commonly referred to as solid, liquid and hybrid propulsion systems and are defined by the propellants' state of matter and mixing method during storage or combustion. A schematic of the representative configurations of these vehicles is illustrated in Figure 1 - 1.
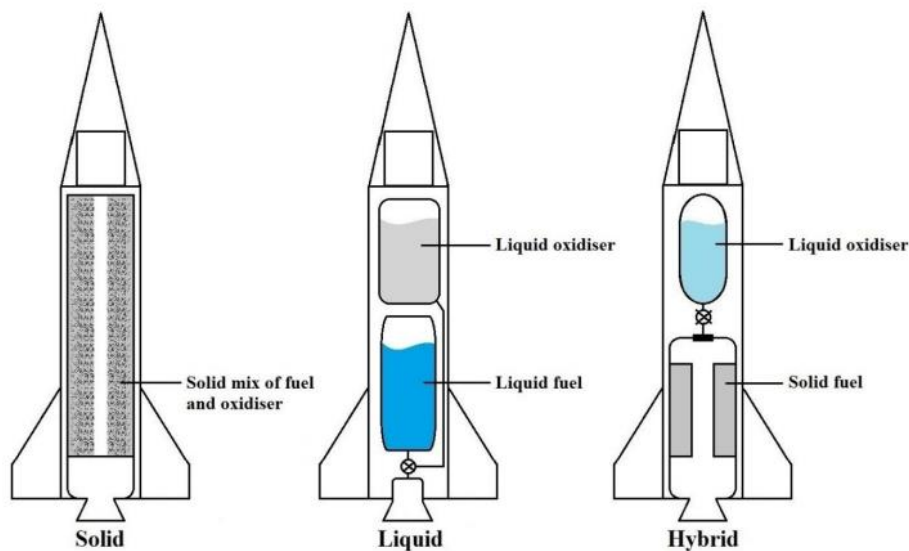
Figure 1 - 1: Chemical rocket propulsion systems (Leverone, 2013)

Hybrid motor propellants generally comprise a liquid or gaseous oxidiser and solid fuel which are stored separately until the ignition sequence is initiated. A reverse configuration, liquid fuel and solid oxidiser is also possible but is rarely used (Sutton and Biblarz, 2001). Combustion of the propellants and the subsequent generation of thrust only occurs when the oxidiser and fuel come into contact with each other. This occurs by allowing the oxidiser stream to flow over the surface of the solid fuel in the presence of a heat source which initiates combustion. Solid fuel grains are generally constructed in a cylindrical form, with one or more axial ports where the

oxidiser can flow towards the nozzle and react with the fuel surface as it passes, depending on nature of the propellants and the motor performance required.

The paramount advantage of this type of combustion method, when compared to that associated with both solid and liquid propellants, is the inherent safety during motor transportation and handling as a consequence of the separation (both in location and in state of matter) of the propellants. Additionally, there are safety and handling advantages during fuel manufacture when compared to solid rocket motors due to the generally inert nature of the hybrid fuel (Sutton and Biblarz, 2001). These advantages make the use of this propulsion technology intriguing for low-cost launch applications and university research. However, their applicability is not limited to just these fields; significant developments in the areas of space tourism and off-Earth space operations, such as the development of the Mars Ascent Vehicle (Chandler *et al.*, 2010) have been achieved.

Unfortunately, there are also numerous shortfalls associated with the technology. One of the major drawbacks to the classical hybrid technology is the relatively slow fuel combustion mechanism. In this regard, the measure of performance is often referred to as the regression rate, which is the rate at which the fuel port burns perpendicular to the oxidiser flow. This has typically limited mission options to those that only require low thrusts, and inherently requires the development of complex fuel grain geometries to increase fuel surface area, taking away from many of the manufacturing and cost advantages that the technology presents.

Multi-port fuel grain designs, such as the wagon wheel design, act to increase the combustible surface area by increasing the number of ports, as shown in Figure 1 - 2. This solution has the potential to increase the overall regression of the fuels sufficiently for use in higher thrust applications, however, the increased number for ports results in additional complexity. Multi-port fuel grain designs require residual fuel to remain between the ports after the burn, or the inclusion of structural matrices (McKinney and Kniffen, 1994), to ensure the maintenance of the structural integrity of the fuel grain throughout the mission. Both options result in a heavier, larger vehicle, taking away many of the performance-enhancing attributes resulting from the multi-port design (Humble, Henry and Larson, 1995).

Multi-port fuel designs generally require a significant amount of fuel to remain after the burn in order to prevent premature collapsing of the ports. This material is referred to as the unused

fuel sliver mass. An example of the remaining fuel slivers and thus unused mass fraction of a wagon wheel type HTPB hybrid fuel after firing can be seen in Figure 1 - 2.
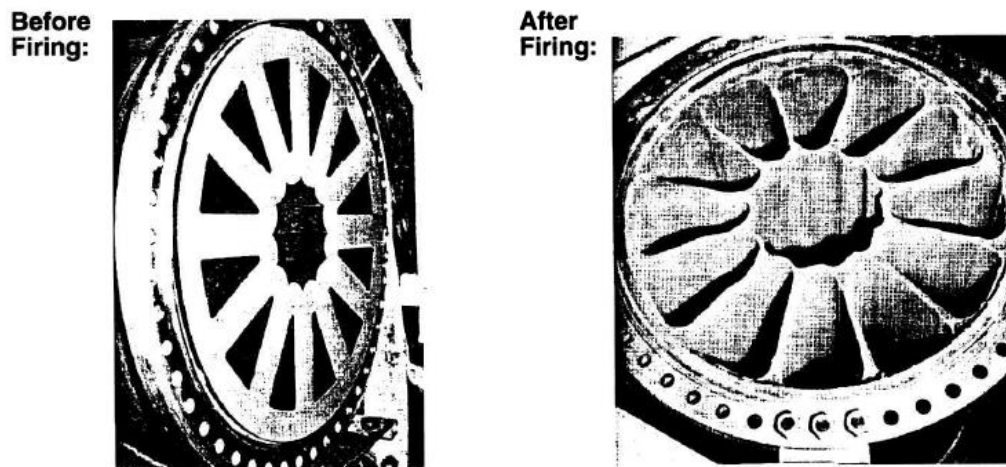
Figure 1 - 2: Before and after images of an HTPB multi-port hybrid fuel grain (Humble, Henry and Larson, 1995)**.**

Noting that many of the advantages of hybrid technology were counteracted by the required complexity of grain geometries, research in the field progressed towards discovering new hybrid fuel options, which would allow for an increased regression rate without having complex port geometries. The focus on this venture was to overcome the restrictions associated with the classical hybrid combustion mechanism.

Classical hybrid combustion relies on the vaporisation of the fuel on the surface, thus creating a narrow flame zone within the oxidiser boundary layer (Marxman, 1965). There are limitations to the speed of fuel burning, known as regression rate, with this form of combustion. The flame zone only occurs within the oxidiser boundary layer, restricting combustion to only the exposed surface. Newer fuels were discovered which allowed the formation of a liquid layer upon the exposed grain surface, becoming unstable under the oxidiser flow.

This mechanism is referred to as non-classical combustion and is initiated when fuels within a certain liquid viscosity range allow for the formation of waves on the liquefied fuel surface. These waves grow and allow droplets of fuel to be mechanically entrained into the oxidiser stream, effectively increasing the combustible surface area and thus the rate at which the fuel

is combusted. Fuels which permit this phenomenon are referred to as liquefying fuels. A more detailed description of the fuel combustion methods, with images, is discussed in Chapter 2.

The increased regression rate of these non-classical hybrid fuels offers hybrid propulsion technology an opportunity to increase the scope of mission applications, and in some cases, be competitive with other chemical propulsion technologies. The regression rate is improved sufficiently to allow fuel grain to be developed with a single oxidiser port, thus reducing manufacturing flow complexities associated with complex port geometries significantly.

A fuel that has been specifically identified as a high regression rate hybrid fuel is paraffin wax. Paraffin wax will be the focus of this research as it is one of the primary liquefying fuels in use. An example of a single port, paraffin wax-based hybrid fuel grain which is considered in this research can be seen in Figure 1 - 3.

<div align="center">(a)   (b)</div>

Figure 1 - 3: (a) Single port blackened paraffin wax grain segment, and (b) fuel grain cartridge with four segments inside (Genevieve *et al.*, 2012)

Unfortunately, paraffin wax is considered to be brittle, and its ability to withstand pressurisation and launch loads is unknown (Freund *et al.*, 1983; Kim *et al.*, 2010, 2015); especially at large motor scales. Numerous researches have considered this an important step in the development of paraffin wax fuels, and have initiated with research into this area with basic structural testing, and structural enhancement additives (Wang, Severtson and Stein, 2006; Cantwell, Karabeyoglu and Altman, 2010; Zaseck *et al.*, 2012; Piscitelli *et al.*, 2015; Cardoso *et al.*, 2017; Paravan, Galfetti and Maggi, 2017). While there is little risk of catastrophic motor failure if the fuel grain was to crack, as in the case of solid rocket motors, there is still a risk of not meeting

the mission requirements due to fuel loss, which, in the scope of space launch missions, may well contribute to mission failure (Marxman and Gilbert, 1963).

There are several possible means to increase the structural performance of paraffin wax as a hybrid rocket fuel. It is possible to embed structural matrices within the fuels grains to ensure the rigidity of the structure during combustion (McCulley, Bath and Whitmore, 2012; Hill *et al.*, 2019), however, whatever material is used could negatively affect the fuel regression, and would increase manufacturing complexity, potentially taking away from the advantages of using a liquefying fuel. Other structural enhancement methods include the use of additives, such as polymers (Mengu and Kumar, 2018; Pal and Ravikumar, 2019). However, if these additives affect the melt viscosity of a liquefying fuel, droplet entrainment would be hindered, and thus the regression rate would decrease. Metallised additives have been used in classical hybrid fuels to increase energetic performance (Risha *et al.*, 2007; Merotto *et al.*, 2011; Pal and Kumar, 2017; Maharaj, 2018), but so far, it is not yet comprehensively known what effect their presence has on the structural performance.

While some structural testing has been conducted on paraffin wax fuels, there is little investigation on complex structural testing and enhancements of paraffin wax fuels for hybrid rockets (Veale *et al.*, 2017). In most existing researched cases, the extent of the testing has considered only basic quasi-static tensile tests, with some metallised or polymer additives to increase structural properties. While these tests are useful in determining the effect of various additives on the basic structural properties of the fuel material, they are not sufficiently conclusive in offering insight to the fuel grain's structural response to dynamic loading. There is a clear requirement at this point in hybrid fuel development to determine a fuel grain's structural properties under conditions similar to that of the loading experienced, and to define a method of structural response modelling which is capable of considering these properties.

1.2 The Phoenix Program

The University of KwaZulu-Natal's Aerospace Systems Research Group initiated their research into the field of hybrid rockets with the development of the HYROPS (Hybrid Rocket Performance Simulator) software, which is a multipurpose hybrid motor design tool and trajectory simulator (Chowdhury, 2012; Genevieve, Pitot de la Beaujardiere and Brooks, 2017). This tool can be used to optimise the motor design of a hybrid rocket and then simulate its

expected trajectory. The tool is capable of reporting simulated combustion values such as the chamber pressure, burn time and port geometrical changes due to regression rate.

Simultaneously, the research group conducted several laboratory-scale motor hot-fire tests as a concept verification for the use of paraffin wax and nitrous oxide as a hybrid rocket propellant combination. Shortly after that, the Phoenix-1A hybrid sounding rocket was developed. This was a vehicle designed to reach an altitude of 10 km and was to be used as a technology demonstrator. The Phoenix-1A vehicle can be seen on its launch rail in Figure 1 - 4. Unfortunately, due to a nozzle failure, the Phoenix-1A did not reach its target altitude, however, it fully demonstrated the capabilities of the technology in use.

Figure 1 - 4: The Phoenix-1A hybrid sounding rocket on the mobile launch platform prior to launch

After this launch, the group continued to develop vehicles with varying mission objectives, such as the Phoenix-2A, 100 km apogee sounding rocket, and the Phoenix-1B 15 km apogee sounding rocket. Each of these vehicles is in varying stages of development, with the Phoenix

1B being successfully hot-fire tested and planned for launch in 2020. The Phoenix-2A vehicle is currently only at the paper design stage due to its significant size, and associated technology and budgetary constraints. In addition, concerns have arisen in terms of the limited understanding of the ability of paraffin wax fuel grains to survive the launch conditions. More detailed information about each of the vehicles above will be discussed in Chapter 4.

The development fuel grains for the vehicles within the Phoenix program, and most other paraffin wax-based hybrid motors, has thus far been guided solely by combustion performance considerations, with little consideration given to the structural performance of the paraffin wax fuel. When considering the Phoenix-1A vehicle, vehicles of similar sizes and propellants have been launched before with no mention of grain failure. However, the launch and recovery of the Phoenix-1A vehicle offered an opportunity to review the remaining grain sliver after flight to determine if in flight or ignition failure has occurred.

1.2.1 Post-launch investigation

in an earlier publication (Veale, Brooks and Pitot de la Beaujardiere, 2015), the Phoenix-1A hybrid fuel grain structural response was modelled after launch using limited quasi-static tensile data in a transient analysis using simplified loading conditions. The model predicted the grain would survive without reaching the material structural limit.

Unfortunately, due to complications with the recovery system, the Phoenix-1A vehicle did not land under its parachute, resulting in most of the vehicle being destroyed. The orientation of landing and the crumpling of the aluminium oxidiser tank on impact did, somewhat surprisingly, allow the combustion chamber to support the remaining fuel grain, almost in its entirety allowing a post launch analysis to still be conducted on the remaining fuel grain sliver, with the knowledge that any cracks or fractures due to impact would show no crack healing or melted fuel ingress.

The regions in the vicinity of the grain segment interfaces showed slight circumferential indentations, noted as areas of increased regression likely caused by the fuel grain discontinuity. This is an effect that would be expected due to the melt layer combustion method causing turbulent regions undercutting the fuel. Similar, and likely more exaggerated flaws, would have resulted in unexpected regression indentations in regions where cracks were present. This grain investigation showed very little indication of grain uneven radial burning. If uneven burning

had been evident, it would have implied that cracks or flaws were present during the burn, thus it was taken that this grain likely did not crack at ignition. Grain failures which were a result of

Radial indentation from segment gap

Fuel melt collecting at fore end after burn

Brittle failure after impact
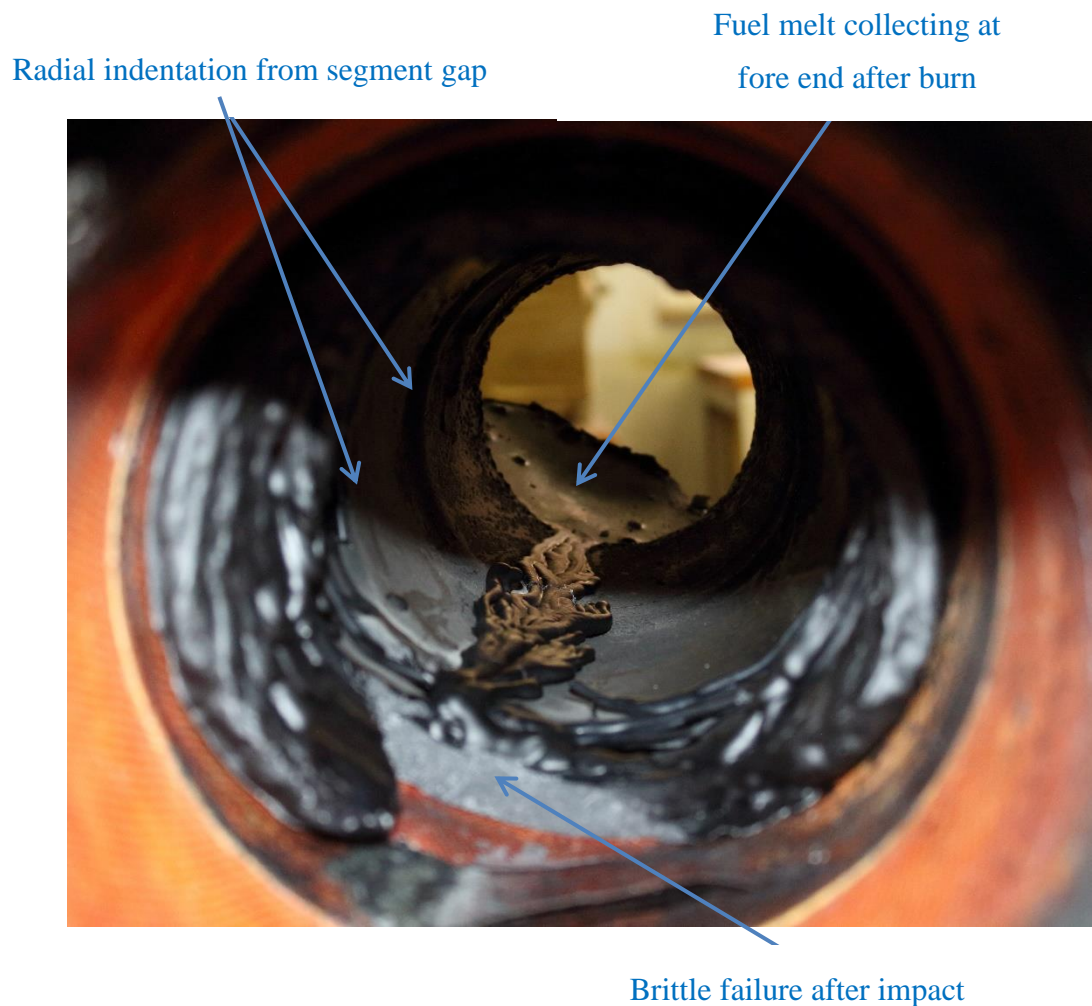
Figure 1 - 5: Inner port of Phoneix-1A grain after launch, taken from aft end

the impact were easily identified as they did not experience any melting and appeared as a clean failed surface similar to brittle failures. An annotated image of the inner port of the recovered Phoenix-1A fuel grain can be seen in Figure 1 - 5. There is no indication of failure, as predicted, except the clear post-burn impact failure.

1.3 Problem statement

The structural performance of paraffin wax hybrid rocket fuel grains under launch conditions is not well understood. Numerous published sources make mention of the need to determine the structural feasibility of paraffin wax fuel grains during the design phase of a vehicle. This is discussed in detail in Chapter 2. Additionally, basic structural testing has been conducted on

paraffin wax fuels doped with materials aimed at improving the grains structural performance. The structural performance of a grain becomes more of a concern as motors tend to the larger scale range of paraffin wax fuel grains, such as those associated with the Peregrine hybrid sounding rocket from NASA Ames (Zilliac *et al.*, 2014) and the Phoenix-2A rocket from the University of KwaZulu-Natal (Leverone, 2013), which are both designed to achieve an altitude of 100 km.

The application of this fuel type requires a full understanding and analysis method of the grain structural feasibility before the need to investigate additives to improve the currently inconclusive structural measure. If the analysis determines that a grain would not remain structurally sound during the specific loading conditions, then the need for structural performance enhancing additives should be considered and understood that they could negatively affect the combustion performance.

It is necessary to investigate the existing research into paraffin wax fuel grains and determine the current state-of-the-art in hybrid rocket fuel grain structural integrity analysis, and performance-enhancing methods. The work conducted on solid rocket fuel grain structural feasibility studies can offer insight into the complexities associated with the material behaviours and the loading conditions expected. In addition, there should be an understanding of the relationship, if any, between additives or structural enhancement methods and their resultant effect on structural response and combustion performance.

Concerns relating to structural failure include the possibility of grain material breaking off and being wastefully ejected from the motor, or potentially blocking the nozzle and resulting in a chamber over-pressurisation failure. This research intends to provide a methodology for comprehensively evaluating the structural characteristics of paraffin wax fuel grains and assessing the structural impact of additives or design modifications.

Important factors to consider when investigating the plausibility of grain failure include material strengths and moduli, combustion characteristics, failure propagation and other aspects that may affect the fuel material characteristics, such as temperature, strain-rate and additives. It is necessary to characterise the fuel material structural properties, particularly in terms of strain-rate or thermal dependencies. Associated investigations require significant experimental testing under specific conditions to ascertain the response of the material in the various loading

situations. Further, the information obtained from experimental testing should enable the formulation of accurate material response models for use in diverse grain structural simulations.

There is currently no existing procedure for structurally characterising and analysing hybrid rocket fuel grains, offering a clear gap in the technological development of paraffin wax hybrid fuels with regard to the structural performance and response modelling. This research aims to develop a procedure for attending to these development deficiencies in order to increase the Technology Readiness Level (TRL) of hybrid rockets. The objective of this research is to focus specifically on the structural aspects of paraffin wax for use in geometrically different fuel grains. Specifically, it is necessary to determine and characterise the complex structural nature of paraffin wax as a fuel and make use of more representative methods of modelling its structural response. The output of this work, while focusing on the Phoenix Hybrid Sounding Rocket Program, should be applicable to all paraffin wax hybrid rocket fuel grains as long as adequate material characterisation is achieved.

1.4 Research objectives

The overall aim of this research is to develop methods and parameters for characterising paraffin wax hybrid fuels, with and without aluminium additives, and applying the information obtained experimentally to an FEA (Finite Element Analysis) structural model in order to determine the feasibility of the material being used in specific hybrid motor designs. The research objectives associated with this aim are as follows:

1. Investigate the current paraffin wax-based hybrid rocket state-of-the-art, and identify the deficiencies associated with fuel grain structural assessment. This investigation should include structural and performance-enhancing additives and the effect these have on the performance of the motor.
   This objective creates an in-depth understanding of the current TRL of hybrid rockets and the degree of research focussed on fuel grain structural assessment and identifies shortfalls in existing fuel grain structural and performance analyses.

2. Develop an experimental testing regime to fully characterise paraffin wax fuel as an input to a structural FEA model.
   This objective identifies and defines empirically the material-specific response considerations, such as the temperature dependence of the material as well as the

strain-rate dependency. Both factors should be considered in a structural analysis that is to accurately represent the structural response of a paraffin wax fuel grain.

3. Verify the use of material constitutive and failure models for structural response modelling considering the specific characteristics of paraffin wax.
   This objective critically analyses the use case of material constitutive and failure models to represent the material properties of paraffin wax for use within the tested range of material characterisation. The defined response models require verification through experimental testing to ensure adequate representation of the material response under load.

4. Develop a computationally efficient structural response model to represent the ignition pressurisation loading condition associated with a set of hybrid rocket motor designs.
   This objective makes use of both theoretical (modelled) motor performance data and experimental motor performance data to predict and compare the structural performance of paraffin wax hybrid rocket fuel grains in response to the transient load of ignition pressurisation.

5. Apply the findings from the above studies to propose recommendations for future work and development.

1.5 Motivation

Hybrid rocket research has been advancing rapidly since the development of high regression fuels such as paraffin wax. The primary objective of most researchers is to consider the combustion performance, often in the form of regression rate, and apply it to their specific mission requirements. This objective often does not consider the structural performance of the fuel grain. Research into fuel grain structural properties has previously been conducted, but only considers the quasi-static tensile properties of paraffin wax with the inclusion of potential structural enhancement additives. Unfortunately, the use of structural enhancement additives generally reduces the advantages of using paraffin wax fuels and may not therefore offer the desired result.

To date, there has been very little research into the structural response modelling of hybrid fuel grains. This seems to be an unusual situation since the response modelling of solid rocket motors is of vital importance in the context of overall motor development.

The lack of research into this field has offered an opportunity to develop a structural modelling methodology for hybrid rocket fuel grains, and wax-based fuel grains in particular. This research will thus focus specifically on applications involving paraffin wax and paraffin wax with aluminium additives, which have frequently been identified to increase combustion performance.

1.6 Presentation of the thesis

The thesis is presented in a manuscript-based format, where each of the core chapters is a manuscript that has either been published or is currently under review. Only small formatting changes have been made to each manuscript, however, the body of the text and the arrangements of headings are as per the original publication. The thesis consists of two articles published in a peer-reviewed journal, and one manuscript currently under review with a peer-reviewed journal. In addition, the work includes this introductory chapter and a concluding chapter which serve to integrate the aspects covered in the publications. Each manuscript was arranged sequentially within the research and aimed to address at least one of the objectives stated above.

The current chapter introduces the research topic, with a brief introduction into hybrid rocket technology development and the use of paraffin wax as a hybrid fuel. It addresses the deficiencies associated with structural response modelling and defines the objectives of this research.

Chapter 2 presents the article "A review of the performance and structural considerations of paraffin wax hybrid rocket fuels with additives" which was published in *Acta Astronautica* (Veale *et al.*, 2017). The article accumulates all of the available data associated with paraffin wax hybrid fuel combustion and structural testing, including with a variety of additives. The work detailed the current extent to which paraffin wax fuel has been investigated in the context of structural concerns. It details a clear deficiency in the development of comprehensive structural testing and modelling methodologies.

Chapter 3 presents the article "The structural properties of paraffin wax based hybrid rocket fuels with aluminium particles" which was published in *Acta Astronautica* (Veale *et al.*, 2018). This article details the full material structural characterisation testing of paraffin wax and paraffin wax containing aluminium particles. This includes assessing the strain-rate dependencies, temperature dependencies and the quasi-isotropic nature of paraffin wax.

An earlier publication, "Structural Performance of Large Scale Paraffin Wax Based Fuel Grains", which was presented at the *51ˢᵗ AIAA Joint Propulsion Conference*, detailed the initial aspects of this study, reporting on the structural properties of paraffin wax tensile specimens machined directly from a fuel grain (Veale, Brooks and Pitot de la Beaujardiere, 2015). A comparison of the results presented in the more recent publication addresses the question of the isotropic nature of paraffin wax crystal structures.

Chapter 4 presents the manuscript "Explicit modelling of the ignition transient structural response of a paraffin wax hybrid rocket motor fuel grain", which is under review with the *Journal of Aerospace Technology and Management*. This manuscript details the application of the Johnson-Cook material constitutive and failure models in explicit FEA modelling of paraffin wax. It presents a methodology for determining the model's material parameters and a verification of the results. After the model use case is confirmed, the chapter then proceeds to addresses the specific motor structural response against both theoretical and hot-fire tested motor combustion test cases.

Chapter 5 provides concluding remarks concerning the scope and findings of the research. This chapter brings together the work from each core chapter and addresses the contributions this research has made to the field. Future research and recommendations are also addressed.

Each chapter has its own abstract, nomenclature and conclusion. This was left as per the format of the publications for completeness. The individual reference lists were moved to the end of the thesis and listed as a single list to prevent duplicate referencing.

CHAPTER 2: A REVIEW OF THE PERFORMANCE AND STRUCTURAL CONSIDERATIONS OF PARAFFIN WAX HYBRID ROCKET FUELS WITH ADDITIVES

2.1 Abstract

Paraffin wax as a hybrid rocket fuel has not been comprehensively characterised, especially regarding the structural feasibility of the material in launch applications. Preliminary structural testing has shown paraffin wax to be a brittle, low strength material, and at risk of failure under launch loading conditions. Structural enhancing additives have been identified, but their effect on motor performance has not always been considered, nor has any standard method of testing been identified between research institutes. A review of existing regression rate measurement techniques on paraffin wax-based fuels and the results obtained with various additives are collated and discussed in this paper. The review includes 2D slab motors that enable visualisation of liquefying fuel droplet entrainment and the effect of increased viscosity on the droplet entrainment mechanism, which can occur with the addition of structural enhancing polymers. An increased viscosity has been shown to reduce the regression rate of liquefying fuels. Viscosity increasing additives that have been tested include EVA and LDPE. Both these additives increase the structural properties of paraffin wax, where the elongation and ultimate tensile strength are improved. Other additives, such as metal hydrides, aluminium and boron generally offer improvements on the regression rate. However, very little consideration has been given to the structural effects these additives have on the wax grain. A 40% aluminised grain, for example, offers a slight increase in the ultimate tensile strength but reduces the elongation of paraffin wax. Geometrically accurate lab-scale motors have also been used to determine the regression rate properties of various additives in paraffin wax. A concise review of all available regression rate testing techniques and results on paraffin wax-based hybrid propellants, as well as existing structural testing data, is presented in this paper.

Keywords: Hybrid rocket; regression rate; paraffin wax; additives

2.2 Introduction

Hybrid rocket technology has advanced since the discovery of liquefying fuels, also referred to as non-classical fuels. Hybrid rockets are named as such due to their propellants, which often comprise a solid fuel and a liquid or gaseous oxidiser. The physical and state separation of the fuel and oxidiser offer an increased safety aspect to rocket design and fuel handling. However, there is compromised performance due to the limiting boundary layer combustion method. The measure of regression rate of the solid fuel is a good indicator of the combustion performance of a propellant combination, which defines how quickly the solid fuel burns, however, the density of the propellant should also be considered. Hybrid fuels, particularly traditional variants such as hydroxyl-terminated polybutadiene (HTPB) are known to have very low regression rates. The regression rate is often improved through the use of performance-enhancing additives, such as high-energy metal particles. The degree to which these additives improve the combustion performance and the effect they have on the structural performance on a solid fuel grain has not been comprehensively determined and is dependent on factors such as particle size and density, as well as the original binder material. Although we can consider the propellant performance independently, the performance of the rocket itself is dependent on various design parameters, such as vehicle size, design thrust, mass and fuel density. In this paper, we review the current state of paraffin wax fuelled hybrid rocket motor performance testing with specific reference to the role of additives in improving metrics such as specific impulse and density impulse. The purpose of this review is to create a link between existing regression testing results, with various additives, in comparison to the available structural characterisation data on those fuel mixtures of paraffin wax-based hybrid fuels to determine their feasibility in launch applications.

Nomenclature

a	regression rate coefficient
A_b	combustion area (m^2)
G_o	oxidiser mass flux (kg/m^2s)
ID	inner diameter
I_{sp}	specific impulse
m	mass (kg)
n	flux exponent
OD	outer diameter
O/F	oxidiser to fuel ratio

$\dot{r}$	regression rate (mm/s)
r_f	regression rate (mm/s)
t_b	combustion time (s)
ρ_f	fuel density (kg/m^3)
HTPB	hydroxyl-terminated polybutadiene
HRM	hybrid rocket motor
SRM	solid rocket motor
LRM	liquid rocket motor
PMMA	polymethyl methacrylate
GOX	gaseous oxygen

2.3 Hybrid combustion models

Combustion within a hybrid rocket motor (HRM) differs from that within a solid rocket motor (SRM) with the separation of the oxidiser from the solid fuel grain, which resides in the combustion chamber. Combustion initiates when the oxidiser is either pumped or allowed to flow under pressure past the fuel grain surface, through either a single port or multiple ports. The number of ports is determined by the regression rate of the fuel material, and the required thrust. This combustion mechanism allows for the development of a flame zone above the exposed fuel surface and varies along the length of the port due to the changing O/F ratio. Classical fuels such as HTPB have very low regression rates as a result of the dominant boundary layer combustion mechanism. Non-classical fuels, such as paraffin wax have a mechanical combustion mechanism referred to as droplet entrainment in addition to the boundary layer mechanism, which promotes faster regression of the fuel. The focus of this review is the effect of additives on the non-classical combustion mechanism of paraffin wax through empirical means. However, a brief overview of both mechanisms is included for reference.

2.3.1 Classical hybrid combustion

Boundary layer combustion is a result of fuel vaporisation. The primary combustion region is shown to be within a relatively narrow flame zone located within the boundary layer (Marxman, 1965), depicted in Figure 1 - 1. The various forms of heat transfer allowing for fuel vaporisation include convection and radiation from the flame zone. Vaporised fuel is transferred away from the heated fuel surface towards the flame zone. Un-combusted oxidiser is moved from the main

oxidiser stream to the flame by turbulent diffusion. The stoichiometric conditions of the reaction define the position of the flame within the boundary layer. The rate of the combustion reaction, which is dependent on pressure and temperature, determines the flame thickness. Other factors which affect the development of the boundary layer include chamber pressure, gas temperature, gas composition, mass flow rate, port length, and port diameter (Sutton and Biblarz, 2001). Classical combustion is limited by the diffusive heat transfer to the fuel surface, resulting in slow regression rates. There has been significant work conducted in the diffusion-limited classical combustion mechanism defining the regression rate of these types of fuels and the reliance on the position of the flame zone within the boundary layer as well as the heat of gasification. This problem is highly complex and is beyond the scope of this review, however detailed work on the heat and mass transfer between chemically reacting liquids has been conducted by numerous researchers leading to adequate regression rate laws (Marxman and Gilbert, 1963; Smirnov, 1985).
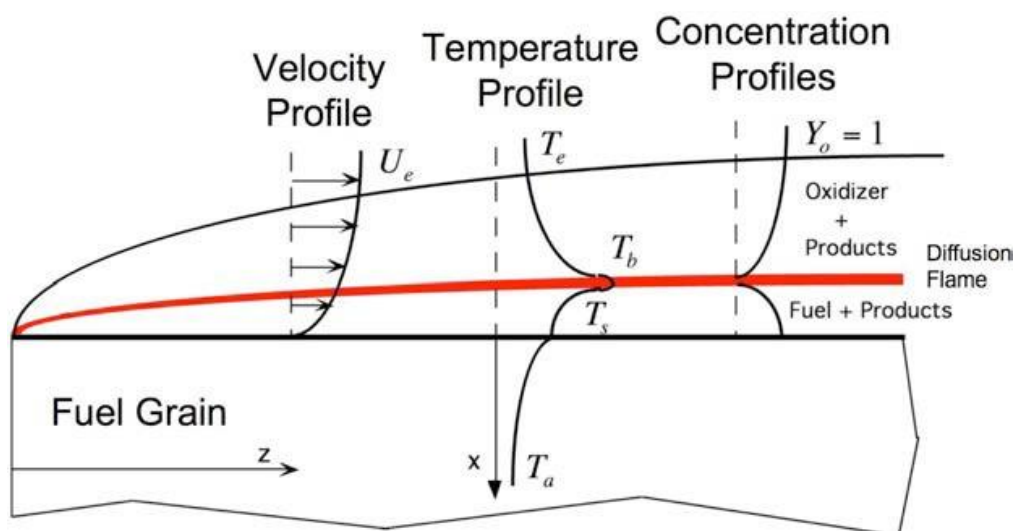
Figure 2 - 1: Schematic of the classical hybrid fuel combustion mechanism
(Cantwell, 2007)

There have been some methods discussed for testing and enhancing the regression rate of classical hybrid fuels. To name a few, authors such as Gariana et al. developed a 2D HTPB/GOX slab motor to compare combustion results to a numerical simulation developed (Gariani, Maggi and Galfetti, 2011). Li et al. investigated the increase in the average regression rate when using swirl injectors. The impinging injectors and oxidiser swirl resulted in an uneven burn (Li, Cai and Tian, 2016). Pei et al. considered the effect of altering the combustion

chamber port geometry on the regression rate and combustion efficiency of the motor (Pei and Hou, 2014). These modifying techniques indicated an increase in performance measures, but the effects did not result in a performance enhancement similar to that of high regression rate fuels which do not rely primarily of diffusive heat transfer.

2.3.2 Non-classical hybrid combustion

The identification of higher regression rate fuels has allowed hybrid rocket motor technology to develop further, addressing more practical requirements. The fundamental difference between the classical and non-classical combustion mechanisms is the formation of a low viscosity liquid layer on the regressing surface. These fuels, known as liquefying fuels, produce a thin, low viscosity, low surface tension liquid layer on the fuel surface during combustion. Instability of this liquid layer caused by the flow of oxidiser over the liquid surface results in the formation of waves, which promote the entrainment of droplets into the gas stream, increasing the overall mass transfer rate and combusting surface area. A schematic of this combustion mechanism can be seen in Figure 2 - 2 (Cantwell, 2007).
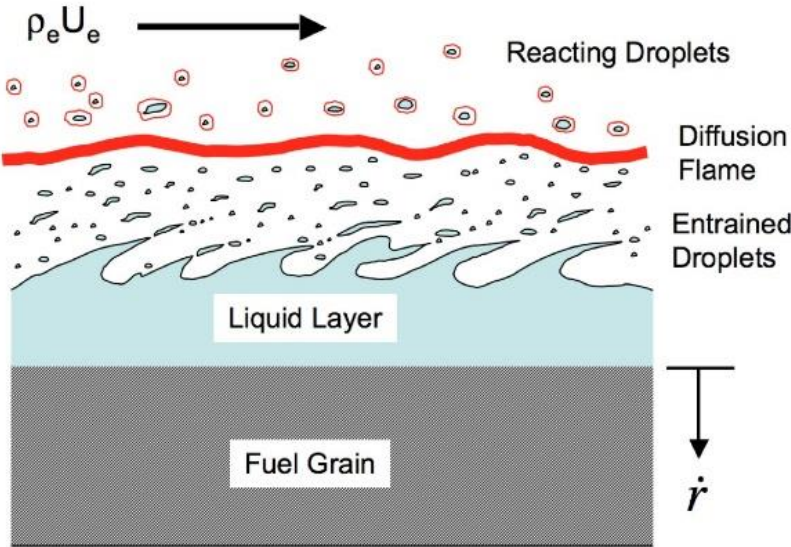
Figure 2 - 2: Liquefying fuel entrainment mechanism (Cantwell, 2007)

The droplet entrainment significantly enhances the speed of regression, and thus addresses some of the classical hybrid performance concerns. The increased regression rate of these fuels reduces the need for multi-port designs, and thus overly complex geometries and manufacturing techniques. This fuel diffusion invention was patented by Karabeyoglu et al. (Karabeyoglu,

Cantwell and Zilliac, 2005, 2007) in which they developed a method of identifying hydrocarbon fuels that are solid at room temperature, have a mean carbon number between 15 and 80, and have a low molecular weight (Karabeyoglu, Cantwell and Zilliac, 2005, 2007). An additional advantage of this regression enhancing combustion mechanism is that droplet entrainment is not affected by blowing as it is not a mechanism of the flame zone heat transfer (Karabeyoglu, Cantwell and Altman, 2001). Mazzetti et al. have conducted an extensive market review on the plausibility of hybrid rocket propulsion in the mid-term future, particularly since the discovery of liquefying fuels such as paraffin wax (Mazzetti, Merotto and Pinarello, 2016). There has been extensive research conducted on the modelling of droplet formation and the combustion process of liquefying fuels considering non-equilibrium and quasi-equilibrium evaporation conditions. The equilibrium model can be considered for large droplet size. However, a non-equilibrium model is necessary for accuracy in the case of small droplets (Tyurenkova, 2012; Guendugov, Smirnov and Tyurenkova, 2013; Tyurenkova, Smirnov and Guendugov, 2013). The development of the droplet formation and the size of the droplets formed for paraffin wax fuels will determine the increased regression rate of the fuel due to droplet entrainment. The focus of this review is the empirical solution to the regression rates of liquefying fuels, but test data should be validated against accurately determined liquid combustion models.

2.4 Performance enhancing additives

An advantage of making use of hybrid propellants with a solid fuel is the ability to include energetic additives in the casting process. Although liquefying fuels already show an improved regression rate, the use of energetic additives can further improve this, and potentially offer control over the regression rate (Cantwell, Karabeyoglu and Altman, 2010). While, metal additives, such as aluminium can increase nozzle erosion, certain metal hydrides, such as magnesium hydride, can reduce this effect, by reducing the oxidising species in the nozzle (Calabro et al., 2007; Cantwell, Karabeyoglu and Altman, 2010). Additives which affect the material strength could be added to improve the structural performance of the fuel grain if it is prone to failure. However, this may alter the fuel liquid viscosity, and reduce the effect of entrainment regression. Consideration should be given to the effect on both the structural and performance properties of a fuel with the addition of any additive. This is apparent from studies where additives offered structural benefits, but in turn increased the melt layer viscosity, reducing entrainment and thus regression rate (Kim et al., 2010). Classical hybrid fuels have little risk of structural failure due to their toughness and strength (Risha et al., 2007). Newer fuels, such as paraffin wax, are comparatively brittle and weak and may be more likely to fail

in use, necessitating a further investigation into their performance in the presence of thermal, pressure and dynamic loading (Risha *et al.*, 2007).

2.4.1 Aluminium

Aluminium additives, both on a micro- and nano-scale have been shown to increase the regression rate of hybrid fuels while serving as a dense energy source (Vickland, 1967; Lips, 1976, 1977b, 1977a; Strand *et al.*, 1992; Strand, Ray and Cohen, 1993; George *et al.*, 1998; Chiaverini *et al.*, 2000; Risha *et al.*, 2001, 2002). The effectiveness of the additive creates an opportunity to make use of other oxidisers, such as nitrous oxide. Data has shown that the use of nitrous oxide with an aluminised HTPB grain can yield a similar regression rate to that of pure HTPB in gaseous oxygen (GOX) (Evans *et al.*, 2009). There are numerous advantages to using nitrous oxide (N2O) such as self-pressurisation, low cost and availability. An added benefit of using aluminium powder is the reduced O/F ratio, resulting in a reduced oxidiser tank size (Cantwell, Karabeyoglu and Altman, 2010).

The inclusion of aluminium particles within fuels can lead to an increase in specific impulse, volumetric heat of oxidation, adiabatic flame temperature, heat of combustion, and radiative heat transfer (Thomas *et al.*, 2015). On a micro-scale, aluminium particles increase the regression rate by improving the radiative heat flux from the diffusion flame zone to the fuel surface as a result of the radiating metallic particulate matter and the higher gas-phase temperature (Risha *et al.*, 2007). Particles also improve the regression rate through the release of energy during metal oxidation (Thomas *et al.*, 2015). In some studies, the addition of aluminium particles in the fuel grain does not significantly benefit the regression rate due to the high melting temperatures associated with the aluminium oxide layer, which coats the aluminium surfaces. The fuel often melts before the aluminium, creating a protective film around the particles, and further impeding the combustion process. The aluminium can be lost in the exhaust, and have little benefit on the regression rate. This scenario is particularly prevalent in oxygen-rich environments, such as the use of a GOX oxidiser. The use of fluorine-based oxidisers reduced the build-up of the oxide layer and allowed for easier combustion (Lips, 1977b).

Nano-sized aluminium particles are known to react differently to micro-sized particles. This can result in higher combustion efficiencies, better heat transfer, and a reduced ignition delay and burn time when compared to micro-sized particle-enriched grains (Risha *et al.*, 2007). The

cost and manufacturing complexities involved are some of the disadvantages associated with the use of nano-sized particles. The reactive effect is similar to that of the micro-sized aluminium particles, however, with the lower ignition time and temperature due to the high specific surface area, the energy release is closer to the fuel surface (Thomas *et al.*, 2015). Production is further complicated by the unreactive, oxide mass fraction which can develop around each particle if not processed in inert environments.

There is a limit to how much aluminium can be introduced to a propellant. The inclusion of aluminium particles increases the regression rate of that propellant combination, but when an excessive amount is added, the near-surface combustion becomes less efficient due to a build-up of particles at the fuel surface (Risha *et al.*, 2007). The mechanism behind the combustion of the aluminium particles themselves relies on their entrainment into the oxidiser stream. The particles can collect on the regressing fuel surface before they are forced into the oxidiser stream, resulting in a reduced regression rate due to limited heat transfer, especially in larger hybrid motors (Thomas *et al.*, 2015). It is also noted that reducing the aluminium particle size increases regression rate insofar as the oxide layer formation is prevented. If methods of altering the oxide layer and coating the particles are used, the regression rate can be increased (Thomas *et al.*, 2015). The inclusion of aluminium additives in hybrid fuels has been considered in applications such as the proposed hybrid design of the Europa and Uranus mission by Jens et al. and the Mars Ascent vehicle design by Chandler et al. The first design considers the addition of 30% micron-sized aluminium particles in PE wax (Jens, Cantwell and Hubbard, 2016), while the second considers the addition of 40% micron-sized aluminium particles to paraffin wax (Chandler *et al.*, 2011). The intended advantage is such that the specific impulse and density impulse will increase, and the optimal O/F ratio will change. They note, however, that the theoretical performance may not be applicable due to the inefficiency attributed to aluminium combustion, reducing the overall combustion efficiency, and the slag formation in the post-combustion chamber.

2.4.2 Boron

Boron is considered to improve regression due to its higher volumetric heat release than aluminium, but its use is limited due to its difficulty with ignition which can lead to low combustion efficiencies (Karabeyoglu and Arkun, 2014). Small amounts (5%) of boron additives in HTPB have shown a reduction in regression rates due to this ignition complexity (Thomas *et al.*, 2015). Tests conducted at Pennsylvania State University (PSU) include the use

of boron and boron carbide particles within HTPB fuels. When the additive amount in HTPB is near 10%, there is an increase in regression rate as compared to pure HTPB combustion (Evans *et al.*, 2009). Extensive boron testing has been conducted by the Israel Institute of Technology for use in solid fuel ramjets (Gany and Netzer, 1986; Natan and Gany, 1993a, 1993b). The difficulties in the combustion of boron and boron carbide is a known problem with the utilisation of this additive. An afterburner can be introduced to assist with full combustion. The boron particles can also be coated with materials such as magnesium, to assist with the combustion process.

2.4.3 Metal hydrides

Metal hydrides, such as magnesium hydride (MgH_2) and lithium aluminium hydride ($LiAlH_4$) have been considered for performance enhancement and their use results in an increase in the regression rate of paraffin wax (Galfetti *et al.*, 2013). Lithium-based particles are extremely reactive. However, the volumetric heat of oxidation is low compared to that of aluminium or boron. Testing which includes $LiAlH_4$ as an additive in paraffin wax has shown a noticeable increase in regression rate (Schultz, 2013). Tests conducted by Smoot and Price (Smoot and Price, 1966) show that the amount of lithium hydride (LiH) added to an HTPB fuel affects the primary combustion mechanism and the pressure dependence of the combustion. At increasing oxidiser mass flow rates, the combustion mechanism moves from the pressure independent diffusion controlled combustion to the pressure dependent kinetic controlled combustion. In this case, higher levels of LiH within the fuel grain cause the transition range to extend, and the pressure sensitivity of the combustion to reduce.

2.4.4 Magnesium

Magnesium is a readily available and affordable metal which has similar thermal capabilities to that of $LiAlH_4$, although it is slightly less reactive. It is easily ignited and burns with a hot flame, which can aid in the development of a liquid layer on the fuel surface (Schultz, 2013). Testing conducted by Schultz (Schultz, 2013) revealed that the regression rate of paraffin wax could be improved with the addition of more than 10% MgH_2. Amounts less than this result in a slight reduction in the regression rate as a consequence of the newly opaque grain surface reducing radiative heat transfer into the fuel.

2.4.5 Polymers

Polymers such as low-density polyethylene (LDPE) and ethylene-vinyl acetate (EVA) have been investigated with paraffin wax. In small amounts, they showed an improvement in the structural properties of the grains, but the regression rate was affected (Nakagawa and Hikone, 2009; Kim *et al.*, 2010; Maruyama *et al.*, 2011). These polymers increase the melt viscosity of the wax, reducing the effect of droplet entrainment, and thus the regression rate. The increase in the structural performance of grains with LDPE indicates a reduced risk of grain slumping due to storage (Kim *et al.*, 2010).

2.5 Density Impulse

Density impulse is a secondary measure of propellant performance. The specific impulse (I_{sp}) of a system is defined as the total impulse per unit weight, while the density impulse is defined as the total impulse per unit volume (Gordon, 1962), and is often used as a performance measure in volume-strict designs (Karabeyoglu *et al.*, 2011; Karabeyoglu, 2014). Propellants with similar specific impulses can result in a different density impulse based on the propellant density. This results in a correlation between the size of the vehicle that is necessary to house the propellant. Energetic additives can be used to change this measure of performance, either resulting in a higher or lower density fuel. Generally, HRMs have a higher I_{sp} than SRMs, and a higher density impulse than liquid rocket motors (LRMs) (Pastrone, 2012). The advantage of the density impulse may be negligible due to the grain sliver fraction, but this is dependent on the HRM port geometry (Pastrone, 2012).

Karabeyoglu et al. (Karabeyoglu *et al.*, 2011) considered an upper stage hybrid motor design to advance the technology readiness level (TRL) of advanced hybrid motors. In doing so, they derived a correlation between performance measures such as I_{sp} and density impulse to determine the performance comparison between HRMs, LRMs, and SRMs. With the addition of energetic particles to HRMs, there is a noticeable increase in I_{sp}, and density impulse, making them feasible for use when compared to LRMs (Karabeyoglu *et al.*, 2011).

Further investigation into performance enhancement of metal additives has led to a comparative study on the theoretical specific impulse at the optimal O/F ratio, and resultant density impulse for a 40% weight addition of various additives. The addition of metal additives (Al, B, Mg, Mg_1B_3) into a paraffin wax has been shown to slightly decrease the optimal specific impulse

when using high-performance oxidisers, such as liquid oxygen (LOX) (Karabeyoglu, 2017). This is attributed to the increased dissociation effect at high temperatures, and the average molecular weight of the combustion products. There is, however, a noticeable increase in the specific impulse for medium- and low-performance oxidisers (N_2O_4 and N_2O respectively) (Karabeyoglu, 2017). The density impulse for these metals, determined with the O/F ratio for the optimal specific impulse, increases for the high- and low-performance oxidisers, while decreases slightly for the medium-performance oxidiser. Metal hydrides (AlH_3, MgH_2, $LiAlH_4$, $LiAlH_4$) indicate an increase in specific impulse for all the oxidisers. However, the Li-based additives tend to decrease the density impulse, most likely because of the element's low density (Karabeyoglu, 2017).

2.6 Combustion testing

Often the regression rate of a propellant is used as a measure of propellant performance. Although this is not the only performance metric, it offers a useful basis for comparison between fuels. The regression rate is dependent on design-specific properties as well as propellant performance properties. A simplified equation which can be used to estimate regression rate, $\dot{r}$, as a function of oxidiser mass flux, G_o, on the basis of empirically derived ballistic coefficients, a and n:

$$\dot{r} = aG_o{}^n \qquad\qquad (1)$$

Techniques for quantifying the regression rate of fuels include the instantaneous measurement of fuel depletion throughout the burn or the time-averaged regression rate which is estimated based on the burn time, fuel mass, and flow rate. Instantaneous regression is determined with the use of slab motor test stands that allow a small section of propellant to be combusted with visualisation by transparent windows or x-ray to measure the instantaneous fuel regression (George et al., 1998; Karabeyoglu, Cantwell and Zilliac, 2005; Evans et al., 2009). The fuel grain height is assessed continuously throughout the combustion process. This technique has several disadvantages, not least that the resultant ballistic coefficients are affected by the geometry of the fuel slab as well as the interaction of the oxidiser flow and the side walls, or the effect of side burning (Nakagawa and Hikone, 2009). Inaccuracies may also arise from the short burn times due to ignition transients. The primary use of a slab motor, however, is to compare the regression behaviour of pure fuels and those with additives and to determine the mechanisms behind the combustion process visually. This is especially informative when

considering the liquefying fuel entrainment mechanism, which has since been visually identified in numerous slab motor tests.

A more physically representative method of determining the regression rate of a propellant combination is through the use of small-scale or full-scale static motors. The regression rate determined through cylindrical motors is an approximation due to the lack of accurate real-time measurements. The regression rate in a cylindrical motor can be determined by measuring the fuel grain before and after the burn and noting the combustion properties throughout the burn. Such measurements are not instantaneous but are rather time- and space-averaged, leading to some errors (Karabeyoglu, Cantwell and Zilliac, 2005, 2007). Sacrificial regression rate measuring devices can be used for an instantaneous result. These sensors are cast within the fuel grain and make use of electrical resistance to determine their total height. As the fuel regresses, the combusting fuel erodes the sensor resulting in a change in resistance and an estimation of the fuel height. This technique has been tested (Thomas *et al.*, 2015) but was found to under-read the regression rate of the grain.

The regression rate data presented in this section include the averaged regression rate for an averaged oxidiser mass flux over the full burn time. Axial variation in regression rate is expected in hybrid combustion (Smirnov, Tyurenkova and Smirnova, 2015; Tyurenkova and Smirnova, 2016), but was not considered in the empirical regression rate data as the difference was either noted to be very small or not mentioned at all.

2.6.1 Slab motor testing

Slab motor test stands are a useful testing apparatus for both flow visualisation and regression rate analysis. Numerous institutions have constructed them with varying testing objectives for the development of hybrid technology. These objectives include either visualising the combustion process through hot gas pyrolysis or full boundary layer combustion, or direct visual regression rate measurements. Hot gas pyrolysis allows the user to visualise the melt layer and any mechanical entrainment that may occur without any combustion. It can be used to define the amount of regression that is attributed to droplet entrainment (Lestrade, Anthoine and Lavergne, 2011).

Table 2 - 1 and Table 2 - 2 include a summary of the existing slab motor test stands that have been developed primarily for paraffin wax and have yielded useful results to date. Each test

stand has been used to capture specific data for the various grades of fuel. In some cases, significant regression rate data has been determined, particularly with the inclusion of additives. Table 2 - 1 addresses the design parameters, including the chamber geometry, fuel, oxidiser and any additives that were included in the fuel.

The French Aerospace Lab (ONERA) and Korea Aerospace University both investigated hot gas pyrolysis to assess the effect of liquid layer entrainment on regression (Pelletier, 2009; Kim *et al.*, 2010, 2015; Lestrade, Anthoine and Lavergne, 2011; Lestrade, 2012). By removing combustion, the effect of normal boundary layer combustion was eliminated, leaving only the effect of the unstable wave formation. In addition to this, Korea Aerospace University compared the pyrolysis result to full combustion results. Tokai University (Nakagawa and Hikone, 2009; Maruyama *et al.*, 2011) and the Korea Aerospace University both investigated the effects of the fuel viscosity on liquid layer formation, and subsequent droplet entrainment. The viscosity was modified by mixing either EVA (ethylene vinyl acetate) or LDPE (low-density polyethylene) into paraffin wax respectively. Stanford University (Chandler, 2012) used a slab motor to study droplet entrainment visually. For clear droplet visualisation, a space was included between the windows and the fuel grain. This introduced side burning but reduced the number of droplets that interacted with the window, distorting vision. The resultant slow motion videos clearly show droplet entrainment of the paraffin wax fuel into the oxidiser stream through the formation of waves in the liquid layer. The boundary layer formation and flame zone are clearly visible and useful in assisting with the understanding of the physical mechanisms at play during combustion. This test stand was not intended to measure fuel regression. Finally, SPLab (Galfetti *et al.*, 2013) and Penn State University (Chiaverini *et al.*, 2000; Evans *et al.*, 2009) both investigated the regression rate effects of fuels doped with metallised particles, specifically aluminium, magnesium and lithium hydride. The various pressure and oxidiser mass flux ranges can be seen in Table 2 - 2.

ONERA yielded an average regression rate result of 0.65 mm/s for pure paraffin wax under hot gas pyrolysis conditions. This is very low compared to commonly high results and is attributed to the lack of combustion regression (Pelletier, 2009). The regression rate was measured through visualisation and an ultrasonic sensor, generating the instantaneous solid and liquid fuel thicknesses (Lestrade, Anthoine and Lavergne, 2011, 2015). The ultrasonic measurements were reported, but due to the lack of combustion within the chamber, the gas temperature did not stabilise affecting the measured regression rate (Lestrade, 2012).

Table 2 - 1: Slab motor design parameters

Institution	Fuel	Oxidiser	Additives	Wall interaction	Slab dimensions (mm)	Windows
ONERA (Pelletier, 2009; Lestrade, Anthoine and Lavergne, 2011; Lestrade, 2012)	Paraffin wax (C31H64)	None (pyrolysis)	None	No	40 x 24.82 x 350	Yes
TU (Nakagawa and Hikone, 2009; Maruyama *et al.*, 2011)	Paraffin wax (C51H104)	GOX	EVA (C5H7O2(CH3))	Yes	10 x 10 x 100	Yes
KAU (Kim *et al.*, 2010, 2015)	HDPE, LDPE, Paraffin wax (C28H58)	GOX	LDPE	Yes	Width of 50 mm	Yes
SU (Chandler, 2012)	Paraffin wax (C32H66), HTPB and HDPE	GOX	Carbon Black	No	25 x 9.5 x 127	Yes
SPLab (Galfetti *et al.*, 2013)	HTPB, Gel wax (C12H26), Solid wax (C24H50)	GOX	Nano-aluminium (Alex50) and (Alex 100), MgH2 powder (50 to 150 µm particle size) and LiH	Not specified	10 x 4 x 50	Yes
PSU (Chiaverini *et al.*, 2000; Evans *et al.*, 2009)	HTPB	GOX	UFAL	Yes	76.2 x 42.8-44.5 x 584.4	None
DLR (Kobald, Ciezki and Schlechtriem, 2013; Kobald *et al.*, 2014, 2016; Kobald, Verri and Schlechtriem, 2015)	Sasol Wax 6003, 6805, 0907, 1276	GOX	Carbon Black, SA, Nanoclay, Common Polymer	Not Specified	90 x 14 x 180	Yes

* ONERA – Le centre français de recherche aérospatiale   * SU – Stanford University   * DLR – Institute of Space Propulsion

* TU – Tokai University   * KAU – Korea Aerospace University   * SPLab – Politecnico di Milano

* PSU – Pennsylvania State University

Table 2 - 2: Slab motor operating conditions

Institution	Operating pressures (bar)	Oxidiser mass flux range (kg/m²s)	Regression error interval	Testing objective
ONERA (Pelletier, 2009; Lestrade, Anthoine and Lavergne, 2011; Lestrade, 2012)	10-30	50-300	Not stated	Liquid layer visualisation, and effect on regression rate through hot gas pyrolysis. Regression rate measured with window visualisation with high-speed cameras and ultrasonic sensor, generating the instantaneous solid and liquid fuel thicknesses.
TU (Nakagawa and Hikone, 2009; Maruyama *et al.*, 2011)	Atmospheric	10-30	Not stated	Control the regression rates of fuels by changing their viscosities with the use of additives. Regression rate determined through window visualisation with high-speed cameras
KAU (Kim *et al.*, 2010, 2015)	1.1-2.6	4-15	Not Stated	Manipulate the liquid layer viscosity of paraffin wax fuels. Tested with both hot gas Pyrolysis and Full boundary layer combustion.
SU (Chandler, 2012)	Up to 17.2	Up to 40	Regression not measured	Visualise the droplet entrainment in liquefying fuels
SPLab (Galfetti *et al.*, 2013)	1.5	100-350	Not stated	Double slab (top and bottom) configuration motor for testing the regression rates of various fuels with additives
PSU (Chiaverini *et al.*, 2000; Evans *et al.*, 2009)	23-46	175-225	±5%	Double slab (top and bottom) configuration motor for testing the regression rates of different fuels with performance additives. Thermocouples were embedded into the fuel during some of the tests to measure surface temperature during combustion
DLR (Kobald, Ciezki and Schlechtriem, 2013; Kobald *et al.*, 2014, 2016; Kobald, Verri and Schlechtriem, 2015)	Atmospheric	6-8	±10%	Determine a relationship between liquid layer viscosity and regression rate.

* ONERA – Le centre français de recherche aérospatiale   * SU – Stanford University   * DLR – Institute of Space Propulsion

* TU – Tokai University   * KAU – Korea Aerospace University   * SPLab – Politecnico di Milano

* PSU – Pennsylvania State University

Both Tokai University and the Korea Aerospace University utilised slab motor test stands to develop an understanding of the effect of the fuel liquid layer viscosity of paraffin wax on regression rate, and if additives could be used to control this property (Nakagawa and Hikone, 2009; Kim *et al.*, 2010, 2015). In the case of the Korea Aerospace University, this was done with the intention of improving structural performance and was tested using both non-reactive hot gas pyrolysis and reactive boundary layer combustion.

Paraffin wax is known to be brittle, and there is a risk of fuel failure in the case of large scale vehicles (Kim *et al.*, 2010, 2015). The addition of LDPE was hypothesised to increase the tensile strength of paraffin wax. The regression rate of paraffin wax with 5% and 10% LDPE addition resulted in a progressive decrease in regression rate to that of pure paraffin wax. This decrease in regression rate still results in a higher overall regression rate to that of pure LDPE. Additionally, the LDPE doped paraffin wax samples showed an improvement in tensile and compressive strength of 24.8% and 34% respectively for the 5% doped samples, and 42.4% and 42.2% for the 10% doped samples (Kim *et al.*, 2010, 2015). The results obtained from Tokai University showed similarly that the addition of EVA in paraffin wax increases the melt layer viscosity, resulting in a lowered regression rate due to a reduction in droplet entrainment (Nakagawa and Hikone, 2009).

Pennsylvania State University and The Space Propulsion Lab (SPLab) from the Politecnico di Milano's Aerospace Engineering Department both used a double slab motor, which has a slab on the top and bottom of the combustion chamber, while still allowing for direct visualisation. The tests conducted by SPLab were extensive and included fuels such as gel wax, solid wax and HTPB, and additives at a wide range of oxidiser mass fluxes. The regression rate was determined based on the fuel volume and burn time (Galfetti *et al.*, 2013) as follows:

$$\dot{r} = \frac{\Delta m}{\rho_f t_b A_b} \qquad\qquad (2)$$

The SPLab tests were conducted on each fuel with varying percentages of nano-aluminium powders of 50 and 100 nm average particle size (named Alex50 and Alex 100 respectively) and MgH2 powder (50 to 150 µm particle size) (Galfetti *et al.*, 2013). The results indicated a superior regression rate for the pure solid wax over the pure gel wax and HTPB fuels. At a mass flow rate of 350 kg/m²s, HTPB regression rate is measured to be about 0.6 mm/s, gel wax is 1.1 mm/s and solid wax is 2 mm/s (Galfetti *et al.*, 2013). Carbon black (0.2%) was added to the

wax to increase the surface radiation heat transfer and limit the sub-surface radiation penetration, thus reducing the effect of sloughing (Dean, 1995). The results indicate only a slight drop in the regression profile over the oxidiser mass flux range, while still also indicating the superiority of solid wax over the HTPB fuel. At 350 kg/m^{2}s the blackened solid wax regression rate measures about 1.94 mm/s (Galfetti *et al.*, 2013).

With the addition of 5% Alex100 aluminium particles to solid and gel wax, the regression rates at 350 kg/m^{2}s increased to 2.2 mm/s and 1.9 mm/s respectively. There was a substantial increase in regression performance of the gel wax (71%), and only a slight increase in performance for the solid wax (10%) when compared to their pure forms (Galfetti *et al.*, 2013). Regression rates with the addition of 5% magnesium hydride (MgH$_2$) into HTPB, gel wax and solid wax at 350 kg/m^{2}s were measured to be about 1.28 mm/s, 1.64 mm/s and 2.5 mm/s respectively. The performance increase for the solid wax and gel wax (relative to the pure fuels at 350 kg/m^{2}s) was 38% and 25% respectively. These results indicate that the performance increase with the addition of MgH$_2$ has a lower dependency on the binder material (DeLuca *et al.*, 2011; Merotto *et al.*, 2011; Galfetti *et al.*, 2013).

Pennsylvania State University used their slab motor for analysing the regression rate of HTPB with the addition of ultrafine aluminium particles (UFAL). These particles have an average size of 0.05 to 0.10 µm. This data was later correlated to other cylindrical motor tests and showed very similar results (Chiaverini *et al.*, 2000; Evans *et al.*, 2009). Results from these slab motor tests indicate a large regression rate advantage for fuels with certain additives, which is a similar conclusion to that drawn by SPLab. The addition of 20% (by weight) UFAL to HTPB increased the fuel mass flux by 70% (Chiaverini *et al.*, 2000). The regression rate data obtained from the Institute of Space Propulsion revealed a slight increase in regression rate with the addition of 2% nanoclay, but a significant decrease in regression rate with 5 and 10% of a common polymer. The regression rate data was measured on a short burn slab motor, and therefore the regression rates are not comparable to the results presented in Figure 3 due to the large ignition transients and should only be used for comparative tests on the same test apparatus (Kobald, Ciezki and Schlechtriem, 2013; Kobald *et al.*, 2014, 2016; Kobald, Verri and Schlechtriem, 2015). The regression rate data obtained from some of these slab motor tests have been plotted on a common set of axes for comparison, as shown in Figure 2 - 3.
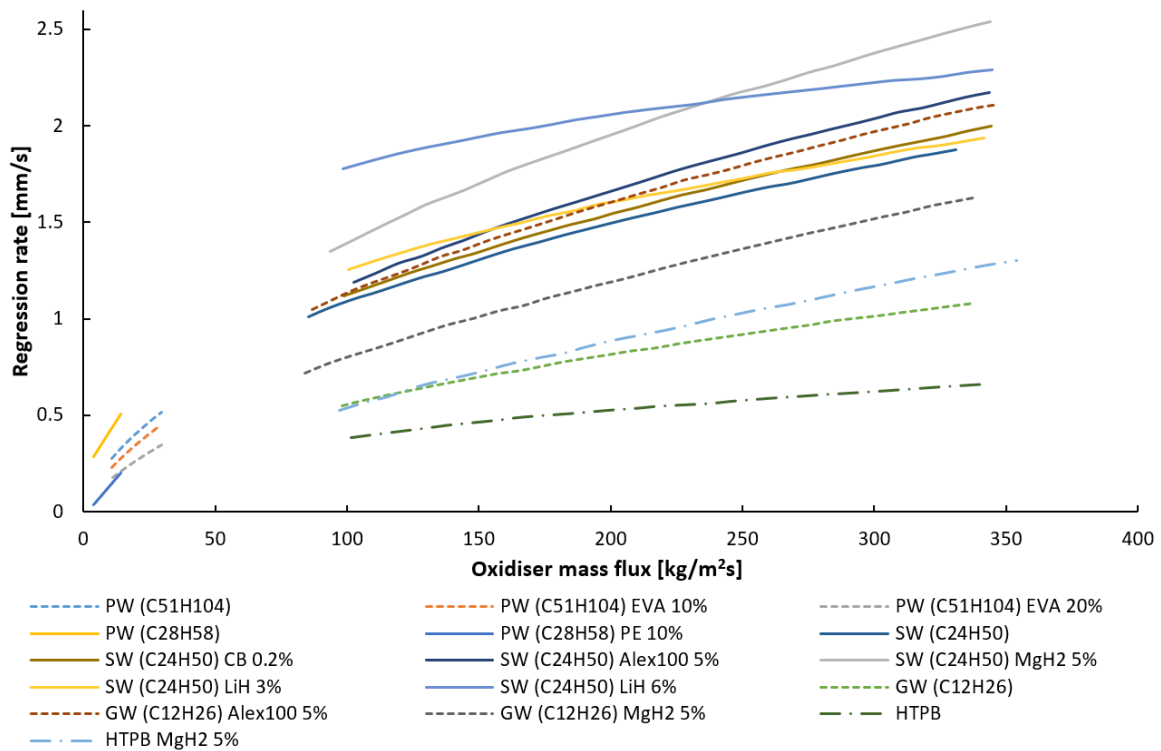
Figure 2 - 3: 2D regression rate results for various wax samples with additives

2.6.2 Laboratory-scale motor testing

Laboratory (Lab)-scale motor testing is one of the most commonly used methods of generating regression rate data. The advantage over a slab motor is the use of a more realistic grain geometry. Regression rate is often determined by time-averaging based on the grain dimensions before and after the burn time, as well as the averaged combustion properties. Numerous institutions have conducted lab-scale motor testing with varying objectives behind their motor designs and testing methodologies. These design attributes are given in Table 2 - 3and Table 2 - 4. The data within these tables were extracted from a number of sources, and is either directly specified as a test condition, or indicated as a design range of the equipment. A shared objective of most of the tests conducted was the determination of the performance characteristics of a propellant combination, and the effect various additives have on the fuel regression rate.

Table 2 - 3 includes the different geometrical properties of the lab-scale motors designed. Some of the tests conducted were either on the same or modified versions of existing lab-scale motors. Table 2 - 4 lists the operating conditions and testing objectives. Before the inception of paraffin wax as a hybrid fuel, a common hybrid fuel was HTPB (Natan and Gany, 1993b). Significant research went into the regression rate improvement of this fuel, in particular with the inclusion

of energetic additives. Since the advantages of liquefying fuels were discovered, researchers began to investigate the improvement of paraffin wax over a doped HTPB fuel (Risha *et al.*, 2001, 2002; Evans *et al.*, 2004, 2009). Finally, to further the regression rate improvement of liquefying fuels, energetic additives were then added to paraffin wax. This gradual development of fuel regression rate improvement has advanced hybrid rocket fuels substantially.

The regression rate data extracted from the publications referenced in Table 2 - 3 and Table 2 - 4 is presented graphically in Figure 2 - 4 and Figure 2 - 5. Figure 2 - 4 includes the pure paraffin and blackened paraffin results from each institution. A trend line has been used to represent the point results from Doran et al. (Doran *et al.*, 2007). This work did not present a regression curve due to insufficient and inconclusive tests. The data was included regardless, as it was the only pure paraffin wax data graphically represented that makes use of N2O as the oxidiser over a range of oxidiser mass fluxes. The University of Brazil (Santos *et al.*, 2005) has conducted tests on pure paraffin wax with nitrous oxide, but this data is tabulated, and the oxidiser mass flux is uncertain due to doubt in the flux measurement technique. The remaining tests make use of gaseous oxygen (GOX).

The regression rate data for most of the tests result in a similar regression profile except for the two distinct outliers from Larson et al. (Larson *et al.*, 2015). These two datasets, although obtained from the same LGCP motor as Evans et al. (Evans *et al.*, 2009), had a critical adjustment to the grain dimensions while keeping the motor dimensions the same. The grain only made up about one-quarter of the chamber length, affecting the flow and regression properties. The short burn times and small diameter design of this motor made its design purpose for comparative tests only (Larson *et al.*, 2015). Additionally, there was a difference between the Pennsylvania State University and Aerospace Corporation paraffin wax compositions. The paraffin wax/N2O experimental data plotted as a trend line from the set test points are noted to be much higher than expected for a nitrous oxide propellant when compared to the GOX propellants (Doran *et al.*, 2007). There is uncertainty in the regression rate data measurements from this set of tests (Doran *et al.*, 2007). The remaining regression profiles correlate closely to each other and do not seem to be affected by the carbon chain length of the known waxes used.

Table 2 - 3: Lab-scale motors design parameters

Institution	Fuel	Oxidiser	Grain OD (mm)	Grain ID (mm)	Grain Length (mm)	Chamber Length (mm)	Regression error interval
SU (Karabeyoglu, 1998; Karabeyoglu, Cantwell and Altman, 2001)	Paraffin Wax (C32H66), Plexiglass, HTPB	GOX	60	12.7 - 30.48	177.8	177.8 - 482.6	Not stated
NASA AR (Karabeyoglu *et al.*, 2003, 2004)	Paraffin Wax (C32H66), Plexiglass and HTPB	GOX	195	76.2 - 152.4	838.2 - 1117.6	1200	± 3 – 8%
SU (Lohner *et al.*, 2006)	HTPB, PMMA, HDPE, Sorbitol	N2O	50.8	19.05	127, 152.4 and 228.6	152.4, 177.8, 254	0.044
SU (Doran *et al.*, 2007)	Paraffin Wax (C32H66), HDPE, PMMA, HTPB	N2O	50.8	12.7 - 19.05	101.6 - 228.6	up to 254	Not stated
UB (Santos *et al.*, 2004, 2006)	Macrocrystalline Paraffin wax	N2O	71	23	220	-	Not stated
UB (Santos *et al.*, 2005)	Macrocrystalline Paraffin wax	N2O	71	23	220	-	Poor results
IIT (Weinstein and Gany, 2013)	MW-704 Paraffin Wax, PMMA	GOX		21	190	310	± 8%
KAU (Kim *et al.*, 2015)	Paraffin Wax (C28H58), LDPE, HDPE	GOX	70	20	200	-	Not stated

Institution	Fuel	Oxidiser	Grain OD (mm)	Grain ID (mm)	Grain Length (mm)	Chamber Length (mm)	Regression error interval
PSU LGCP (Risha *et al.*, 2001, 2002; Evans *et al.*, 2004, 2009)	Paraffin Wax (C32H66), HTPB	GOX	38	8.86	410	-	± 3%
PSU XTC (Evans *et al.*, 2004, 2009)	Paraffin Wax (C32H66), HTPB	GOX	114	64	457	-	± 3%
PSU LGCP (Larson *et al.*, 2015)	Paraffin Wax (C32H66), Paraffin Wax (Aerospace Corporation)	GOX	38	8.89 - 12.97	101.6 - 139.7	-	± 3 – 7%
UN (Scaramuzzino *et al.*, 2013)	HTPB, Paraffin Wax (C24H50)	GOX/N2O	69.2	19.1 - 28.8	220 - 240	350	Only defined for failed tests
IITM (Kumar and Ramakrishna, 2013, 2014)	30% Micro-Crystalline wax, 70% Paraffin Wax	GOX	42	9	134	134	± 2.4 – 4%
IITM (Kumar and Ramakrishna, 2013)	30% Micro-Crystalline wax, 70% Paraffin Wax	GOX	100	20	300	300	± 1.7 – 2.5%

* SU – Stanford University   * NASA AR – NASA Ames Research Centre   * PSU – Pennsylvania State University
* UB – University of Brazil   * IIT - Israel Institute of Technology   * KAU – Korea Aerospace University
* UN – Università di Napoli   * IITM – Indian Institute of Technology Madras

Table 2 - 4: Lab-scale motors operating conditions

Institution	Additives	Operating pressures (bar)	Oxidiser Mass flux range (kg/m²s)	Objective
SU (Karabeyoglu, Cantwell and Altman, 2001)(Karabeyoglu, 1998)	None	3.8 - 13.8	5 - 150	Lab scale motor was designed to fulfil the experimental requirements of determining the transient combustion properties, as well as the regression rates of liquefying hybrid fuels
NASA AR (Karabeyoglu *et al.*, 2003, 2004)	None	10 - 68	74.3 - 368.7	Designed as a scaled up version of the above lab scale motor to determine the effect pressure, oxidiser mass flux, and fuel grain length have on the regression rate
SU (Lohner *et al.*, 2006)	None	20 - 45	25 - 270	Lab scale motor designed to characterise the regression rate of traditional and novel hybrid fuels using nitrous oxide as the oxidiser
SU (Doran *et al.*, 2007)	5 um aluminium	27.5 - 48	25 - 300	Utilising the same lab scale motor as above, these tests were conducted to characterise the effect of aluminium particles on the regression rate of some hybrid fuels.
UB (Santos *et al.*, 2004, 2006)	Carbon black	12 - 20	200 - 700	This lab scale motor was developed with the intention of investigating and comparing the ignition of solid fuels, regression rates, and combustion performance of paraffin wax with nitrous oxide and HTPB and gaseous oxygen
UB (Santos *et al.*, 2005)	Carbon black	12 - 20.	96 - 585	The further testing conducted on the above lab scale motor was conducted with the intention of presenting a mathematical correlation for the combustion velocity as a function of the oxidiser mass flux.
IIT (Weinstein and Gany, 2013)	None	12 - 18.	5 - 100	Experimental testing conducted for the correlation of test data to a theoretical model for liquefying fuels
KAU (Kim *et al.*, 2015)	LDPE	Unknown	33 - 475	Testing conducted to determine the performance of paraffin wax doped with varying percentages of LDPE with the intention of increasing the structural properties of paraffin wax.

Institution	Additives	Operating pressures (bar)	Oxidiser Mass flux range (kg/m²s)	Objective
PSU LGCP (Risha *et al.*, 2001, 2002; Evans *et al.*, 2004, 2009)	Carbon black in paraffin wax, aluminium in HTPB	23 - 46	140 - 850	Compare the differences between aluminium loaded HTPB and paraffin wax as a means to improve regression rate in hybrid rockets
PSU XTC (Evans *et al.*, 2004, 2009)	Silberline nano-sized aluminium in paraffin wax	21.7 - 42.4	163 - 320	Determine the regression rate of aluminised paraffin wax fuel grains.
PSU LGCP (Larson *et al.*, 2015)	Lithium aluminium hydride (LiAlH4), cyclotrimethylenetrinitramine (RDX) ($C_3H_6N_6O_6$), and multi-walled carbon nanotubes (MWNT).	13.8 - 24.1	49 - 115	The addition of LiAlH4 and RDX for regression rate and performance enhancement. Addition of MWNT for structural enhancement
UN (Scaramuzzino *et al.*, 2013)	SEBS in Paraffin Wax, aluminium powder in HTPB	4 - 18	30 - 130	Compare the differences between aluminium loaded HTPB and paraffin wax with SEBS as a means to improve regression rate in hybrid rockets
IITM (Kumar and Ramakrishna, 2013, 2014)	None	9	- 160	Comparing regression rate measuring techniques. Weight measurement vs. pressure measurement
IITM (Kumar and Ramakrishna, 2013)	None	9	- 350	Measure the regression rate

* SU – Stanford University   * NASA AR – NASA Ames Research Centre   * PSU – Pennsylvania State University

* UB – University of Brazil   * IIT - Israel Institute of Technology   * KAU – Korea Aerospace University

* UN – Università di Napoli   * IITM – Indian Institute of Technology Madras

The data presented by Karabeyoglu et al. (Karabeyoglu, 1998; Karabeyoglu, Cantwell and Altman, 2001), investigated transient combustion within hybrid rocket motors. A choked sonic orifice placed in the feed line was used to control the mass flow rate. The regression rate data were obtained for very low oxidiser mass fluxes but remains useful in indicating the regression rate advantage of paraffin wax over a standard HTPB/GOX system. The NASA Ames Research Centre established a scaled-up test facility for further regression rate testing at higher oxidiser mass fluxes (Karabeyoglu *et al.*, 2003, 2004). Their results indicate that scale has little effect on the regression rate of paraffin wax, thus small-scale motor data can be applied to larger scale motors. Also, the oxidiser mass fluxes and chamber pressures observed in these scaled-up tests are more realistic when compared to those expected in a flight motor. Additional data obtained from these scale-up tests indicate that grain length and chamber pressure do not affect the regression rate of the fuels (Karabeyoglu *et al.*, 2004).

Rajiv and Ramakrishna from the Indian Institute of Technology Madras conducted lab-scale motor testing with the intention of comparing combustion chamber pressure and weight change regression rate measuring techniques (Kumar and Ramakrishna, 2013, 2014). Their tests were conducted on two motors of 134 mm and 300 mm grain length. The regression rate measurement techniques correlated well to existing data. However, there is a noticeable difference as a result of scale. The fuel used in their testing was a mixture of 30% microcrystalline and 70% paraffin wax. The carbon chain length was not noted in their publications.

For the purposes of this review, further regression rate data was obtained with the inclusion of a variety of additives within a paraffin wax binder and other novel hybrid fuels. The various regression data from Table 2 - 3 and Table 2 - 4 are given in Figure 2 - 5 to allow for the graphical comparison of the effects of additives. Stanford University designed a new lab-scale motor for the regression rate testing of HTPB, polymethyl methacrylate (PMMA), high-density polyethylene (HDPE) and sorbitol (Lohner *et al.*, 2006). This apparatus was later used for the regression rate testing of aluminised grains, as well as paraffin wax (Doran *et al.*, 2007). The system was designed to be modular in an attempt to fit different grain diameters and lengths, accommodating a variety of fuels. Tests were conducted with nitrous oxide as the oxidiser due to its safety advantages over GOX. Trend lines for the 5, 10, and 20% aluminised paraffin wax fuels grains are given in Figure 2 - 5 (Doran *et al.*, 2007) and compared against the most conclusive pure paraffin wax regression sample from Karabeyoglu et al. (Karabeyoglu *et al.*,

2003, 2004). The scattered data does not show a conclusive increase in regression rate with each percentage of aluminium. Doran et al. (Doran *et al.*, 2007) attribute this to the short burn times and few results. A similar conclusion was drawn for the pure paraffin results represented in Figure 2 - 4.
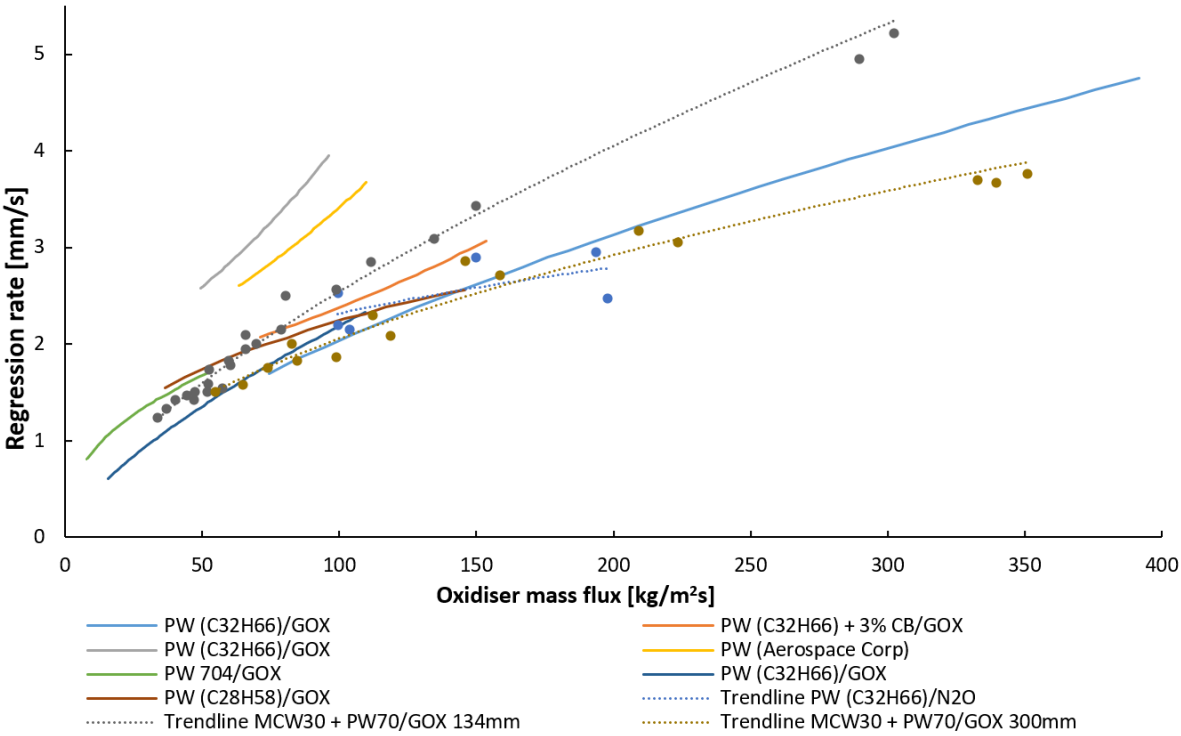
Figure 2 - 4: Regression rate results for pure paraffin wax samples

Other energetic additives such as LiAlH₄ were tested by Larson et al. (Larson *et al.*, 2015). Results of a 5 and 10 % addition of this hydride are plotted in Figure 2 - 5. There is a 7 to 10 % increase in the regression rate of this fuel over that of the pure paraffin tests conducted. Larson et al. (Larson *et al.*, 2015) attribute a portion of this increased regression rate to the lower fuel density when compared to pure paraffin wax. However, there is still an increase in fuel mass burn rates in fuels with additional LiAlH₄. Evans et al. (Evans *et al.*, 2009) demonstrated a 30% increase in regression rate with the inclusion of 13% Silberline aluminium particles. It was hypothesised that the aluminium flakes are encapsulated with molten wax when they leave the fuel surface and burn rapidly near the fuel surface promoting the ignition of the aluminium particles.

Kim et al. (Kim *et al.*, 2015) conducted tests to increase the structural performance of the paraffin wax with the addition of LDPE. Figure 2 - 5 indicates the resultant regression rate data,

showing a reduction of the average regression rate at increasing percentages on LDPE. The addition of LDPE increased the liquid layer viscosity, reducing the regression due to droplet entrainment. Scaramuzzino et al. (Scaramuzzino *et al.*, 2013; Carmicino, Scaramuzzino and Russo Sorge, 2014) added an energetic additive referred to as SEBS, which is a thermoplastic polymer. These test results indicated a higher regression rate when compared to aluminised HTPB, however many of the results were uncharacteristically high due to structural failure of the grain, resulting in fragment loss. A new casting method was then considered which reduced the fragment loss occurrence, but the wax still did not meet structural requirements.
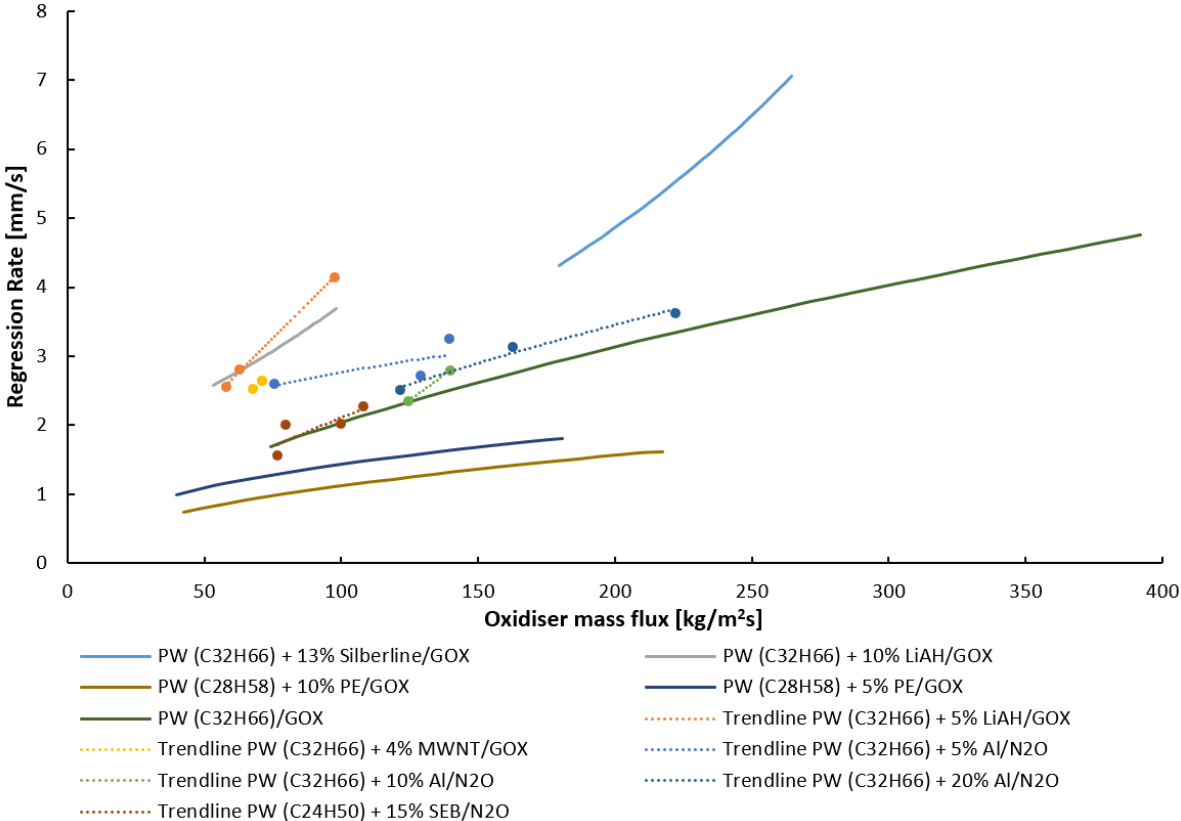
Figure 2 - 5: Lab-scale regression rate results for various wax samples with additives

Other performance testing with the inclusion of aluminium particles includes the work done by Sun et al. (Sun *et al.*, 2016) and Li et al. (Li *et al.*, 2014) where the regression rate of aluminium and aluminium and magnesium doped HTPB fuels grains were tested. The results show a noticeable increase in the regression rate of the fuel with up to 35% Al, and 10% Mg over that of pure HTPB.

The results presented indicate similar regression trends, with most metalized additives improving the regression rate, polymer additives reducing the regression rate, as well as a general increase in regression rate with an increasing oxidiser mass flux. There is unfortunately, very little consistency across testing platforms, due to the differences in measurement methods, averaging techniques and testing procedures. Rajeshwar and Gany (Swami and Gany, 2003) investigated the effects of similarity and scaling in hybrid testing and concluded that for a test motor to accurately simulate a full-scale motor, geometric similarity, oxidiser fuel combination, and scaling of the oxidiser mass flux to the port diameter is required. Further, recent testing conducted by Cai et al. demonstrated the significant effect the length-to-diameter ratio has on the regression rate and combustion efficiency (Cai *et al.*, 2016) of a hybrid motor. It is advised that a set of testing standards be determined for regression rate testing of hybrid rocket motors so that results can be reasonably compared.

2.7 Structural assessment of fuel grains

Both HRMs and SRMs make use of a solid fuel in the combustion chamber. This solid fuel mass is geometrically designed to meet the mission thrust requirements. There are numerous publications available defining the structural assessment of a SRM due to the high-risk nature of a failure (Fitzgerals and Hufferd, 1971; Simo, 1987; Sutton and Biblarz, 2001; Ho, 2010; Kumar and Rao, 2014). The development of a crack in a solid propellant can result in motor over pressurisation or vehicle loss (Gondouin, 1993). There is, however, very little information on the structural performance of hybrid fuels grains. This has not been a primary concern in the development of hybrid technology. Hybrid fuel cracks do not carry as much risk of explosive failure as those in solid fuels. The separation of the fuel and oxidiser limits the fuel reaction to surfaces directly exposed to the oxidiser stream. Further, liquefying fuels may offer a crack healing phenomenon, where the liquid fuel is allowed to flow into any void created as a result of structural failure. The primary failure concern in hybrid fuels is the loss of fuel through the nozzle, which is then at risk of damage or of nozzle blockage resulting in a partial mission altitude (Sutton and Biblarz, 2001). Multiport fuel grain designs commonly used with classical hybrid fuels are at high risk of failure due to sliver fracture of thin-walled ribs. High regression fuels such as paraffin wax do not require multiple ports and can offer some structural rigidity with a single port geometry. However, the brittle nature and low material strength of paraffin wax create uncertainty in its ability to withstand launch loads in its pure form.

Paraffin wax is known to be a soft, weak material. Its low strain failures make its use in high load launch situations concern for structural failure (Wang, Severtson and Stein, 2006; Karabeyoglu and Arkun, 2014). Karabeyoglu (Karabeyoglu, 2017) and Cantwell et al. (Cantwell, Karabeyoglu and Altman, 2010) have commented on the negative impact that metal additives will have on the structural properties of paraffin wax; however little work has been conducted to verify this.

2.7.1 Material testing

Characterising the structural response of propellants is necessary to determine the feasibility of a fuel for the launch conditions, and numerous sources have conducted tensile tests on paraffin wax fuels, with additives. A full characterization is required to determine the temperature and strain rate dependency, but most tests to date are less comprehensive than this. The lab scale tests conducted by Scaramuzzino et al. (Scaramuzzino *et al.*, 2013; Carmicino, Scaramuzzino and Russo Sorge, 2014) documented many fragment losses due to structural failure which resulted in nozzle damage. They attributed this failure to the poor mechanical properties of the SEBS doped paraffin wax grain as a consequence of the low-temperature casting method. Additives such as LDPE have been added to paraffin wax with the intention of improving the structural performance. The effect of this material is to lower the regression rate, as discussed. DeSain et al. (Desain *et al.*, 2009) conducted structural tests on paraffin wax with 0 to 4% LDPE addition following the ASTM 638-03 international standard. The results indicated that LDPE increases the stiffness of the material and increases the ultimate tensile strength (UTS) to a similar range of HTPB. Unfortunately, the stiffness is higher than HTPB, resulting in a fragile grain. They determined the optimal LDPE addition to be 2%, which increases the UTS of paraffin wax to an average of 2.5 MPa at a strain rate of 5.1 mm/min (Desain *et al.*, 2009). This is an improvement of 150% over the pure paraffin wax average UTS of 0.94 MPa. Kim et al. (Kim *et al.*, 2015) conducted tests of a similar nature but followed the procedure stipulated in ASTM D1320-73. This standard has a vastly different testing geometry and has been withdrawn with no replacement. LDPE percentages of 5 and 10% were tested in compression and tension. Similar to DeSain et al. (Desain *et al.*, 2009) the UTS increased with an increasing proportion of LDPE. The average UTS at 0, 5 and 10% LDPE is 1.57, 1.96, and 2.23 MPa respectively at a rate of 5 mm/min.

Kobald et al. (Kobald *et al.*, 2014) conducted extensive mechanical testing on various paraffin wax formulations (Sasol,6003, 6805, 0907, 1276) both macro and microcrystalline, with the

additives such as nanoclay, stearic acid (SA), and what is referred to as a common polymer. The results presented offer the tensile properties of Sasol 6805 with the various additives, normalised to Sasol 6805 + 10% SA. A 2% addition of nanoclay doubles the elongation of the wax but does not significantly improve the tensile strength. It does however slightly increase the regression rate. The addition of 5 and 10% polymer increased the strength by two and three times respectively and the elongation by three and five times respectively. The regression rate of the paraffin wax doped with the polymer had a reduced regression rate. Finally, the addition of a combination of 5% polymer and 2% nanoclay gave an increase similar to that of the 10% polymer (Kobald *et al.*, 2014). A similar evaluation of the effects of organically modified montmorillonite (OMMT) on the structural properties of paraffin wax was conducted by Wang et al. (Wang, Severtson and Stein, 2006) where percentages between 0 and 5% were added to paraffin wax. The structural properties of pure paraffin wax were identified as a ductile failure at low strain rates. The addition of 2% OMMT increased the elongation by 450% (Wang, Severtson and Stein, 2006).

Other additives such as EVA were structurally tested. The addition of 0 to 20% EVA was characterised by Maruyama et al. (Maruyama *et al.*, 2011) who followed the JANAF standards for tensile tests. These tests yielded an increasing UTS with an increasing percentage of EVA addition. The addition of 20% EVA increased the UTS by 1.6 times and the strain by 2.3 times (Maruyama *et al.*, 2011). The effects of the structural properties of paraffin wax grains with aluminium particles were investigated by Veale et al. (Veale, Brooks and Pitot de la Beaujardiere, 2015) and Ryu et al. (Ryu *et al.*, 2016). Veale et al. noted a slight increase in the UTS of Sasol 0907 with a 15% drop in elongation with the 40% aluminised grain. Ryu et al. considered the effect of varying percentages of nano- (100 nm) and micro- (8 µm) sized aluminium particles at varying weight percentages. It was noted that the grains doped with nano-AL displayed a noticeable improvement in structural properties, while the micro-AL doped grains showed less of an improvement, although the tensile strength was still improved.

Table 2 - 5 lists the average UTS obtained from these sources. It can be noted that there are no sources that have conducted a conclusive characterization of the material. Most cases include room temperature tensile and occasionally compressive tests. In this case, each of the sources made use of different standards for testing, none of which are specifically suited to this material.

Table 2 - 5: UTS for paraffin wax tensile tests

Sample (+wt% additive)	Pull rate (mm\min)	Average UTS (MPa)	Experimental standard followed
PW (Desain *et al.*, 2009)	5.1	0.9395	ASTM D638-03
PW	508	0.8915	ASTM D638-03
PW + 2% LDPE	5.1	2.5	ASTM D638-03
PW + 4% LDPE	5.1	1.81	ASTM D638-03
PW + 5% PE (Kim *et al.*, 2010, 2015)	5	1.96	ASTM D1320-73
PW + 10% PE	5	2.23	ASTM D1320-73
PW (Wang, Severtson and Stein, 2006)	10	0.77	ASTM D638-95
PW + 0.5% OMMT	10	0.91	ASTM D638-95
PW + 1% OMMT	10	1	ASTM D638-95
PW + 2% OMMT	10	1.06	ASTM D638-95
PW + 3% OMMT	10	1.15	ASTM D638-95
PW + 4% OMMT	10	1.13	ASTM D638-95
PW + 5% OMMT	10	1.22	ASTM D638-95
PW (Ryu *et al.*, 2016)	5	2.118	ASTM D638-95
PW + 10% Nano Al	5	2.759	ASTM D638-95
PW + 20% Nano Al	5	3.068	ASTM D638-95
PW + 30% Nano Al	5	2.764	ASTM D638-95
PW + 5% Micro Al	5	1.768	ASTM D638-95
PW + 10% Micro Al	5	2.014	ASTM D638-95
PW + 15% Micro Al	5	2.601	ASTM D638-95
PW (Maruyama *et al.*, 2011)	1	0.8	JANAF
PW + 10% EVA	1	1.1	JANAF
PW + 20% EVA	1	1.42	JANAF
PW (Veale, Brooks and Pitot de la Beaujardiere, 2015)	1	1.73	JANAF
PW + 40% AL (Veale, Brooks and Pitot de la Beaujardiere, 2015)	1	1.86	JANAF

The results available are not sufficient to accurately represent the loading conditions that a hybrid rocket fuel grain would encounter during flight. It is advised that once a suitable additive is found to meet the performance requirements, comprehensive structural testing is conducted to characterise the nature of the propellant fully. These tests should follow similar procedures used in solid rocket motor analysis, and include properties such as strain rate dependence, temperature dependence, and creep to name a few.

2.8 Conclusion

Hybrid fuels, particularly liquefying fuels, have shown potential as an applicable form of chemical propulsion. Despite the advances in this technology, no detailed review of the existing performance and structural test results or methods are available for paraffin wax in particular.

In this work, an extensive review of paraffin wax hybrid fuel structural properties versus its regression rate has been presented. This was done with the intention of creating a link between existing structural additives, and performance measures. The density impulse in conjunction with the regression rate as a performance measure is a good indication of the expected performance of a propellant combination in volume-limited designs.

The regression rate data presented indicates a strong link between regression rate improvements in paraffin wax with the addition of metalized additives. Unfortunately, very little testing has been conducted in the structural performance of the grains with these additives. The structural tests that have been conducted have been done under varying conditions, with numerous inconsistencies between sources. In general, there seems to be an improvement in the UTS of the material with small percentages of aluminium, while some report an improvement in elongation, and others report a reduction in elongation. Paraffin wax with a small percentage of a polymer additive, such as EVA or LDPE was investigated with the objective of improving on the materials naturally brittle nature. Small percentages of both EVA and LDPE showed an increase in the UTS and the elongation of paraffin wax. Performance testing of these additives resulted in a reduction in the regression rate. This was due to the increased liquid viscosity, reducing the number of droplets that are entrained into the oxidiser stream. This has been verified in 2D slab motor tests. The structural tests performed have only been conducted at room temperature and at slow speeds, limiting the use of the results. High strain rate tests and temperature dependence of the material should be considered for in-flight loading conditions, while creep and relaxations testing should be considered for storage-related structural analysis. The data presented in this paper indicates a gap in the development and use of paraffin wax hybrid fuels for launch applications. It is important to consider both the propellant performance and its ability to withstand the loads induced during launch. A fuel structural analysis requires comprehensive material characteristics before the structural feasibility can be determined. When considering a new additive, the fuel formulation should be tested with considerations to strain rate dependence and temperature effects. Additionally, the performance of any propellant combination needs to be determined. There are numerous inconsistencies between the test procedure presented above, including chamber size, fuel dimensions, burn times, measurement techniques, averaging methods, and finally, the number of tests conducted.

The next step in the development of paraffin wax-based hybrid fuels and their feasibility in propulsion is to develop a standard procedure for testing which considers which variables need

to be reported, how they should be measured, and finally how they should be reported. The ballistic coefficients, *a* and *n*, in hybrid propulsion can often only be determined empirically, and then used to model flight size motors. These flight size motors also need to carry a structurally sound solid fuel grain, which shows no risk of in-flight cracking or failure. This is a similar process to that used in solid rocket propellants, which should be applied to enhance the future development of hybrid fuels.

CHAPTER 3: THE STRUCTURAL PROPERTIES OF PARAFFIN WAX BASED HYBRID ROCKET FUELS WITH ALUMINIUM PARTICLES

3.1 Abstract

Paraffin wax has been identified as a feasible high regression rate hybrid fuel. For this reason, paraffin wax needs to undergo stringent performance measures to qualify it to meet the requirements necessary for a large-scale launch vehicle. Energetic additives such as aluminium powders have been considered for their performance-enhancing possibilities. This research focusses on measuring the structural performance of the fuels similar to what would be required for a solid propellant. Thus, the structural properties of both pure and 40 wt% aluminised fuels are investigated. Additionally, both elastic and plastic structural properties of the fuel need to be determined for complete material characterisation. Strain rate and temperature dependence of the material structural properties are investigated in this work through compression and tension testing. Results indicate that the addition of aluminium increases the strength of the fuel. Also, a slight increase in temperature was seen to decrease the structural performance significantly. This means that the rate of thermal propagation within the fuel grain is an important consideration. Finally, strain rate dependence is evident in paraffin wax. Higher strain rates result in higher Ultimate Tensile Strength (UTS) failure points, at lower levels of strain.

Keywords: *Hybrid rocket; paraffin wax; additives; structural properties*

3.2 Introduction

The structural performance of solid rocket fuel grains has been considered important for many years (Kelley, 1969; Fitzgerals and Hufferd, 1971; Douglass *et al.*, 1973; Ho, 2010). This is due to the stringent structural requirements of solid rocket propellants, where any unintentional fuel area exposure from crack formation or case debonding could result in catastrophic failure and loss of the vehicle due to over-pressurisation (Gondouin, 1993). Throughout the years, methods of material characterisation and structural simulations have been developed, particularly for solid propellant grains. The primary concern for solid propellant grains is attributed to the fuel and oxidiser being premixed into a single grain. In the case of hybrid

propellants, the solid fuel and liquid (or gaseous) oxidiser are separate, and in different phases. It is not yet known to what extent a vehicle might fail, if at all, if a large crack was to form in a hybrid fuel grain, however, there is still at the least the risk of fuel loss if fuel fragments were to be ejected through the nozzle. Over-pressurisation as a result of excess fuel exposure is less of a concern due to the separation of fuel and oxidiser, and the boundary layer combustion process, however, if a large enough fragment was to break away from the fuel grain, there is a risk of it blocking the nozzle resulting in over-pressurisation. This would result in a pressure shock throughout the motor which may result in motor failure or an altered motor burn performance. In the case of both hybrid and solid fuel grains, a few small surface cracks may not affect the structural integrity of the fuel grain. However, numerous small cracks, a few deep cracks, or large areas of debonding may result in motor failure (Sutton and Biblarz, 2001). With the recent interest in hybrid technology since the inception of high regression rate liquefying fuels, considerations need to be made for the full functionality of the fuels in question.

Paraffin wax has been identified as a viable fuel for large scale hybrid rockets. In addition, additives such as aluminium powders are considered for their theoretical performance-enhancing properties. SasolWax 0907, which is used in this research, has been identified as a brittle material, which allows for relatively little deformation before failure. Before any structural analysis can be conducted, similar to that which would be done for a solid propellant, material characterisation is required to develop a sufficiently accurate constitutive model for the material (Zalewski and Wolszakiewicz, 2011). This paper will detail the experimental technique conducted to determine material properties such as the strain rate and temperature dependencies of paraffin wax, as well as paraffin wax with aluminium additives.

Testing has been conducted over the years on various hybrid fuels with and without additives, and the effects these have on structural properties. Pal and Kumar (Pal and Kumar, 2017) recently conducted a study on the effects of aluminium and polyethylene as additives in paraffin wax hybrid fuels. The study considered only the compressive strength for various combinations of the additives. The fuels were then also compared to view the effects the additives had on the ballistic performance. Ryu et al. (Ryu *et al.*, 2016) investigated the tensile and compressive strength of SasolWax 0907 (Sasol Wax GmbH, 2010) with varying percentages of aluminium additive, however, did not investigate the thermal and strain rate dependence. The results presented in this work, when compared to the results obtained from Ryu et al. (Ryu *et al.*, 2016), show a strong correlation.

A number of other researchers have also conducted introductory-level structural and thermal testing of paraffin-based hybrid fuels, with additives such as hydroxyl-terminated polybutadiene (HTPB), ethylene vinyl acetate, low-density polyethylene (LDPE) and nanoclay. All sources show potential for an improvement in the structural properties of the material with certain amounts of these additives. However, the extent of the mechanical testing was limited in all cases (Wang, Severtson and Stein, 2006; Desain *et al.*, 2009; Maruyama *et al.*, 2011; Kobald *et al.*, 2014; Kim *et al.*, 2015; Sinha, Sridhar and Kishnakumar, 2016; Cardoso *et al.*, 2017; Paravan, Galfetti and Maggi, 2017). Zalewski and Wolszakiewicz (Zalewski and Wolszakiewicz, 2011) presented their findings on the strain rate and temperature dependence of a solid propellant, indicating the importance of this type of investigation beyond just the room temperature, single strain rate scenario, for a complete material characterisation.

Nomenclature

E	modulus of elasticity (MPa)
s	stress (MPa)
e	strain (%)

3.3 Specimen preparation

Before approaching structural testing of a material, its expected structural response needs to be understood. In the case of SasolWax 0907, the effects of the casting technique on the quality of the specimen also need to be considered. To understand the necessary casting techniques required for an adequate test specimen, the crystallisation process should be investigated.

SasolWax 0907, a branched hydrocarbon with the chemical formula of $C_{50}H_{102}$, is defined as a microcrystalline paraffin wax (Piscitelli *et al.*, 2015). These waxes generally have higher densities, molecular weights and refractive indices than macrocrystalline paraffin waxes (Freund *et al.*, 1983). Microcrystalline paraffin waxes can be separated into two categories, these being brittle and ductile. SasolWax 0907 has a congealing range of 83 – 94°C with an overall melting point of 108°C according to the supplier datasheet. This puts it in the category of a brittle paraffin wax, which by definition will offer very little deformation when stressed (Freund *et al.*, 1983). Existing structural properties of paraffin wax indicate that the wax, which is crystalline at room temperature, behaves like a viscoelastic material within the range of -20°C to +40°C. The structural testing conducted here falls within this temperature range.

In order to make use of the paraffin wax, it needs to be formed into the dimensions required for its application. In the case of hybrid motors, this will generally be a cylindrical shape, with a circular port running through the length. For material characterization, specific specimen shapes, defined by testing standards, need to be created. In both cases, the paraffin wax has to be fully melted and poured into a mould of the desired shape. The crystallization of the paraffin wax begins with the formation of nuclei. These nuclei are small crystals with atoms or molecules effectively exerting a force of attraction onto other atoms or molecules from the melted wax. This allows the crystal structure to grow at what is defined as the rate of crystallization. It is important that the nuclei remain randomly orientated, and therefore the anisotropy of the crystals defines the wax as a quasi-isotropic material (Freund *et al.*, 1983). This means that the orientation of casting does not affect the crystal formation, and thus the material properties. Initial test specimens were machined directly from full-size fuel grains. However, this was later shown to be unnecessary due to the crystal formation process, and individual test specimens were then cast for the test campaign. When the structural properties of the machined specimens and the individually cast specimens were compared, no noticeable difference was found. Saccone et al. (Saccone *et al.*, 2015) have detailed the effect various casting procedures can have on the formation of internal cracks in paraffin wax. They have shown that for large grains, slow cooling is not sufficient to prevent internal voids, and thus a force should be applied to the grain during solidification to prevent shrinkage voids. The necessity of this is dependent on the volume of the cast and is not the case for the smaller test specimens. This was however found to be important during the full grain casting, and void formation was often a problem.

The addition of impurities, such as aluminium powder can affect the formation of the crystal nuclei and will inevitably modify the coarseness of the crystal formation. The rate of cooling also affects the crystal formation, with slower cooling rates resulting in a coarser structure. Fast and uneven cooling can also result in internal stresses or voids, and this must be avoided. The shape and size of the crystal formation, however, is defined by a number of factors such as the chemical composition of the wax and the cooling rate. There are three general shapes of crystal formation in paraffin waxes. These are plate, mal and needle shapes (Freund *et al.*, 1983). The properties of SasolWax 0907 paraffin wax indicate that the crystal formation is characterised by needle and mal shapes based on its melting temperature and branched hydrocarbons. The crystal size of needle- and plate-shaped crystals is affected by the cooling rate, while for mal-

shaped crystals, there is only a slight dependency. Slower cooling rates, particularly for needle and plate shapes, result in larger crystal structures. This means that for any specimen casting, temperature rates should be carefully controlled and kept consistent between specimens, based on the casting procedure used for the full-scale grain. The randomly orientated formation of the crystal nuclei also allows for the structural test specimens to be cast individually, instead of being cut out of a full-scale grain.

The testing which was conducted for this research included a range of tensile and compressive tests. There are multiple testing standards available for various materials. However, none specifically define the testing criteria for paraffin wax or a similar material. For that reason, the ASTM tensile and compression testing standards for plastics were employed. These standards are the ASTM D 638 (ASTM International, 2014) and D 695 (ASTM International, 2015) for tension and compression testing, respectively. The specimens were cast individually in purpose-made moulds, depicted in Figure 3 - 1. The tensile specimens used were the Type III plate dog-bone-shaped specimens manufactured as per the dimensions indicated in Figure 3 - 2, with a thickness of 10 mm. The compression specimen shapes were the standard cylindrical specimens defined in the ASTM standards, with a diameter of 12.7 mm and a length of 25.4 mm.
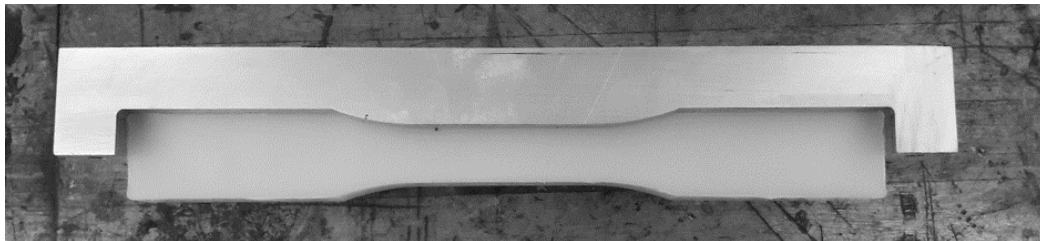
Figure 3 - 1: Half of the specimen split mould

The moulds were manufactured as split moulds so that the specimens could be easily removed without any damage or stresses being induced. Specimens of pure paraffin wax and paraffin wax doped with 40 wt% aluminium power (referred to as aluminised specimens) were investigated. Numerous applications for the use of aluminised fuels have been identified, such as the Mars ascent vehicle proposed by Chandler et al. (Chandler *et al.*, 2011) and the propulsion system for outer planet exploration proposed by Jens et al. (Jens, Cantwell and Hubbard, 2016). The aluminium power used in these tests has an average size of 100 µm and is not treated in an inert environment.
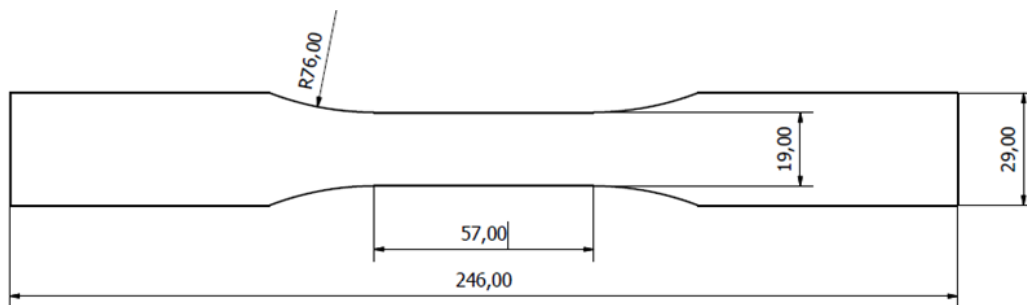
Figure 3 - 2: Type III ASTM638 specimen dimensions (mm)

The casting procedure for the pure specimens is slightly different to that of the aluminised fuel specimens, due to the complexities associated with settling of the aluminium power within the paraffin melt. The two casting procedures were as follows:

Pure specimen casting procedure

1. Melt paraffin wax pellets at 110°C in temperature-controlled kiln – visually inspect until a clear liquid is obtained

2. Preheat specimen mould to 110°C - clean and prepare prior to use, ensuring interaction surface between mould halves are clear of all impurities before assembly to prevent leaking

3. Pour wax melt into now-assembled preheated specimen mould

4. Allow wax to cool slowly within the preheated kiln (now off) – cooling time ±12 hours

5. After cooling, remove specimen mould assembly bolts

6. Pour boiling water (±95°C) on the underside of the mould to allow softening of specimen surface and easy removal from the mould

7. Inspect for damage and shrinkage

8. Prepare surface to remove any shrinkage effects or surface stress concentrations

Aluminised specimen casting procedure

1. Melt paraffin wax pellets with aluminium powder at 110°C in temperature-controlled kiln – visually inspect until a clear liquid is obtained

2. Preheat specimen mould to 90°C - clean and prepare prior to use, ensuring interaction surface between mould halves are clear of all impurities before assembly to prevent leaking

3.   Remove paraffin wax melt from kiln and continuously stir until it reaches a temperature of 90°C

4.   Pour wax melt into now assembled preheated specimen mould

5.   Follow steps 4-8 as above

If the cooling procedure for the aluminised grains is not followed carefully, the resultant specimen will not form homogenously. In the case of cooling from too hot a pour temperature, the aluminium particles will settle to the bottom. If left to cool from too low a pour temperature, the specimen will have distinct layer separation or void formation, or if not continuously mixed during the initial cooling phase, small localised solidification regions will be present. This is evident in Figure 3 - 3. Figure 3 - 3 (a) shows the layer formation from pouring the mix too cold, while (b) shows the resultant settling from pouring the aluminised mix too hot. Figure 3 - 3 (c) shows an image of localised solidification from inadequate mixing and (d) shows the resultant void formation from pouring a mix too cold.

a)   b)

c)   d)
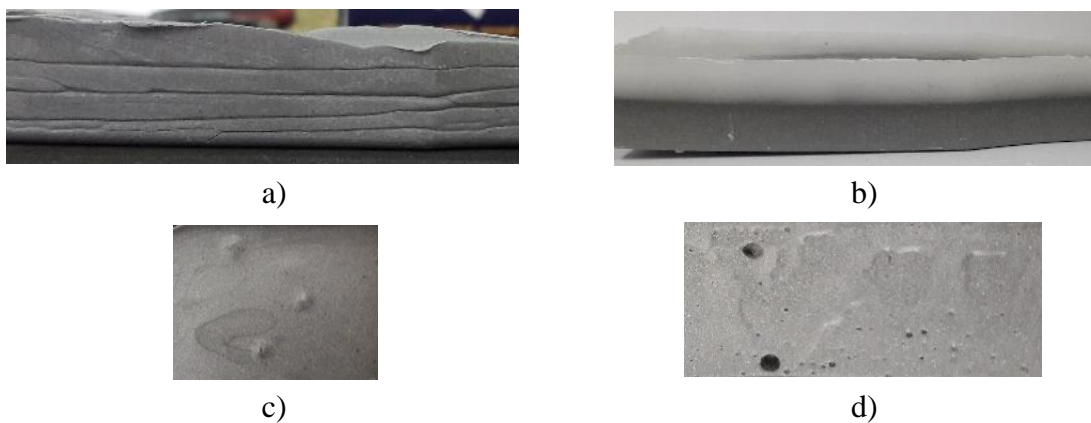
Figure 3 - 3: Photographs of rejected specimens due to a) layer formation, b) settling, c) localised solidification, and d) void formation.

A sufficient number of specimens were cast to ensure that five or more tests could be conducted for each scenario. While the specimen preparation procedure was kept as consistent as possible, there was a rejection of five percent of the cast specimens as a result of the inconsistencies discussed above. An image of a fully prepared tensile and fully prepared compressive specimen, in the testing configuration, can be seen in Figure 3 - 4.

<div align="center">a)   b)</div>

Figure 3 - 4: (a) Tensile and (b) compression specimens

3.4 Testing procedure

The primary objective of the testing regime is to determine the material's structural response under the loading conditions induced during launch. This means that properties for a full, non-linear characterisation need to be considered for the dynamic and thermal loads applied to the fuel grain during launch. Testing was conducted with tensile tests at three different temperature points, and at three different strain rates. The compression testing was conducted at different strain rates only.

The ASTM standards referenced for this testing require a constant temperature environment, with the specimens held at the test temperature for at least 8 hours prior to testing to ensure thermal equilibrium. For all the tests, particularly the elevated temperature tests, the test environment needed to be held at the set temperature for the full duration.

The testing was conducted on an Instron 5500R testing machine with a 5 kN load cell and a 50 mm gauge length extensometer. A purpose-built thermal chamber was installed and used to preheat the grips and environment prior to mounting the test specimens. The test specimens were allowed to preheat for at least 8 hours at the test temperature in a separate kiln, and were then moved directly to the testing machine. The specimen was then checked with a thermal imaging camera to ensure a consistent surface temperature was present prior to testing.

The maximum testing temperature and crystallisation temperature was determined from the Differential Scanning Calorimetry (DSC) results of a paraffin wax sample. The DSC heating result can be seen in Figure 3 - 5. The DSC test measures the heat flow (heat per unit time) required for a sample to maintain a set heating rate when compared to a control volume. The difference in heat flow reveals a phenomenon that either releases or absorbs extra heat. The melting onset temperature, which is taken as a tangent to the average melt curve, is given as 39.75 °C. Temperatures above this will likely result in the wax being too soft for mechanical testing. The crystallisation onset temperature was determined to be 89.27°C by the DSC cooling cycle.
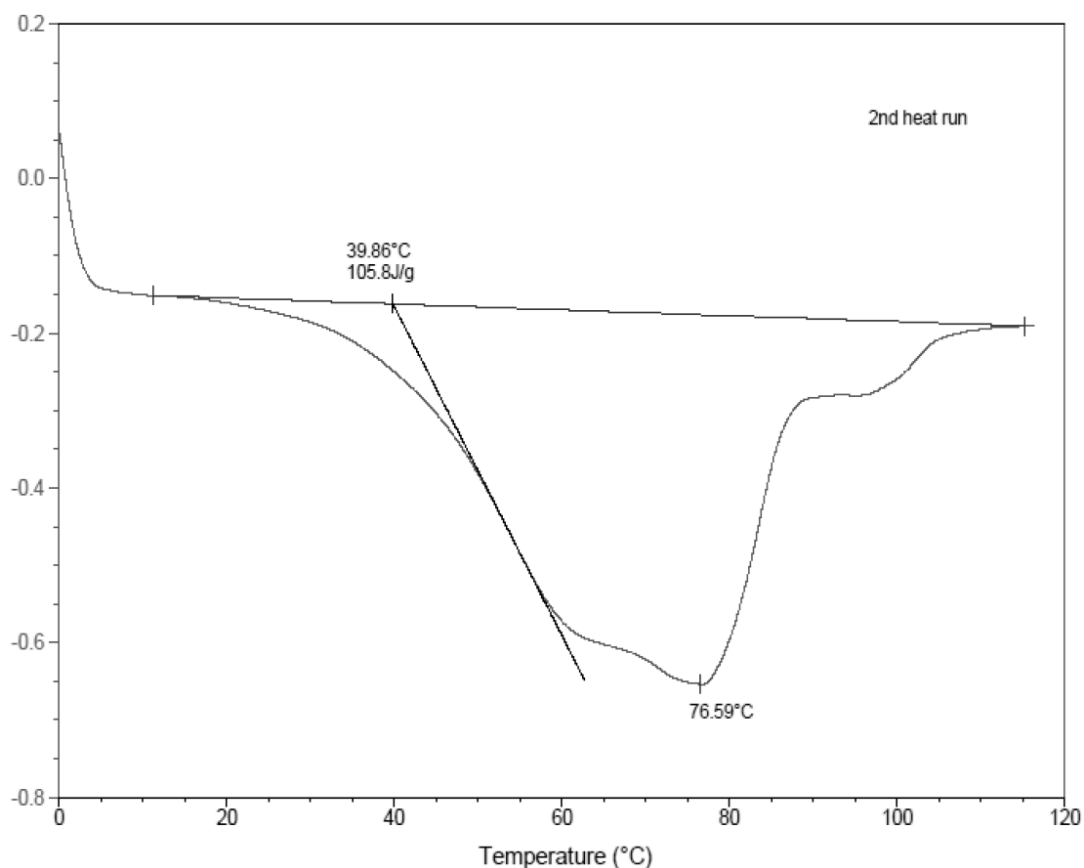
Figure 3 - 5: Differential Scanning Calorimetry results for SasolWax 0907

Tensile tests were conducted at room temperature (23°C), 30°C and 40°C, while compression tests were only performed at room temperature. The extension rates considered were 1, 10 and 100 mm/min for tension, and 1 and 10 mm/min for compression. Some testing was outsourced to verify the results obtained on the testing machine. These results came back as a match to the tests conducted in-house.

Additional material properties such as the difference in thermal conductivity between the pure paraffin wax samples and the aluminised paraffin wax samples were determined. The potential thermal penetration into the grain due to combustion would need to be a consideration during structural modelling of a fuel grain, especially considering the material's low melting onset temperature. It was determined through the use of a TIM Tower testing apparatus, that the thermal conductivity of pure wax is 0.46 (±0.03) W/mK and for the aluminised grains, 1.36 (±0.03) W/mK.

Santi et al. (Santi *et al.*, 2017) conducted tests to determine the thermomechanical properties of paraffin wax by embedding thermocouples into a motor designed to burn for up to 80 seconds. The results of these tests showed no measurable thermal propagation radially into the grain. The thermal diffusivity of paraffin wax is known to be relatively low, and propagation is further limited by the formation and subsequent removal of the liquid layer on the fuel surface. Their observation, however, may not necessarily be the case for aluminised grains, which may suffer a higher level of thermal penetration due to the three times higher thermal conductivity. Combustion testing is necessary to empirically determine the heat flux at the fuel surface in order to accurately determine the thermal penetration into the fuel.

For the purposes of this work, it is beneficial to determine the degree of heat penetration due to conduction from the melted fuel on the surface. In the case of this base approximation, radiation and convective heat transfer effects were neglected. The known thermal data of the materials were applied to a semi-infinite 1D transient conduction model where a temperature boundary condition of 120°C (DSC upper melting temperature) was applied to the fuel surface. After one second, the temperature wave of 30°C reached a depth of 1.37 mm for the pure wax and 1.69 mm for the aluminised wax. The resultant thermal penetration depths are not significant, and less than the theoretical regression rates for pure and aluminised wax, which are dependent on the oxidiser mass flow rate. This estimation is corroborated by the work conducted by Santi et al. (Santi *et al.*, 2017), which indicates no measurable temperature increase into the pure wax grain. The development of a nitrous oxide lab-scale motor using these fuel types predicted a time-averaged theoretical regression rate of 1.63 mm/s and 1.82 mm/s for the pure and aluminised fuels, respectively. The actual combustion testing of this motor designs yielded a measured time-averaged regression rate of ~1.4 mm/s and ~1.6 mm/s for the pure and aluminised wax grains, respectively, which is slightly lower than estimated in both cases

(Maharaj, 2018). However, the regression rate for the aluminised motor was not determined at peak performance. Regression rates for these fuels can generally be significantly higher for higher oxidiser mass flow rates and higher performance oxidisers. In the case of the aluminised grain, it appears that there may be a risk of grain structural deficiency due to heat penetration and that this matter should be considered experimentally in a study similar to that of Santi et al. (Santi *et al.*, 2017).

3.5 Results and discussion

3.5.1 Tensile testing

The first set of testing was aimed at determining the strain rate dependence of the fuels. The graphs of the room temperature results for a 1, 10 and 100 mm/min extension rate for both the pure and aluminised paraffin wax are presented in Figure 3 - 6 and Figure 3 - 7 respectively. Table 3 - 1 summarises the important values of the test results. The standard deviation for each set of test data has been provided to indicate the accuracy of the result grouping at certain points. In all the results presented below, 5 samples of each type cast from the same batch of wax were tested in each case.

In both the pure and aluminised specimens, the strain rate dependence is evident in that at higher strain rates, the ultimate tensile strength (UTS) of the material increases, while the allowable elongation or strain decreases. When comparing the pure and aluminised results, it is evident that the maximum strain is similar for each material at the respective pull rates, with pure wax being slightly higher. However, the UTS is between 10% to 20% higher for the aluminised grain, when compared to pure wax, at the various pull rates. What is also evident from the results is the change in the modulus of elasticity (E) with pull rate, with that of the aluminised specimens being higher, but also with an increase in the linear slope at higher pull rates.
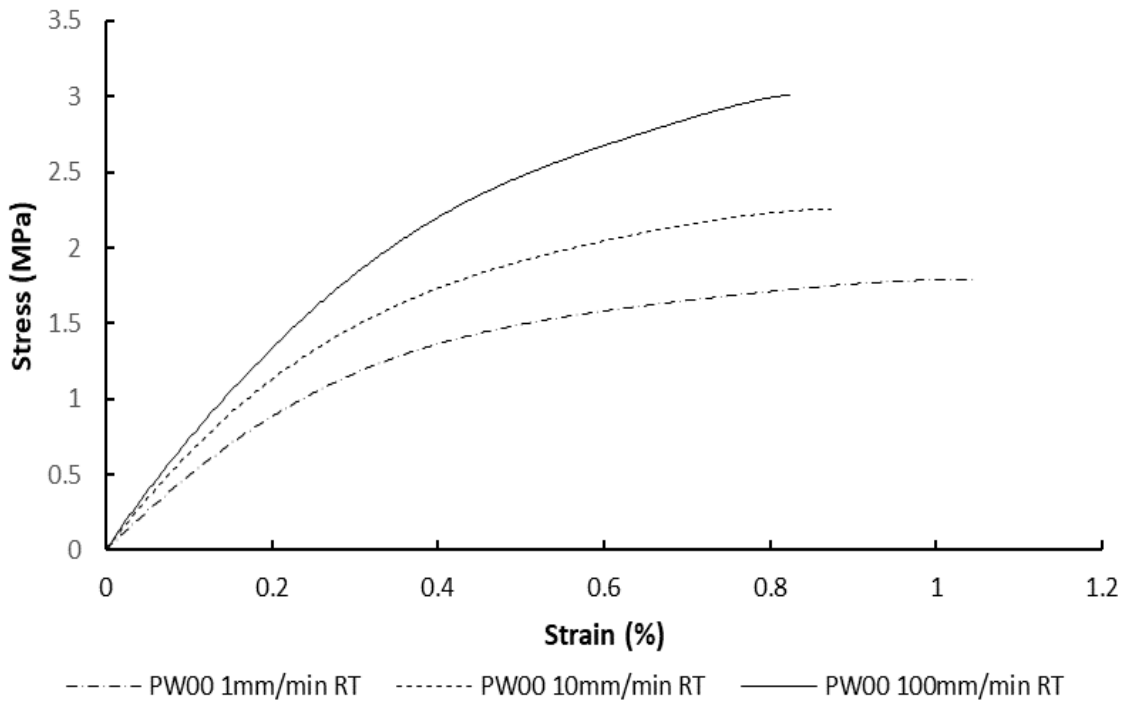
Figure 3 - 6: Impact of the rate of extension on the stress-strain curve of pure SasolWax 0907 at room temperature
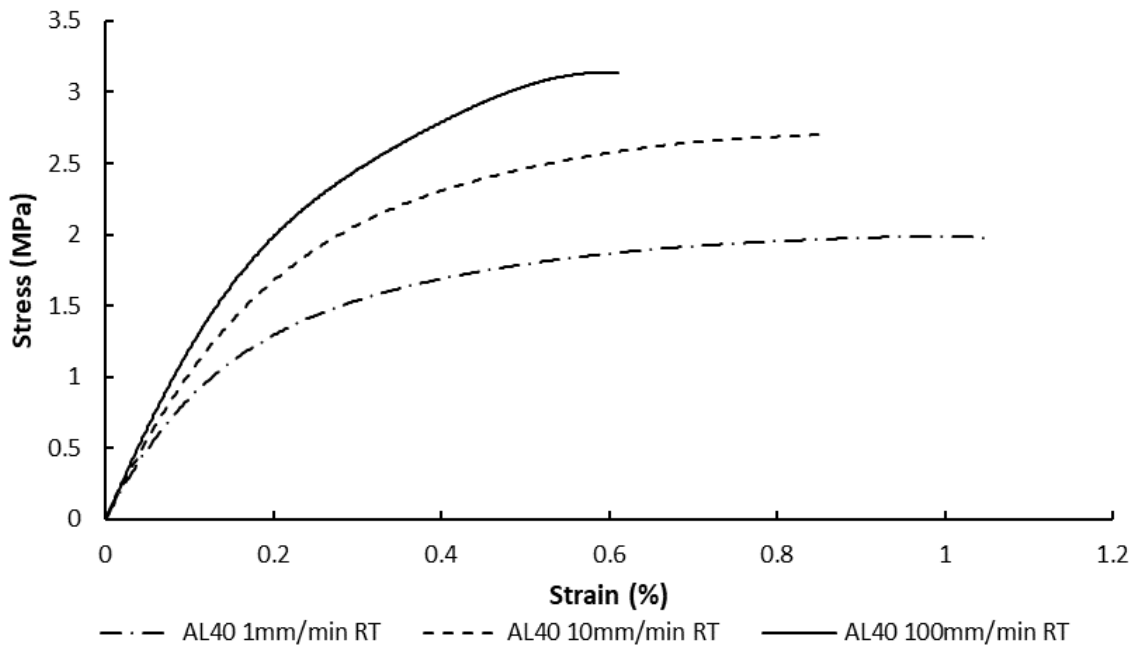
Figure 3 - 7: Impact of the rate of extension on the stress-strain curve of 40% aluminised SasolWax 0907 at room temperature

The material thermal dependency was also investigated, with specimens tested at 30 and 40 °C and at pull rates of 1 and 10 mm/min. The results of the tests for pure paraffin wax at 1mm/min and 10mm/min pull rate can be seen in Figure 3 - 8 and Figure 3 - 9. Both materials show a trend of decreasing UTS and increasing strain with an increasing temperature. A higher pull rate still increases the UTS, however at elevated temperatures, the increase is noticeably less. This implies that the strain rate dependence of this material is less evident at higher temperatures.

A list of notable results extracted from the graphs can be seen in Table 3 - 2, along with that of the aluminised grain results which will be discussed next. A noticeable difference between the elevated temperature tests and the room temperature tests is the location of the UTS point. In the case of room temperature, the UTS point is located at the failure point. This is to be expected in the case of brittle failure. In the case of the elevated temperature tests, the UTS point is not located at the failure point, and the material is able to elongate significantly before failure occurs. The implication of this result is that failure occurred in a ductile manner, with necking present. The results depicted in Figure 3 - 8 and Figure 3 - 9 show the engineering stress, while true stress would include the necking effects. However, the extent of the necking was minimal, and none was visibly evident during this extended elongation.

The 40% aluminised tests conducted at elevated temperatures follow the same trend observed for the pure wax test specimens. The results are presented in Figure 3 - 10 and Figure 3 - 11. Similarly, to the room temperature results, the UTS is noticeably higher for all aluminised scenarios when compared to the pure wax counterparts. The strain rate dependence is also less prominent at elevated temperatures. What is particularly interesting is the significant increase in the peak strain for the 40°C, 1mm/min scenario. The increase in temperature, although decreasing the allowable maximum stress, significantly improves the ductility of the material. The estimated modulus of elasticity rapidly decreases at elevated temperatures, indicating the material's inability to resist plastic deformation at higher temperatures.
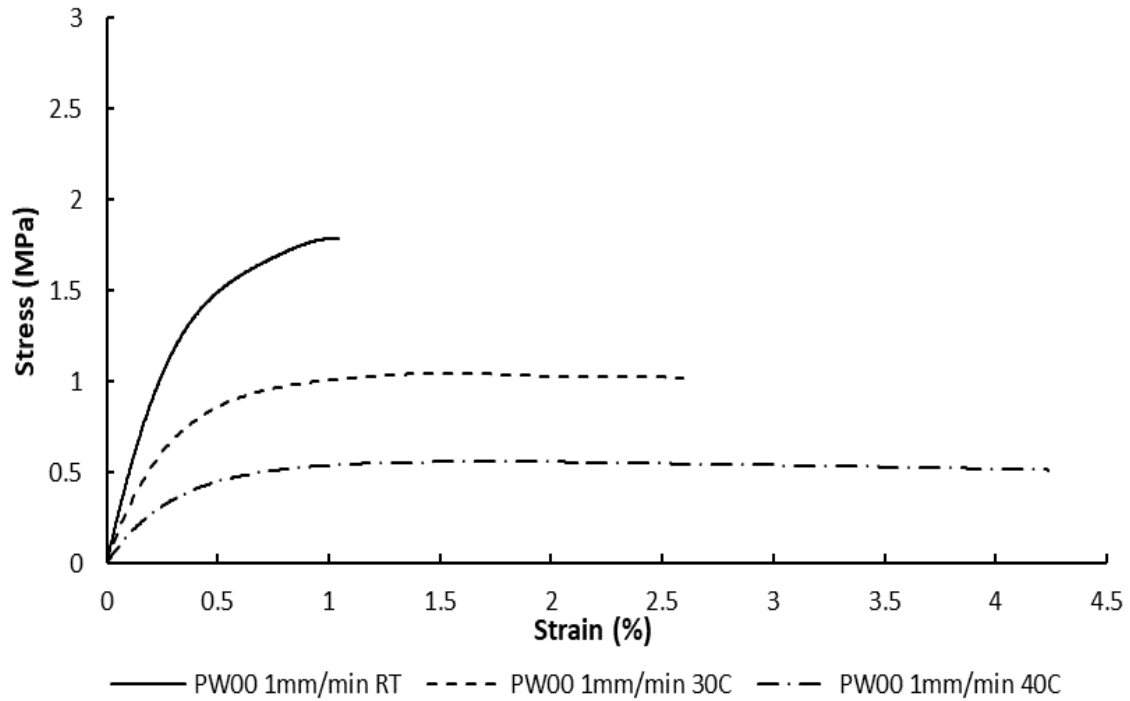
Figure 3 - 8: Impact of the temperature effects on the stress-strain curve of pure SasolWax 0907 at a pull rate of 1 mm/min
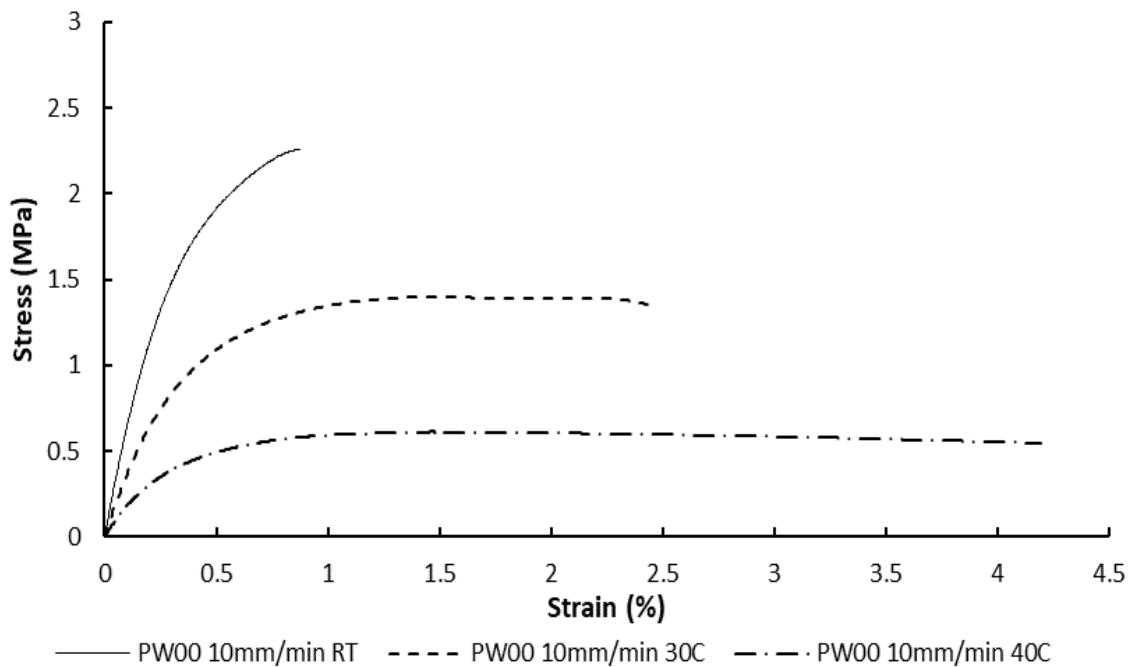
Figure 3 - 9: Impact of the temperature effects on the stress-strain curve of pure SasolWax 0907 at a pull rate of 10 mm/min
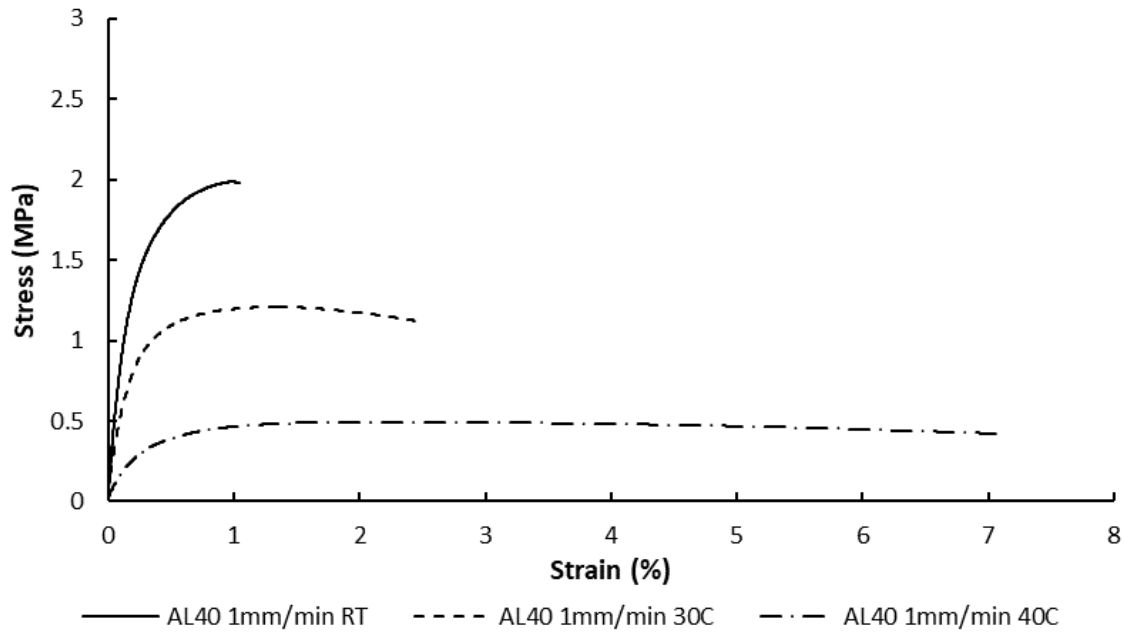
Figure 3 - 10: Impact of the temperature effects on the stress-strain curve of 40% aluminised SasolWax 0907 at a pull rate of 1 mm/min
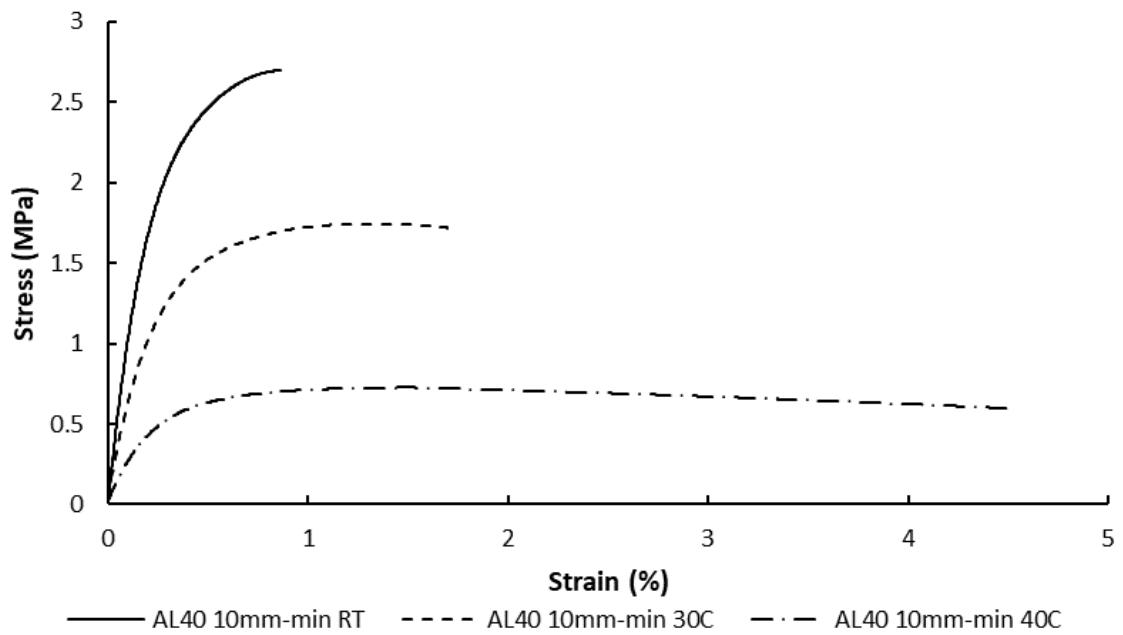
Figure 3 - 11: Impact of the temperature effects on the stress-strain curve of 40% aluminised SasolWax 0907 at a pull rate of 10 mm/min

Table 3 - 1: Comparison of room temperature tensile results for pure and aluminised fuel samples

Material	Pull rate (mm/min)	Temperature (°C)	σ UTS (MPa)	σ StdDev UTS	ε UTS (%)	ε StdDev UTS	E (MPa)	No. tests
PW00	1	23	1.78	0.07	1.05	0.24	512	5
PW00	10	23	2.27	0.1	0.86	0.12	678	5
PW00	100	23	2.97	0.32	0.8	0.22	781	5
AL40	1	23	2.02	0.088	1.01	0.28	1025	5
AL40	10	23	2.71	0.064	0.82	0.094	1162	5
AL40	100	23	3.30	0.15	0.68	0.12	1282	5

Table 3 - 2: Comparison of elevated temperature tensile results for pure and aluminised fuel samples

Material	Speed (mm/min)	Temp (°C)	σ UTS (MPa)	σ StdDev UTS	ε UTS (%)	ε StdDev UTS	σ Failure (MPa)	σ StdDev Failure	ε Failure (%)	ε StdDev Failure	E (MPa)
PW00	1	30	1.07	0.04	1.86	0.16	1.03	0.05	2.6	0.81	308
PW00	1	40	0.57	0.008	1.59	0.31	0.51	0.02	4.2	1.24	156
PW00	10	30	1.43	0.04	1.56	0.26	1.37	0.07	2.43	1.3	368
PW00	10	40	0.64	0.03	1.51	0.44	0.55	0.025	4.17	0.46	189
AL40	1	30	1.24	0.038	1.28	0.15	1.14	0.088	2.45	0.611	583
AL40	1	40	0.51	0.04	2.3	0.36	0.41	0.042	7.06	1.64	171
AL40	10	30	1.75	0.059	1.29	0.18	1.7	0.064	1.73	0.36	677
AL40	10	40	0.74	0.042	1.42	0.182	0.58	0.044	4.55	0.82	272

3.5.2 Compression testing

The compression testing was conducted at room temperature and at compression rates of 1 and 10 mm/min for both the pure and aluminised fuel samples. As expected for a compression test, the ultimate compressive strength (UCS) is higher than the UTS of the same material at the same pull rates. These results are presented in and in Figure 3 - 12 and in Table 3 - 3. The compressive modulus of elasticity, however, is lower than the associated tensile property. This indicates the material's reduced resistance to deformation under compression compared to tension. 5 samples cast from the same batch of wax were tested for each load case.
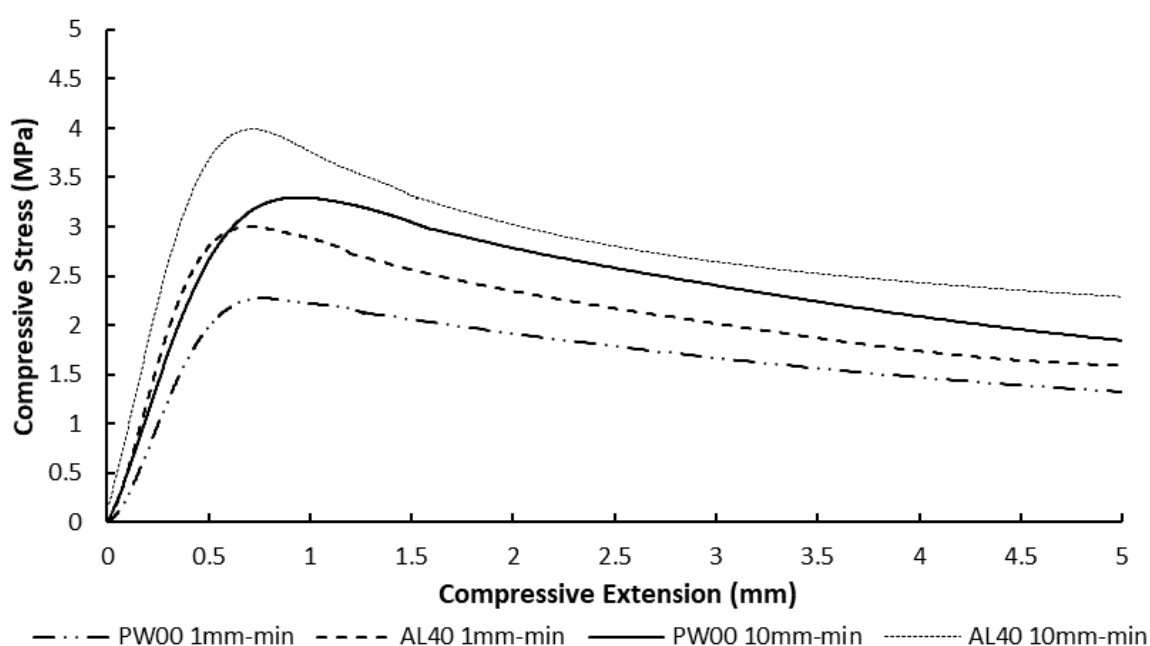
Figure 3 - 12: Impact of the strain rate effects on the compressive strength of 40% aluminised and pure SasolWax 0907

Table 3 - 3: Comparison of compression stress results for pure and aluminised fuel samples

Material	Pull-rate (mm/min)	Temperature (°C)	σ UCS (MPa)	σ StdDev UCS	ε UCS (%)	ε StdDev UCS	E (MPa)	No. Tests
PW00	1	23	2.36	0.075	0.81	0.086	483	5
PW00	10	23	3.34	0.433	1.01	0.11	547	5
AL40	1	23	3.11	0.29	0.75	0.02	700	5
AL40	10	23	4.03	0.45	0.71	0.09	882	5

The deformation of the material under compression is evident throughout the load application. The material begins its deformation by bulging out, with cracks forming along the base region. After a short period of time, the material shears at an angle to the applied force and fails, similar to what would be expected during a brittle failure. A series of photographs of the compression tests on both the pure and aluminised fuel samples can be seen in Figure 13. The photographs show the initial deformation, the formation of the angled cracks, and finally the complete failure of the material. The failure point is where the compression stress-strain curve reached its maximum. Thereafter, the material proceeds to crush beyond failure, however, beyond the point of UCS, the results are of no use.

In general terms, the overall structural behaviour of the wax was as expected for a microcrystalline paraffin wax. Distinct temperature and strain rate dependence is evident in the above tests. An important observation is the dramatic deterioration in structural properties with such a small increase in temperature. This generates concern with regard to the combustion temperatures encountered with hybrid motors. Although the fast-acting shedding of the liquid layer does reduce the level of thermal penetration, it should still be investigated experimentally as a next step.

Results presented by Ryu et al. (Ryu *et al.*, 2016) for varying percentages of aluminium at room temperature and 5 mm/min pull rate correlates well with the results presented in this paper. This is particularly evident in the tensile test, where the UTS of paraffin wax was found to be 2.118 MPa, while in this set of test data it is 2.27 MPa. The compression tests conducted by Ryu et al. (Ryu *et al.*, 2016) made use of different specimen dimensions. These results were also quite similar for the pure wax, but with a larger discrepancy for the aluminised fuel. The average UCS determined by Ryu et al. (Ryu *et al.*, 2016) for pure paraffin wax was 3.503 MPa, while for this study it was only 3.34 MPa.

Kobald et al. (Kobald *et al.*, 2014) also investigated the thermal effects on the structural performance of paraffin wax, who conducted tests at temperatures of 15°C, 25°C and 30°C. These results were on a different grade of paraffin wax which resulted in a significant difference in elongation before failure. An in-depth review on all existing structural tests on paraffin wax hybrid fuels has been conducted by Veale et al. (Veale *et al.*, 2017) as a prelude to this research.

What can be deduced from this accumulation of data is that the paraffin wax reacted similarly in that at elevated temperatures the UTS decreases and the elongation increases significantly.
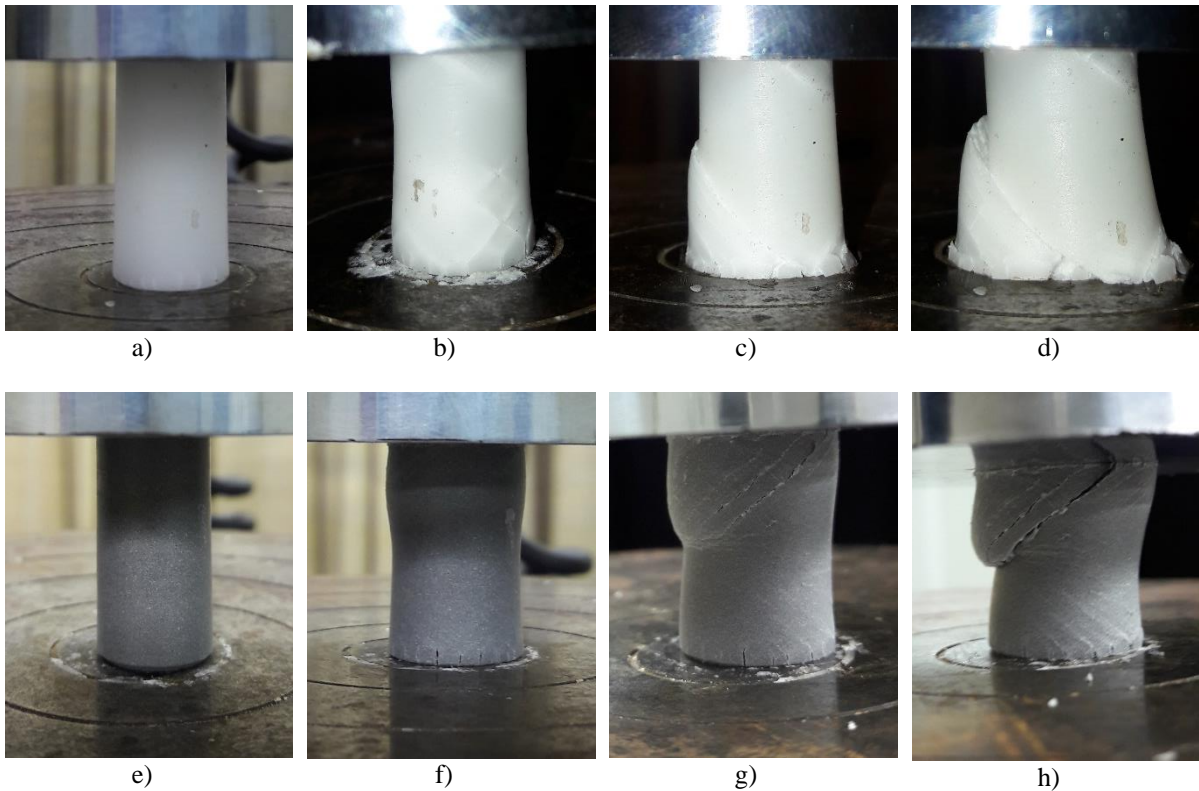
Figure 3 - 13: The process of compression failure for paraffin wax and aluminised fuel samples. a) PW00 initial mounting, b) PW00 application of load, c) PW00 nearing failure, d) PW00 failure point, e) AL40 initial mounting, f) AL40 application of load, g) AL40 nearing failure, h) AL40 failure point.

3.6 Conclusion

The data presented in this research detail some important structural properties of paraffin wax and aluminised paraffin wax that should be considered prior to use in any large-scale hybrid motor. The material itself is very susceptible to rapid load application and thermal effects. This should be considered for launches in areas with high ambient temperatures. Additionally, with combustion temperatures reaching 2000-3000 K, the thermal propagation into the grains should be considered, especially for long-duration burns. It is particularly important to experimentally determine the relationship between regression rate and thermal penetration into the grain to determine what level of fuel softening occurs throughout the burn.

The results presented show a strong strain rate dependency of the material which is an important aspect when considering ignition pressure and high inertial loads. The UTS increases by 60-70% between a pull rate of 1 and 100 mm/min for both the pure and aluminised samples at room temperature. The strain rate effect is not as evident at elevated temperatures, due to the thermal softening of the material. The results from the elevated temperature tests show a UTS drop of 65 – 75% between temperatures of 23°C and 40°C for the pure and aluminised samples, while the strain increased significantly.

The results obtained from these set of tests are to be utilised for a dynamic analysis of a fuel grain considering actual launch and thermal considerations. This is a standard analysis conducted on solid propellant grains due to the inherent danger associated with grain cracking. Although a failure in a hybrid grain may not have as catastrophic an impact, any failure should be avoided. Full material characterisation followed by computational modelling and full-scale experimental testing should be the next steps in determining the structural feasibility of these fuels.

CHAPTER 4: EXPLICIT MODELLING OF THE IGNITION TRANSIENT STRUCTURAL RESPONSE OF A PARAFFIN WAX HYBRID ROCKET MOTOR FUEL GRAIN

4.1 Abstract

Paraffin wax has been identified as a hybrid rocket motor fuel which offers enhanced regression rates and improved combustion performance. While various investigations into the performance of this class of fuels are being conducted around the world, the consideration of its structural performance is often overlooked. The grain geometry and design chamber pressure are often defined early on in the motor design process, and without adequate verification. The research presented here establishes a simplified, yet accurate method of defining the structural performance of a paraffin wax hybrid fuel grain to be introduced early in the design phase of a motor. The use of the Johnson-Cook material model has been verified to work within the 'low speed' ignition range experienced in paraffin wax/N2O hybrid motors, and therefore is used to predict failure in a variety of motors designed and tested by our group. The resultant stress profiles within the grains indicate that the grain outer- to inner-diameter (OD/ID) ratio as well as the OD itself play an important role in the grain's ability to withstand the loading conditions applied. Additionally, the grain structural properties and the stiffness of the combustion chamber affect the severity of the internal stresses in the grain. The feasibility of large-scale pure paraffin wax grains without structural enhancement additives is thus found to be poor. Fuel additives should thus be considered for structural enhancement.

Keywords: Hybrid rocket; paraffin wax; mechanical properties, structural integrity

4.2 Introduction

The structural performance of a solid fuel grain is a necessary factor to consider for the propulsion of any solid rocket motor. In the past, solid rocket fuel structural performance has been investigated to reduce any risk of in-flight failure due to the development of cracks from flight loading and fuel storage (Kelley, 1969; Fitzgerals and Hufferd, 1971; Douglass *et al.*, 1973; Ho, 2010). A simple crack in the body of a solid rocket fuel is considered a structural failure due to the risk of exceeding the design grain surface exposure. The rapid exposure of

combustible surface area, in this case, where the fuel and oxidiser are premixed, can result in a catastrophic failure of the vehicle due to over pressurisation (Gondouin, 1993). The boundary layer combustion mechanism of hybrid rocket motors means that there is less risk associated with crack formation in terms of vehicle loss. However, there are still concerns attributed to fuel loss, which can result in an incomplete mission if fuel fragments were to dissociate from the grain body. Additionally, if the fuel fragments were to block the nozzle, over pressurisation of the combustion chamber may occur, and the vehicle may be lost. While a few small surface cracks may not cause failure, many small cracks or few large cracks can cause a potential failure situation in hybrid fuel grains (Sutton and Biblarz, 2001).

The propellant combination of interest in this research is SASOL 0907 paraffin wax as fuel with nitrous oxide as the oxidiser. This propellant combination is utilised as the primary propulsion mechanism for the University of KwaZulu-Natal's Phoenix Hybrid Sounding Rocket Program (Genevieve *et al.*, 2012, 2015; Leverone *et al.*, 2013, 2019; Balmogim *et al.*, 2015). Additionally, the Phoenix program plans to utilise aluminium powder additives in the paraffin wax at varying percentages to improve the performance and density specific impulse of the motors (Maharaj *et al.*, 2016). Paraffin wax has been selected as the base fuel due to the high regression rate when compared to classical hybrid fuels (Karabeyoglu, Cantwell and Altman, 2001). Nitrous oxide is used as the oxidiser due to the less stringent safety and handling requirements when compared to oxygen, as well as its self-pressurisation nature. Energetic additives such as aluminium add some performance advantages such as higher combustion efficiencies and better heat transfer, while they may also result in excessive nozzle erosion (Calabro *et al.*, 2007; Cantwell, Karabeyoglu and Altman, 2010). The effects of aluminium powders on the combustion performance have shown a dependency on the particle size (Risha *et al.*, 2007). Numerous performance tests have been conducted on various aluminium doped grains, and have generally shown an increase in regression rate while increasing the density specific impulse of the vehicle. When considering aluminium as an additive, it is primarily viewed as a performance enhancer, while little attention is given to its effect on the structural performance of the fuel grains, in which it makes the wax more brittle (Veale *et al.*, 2018). A comprehensive review between existing combustion performance testing and mechanical testing conducted by various researchers was conducted and presented in (Veale *et al.*, 2017).

List of Symbols

A	Quasi-static yield stress
a	Grain inner diameter
B	Hardening constant
b	Grain outer diameter
C	Material speed of sound
c	Strain rate dependency constant
D_c	Critical damage
D_1	Strain at initiation of necking
$D_{2,3}$	Triaxility constant
D_4	Strain rate dependency failure constant
D_5	Temperature dependency failure constant
E	Modulus of elasticity
ε_f	Fracture strain
ε_p	Accumulated plastic strain
$\varepsilon_{p,d}$	Damage threshold
$\dot{\varepsilon}_o$	Reference strain rate
$\dot{\varepsilon}_p$	Plastic strain rate
$\dot{\varepsilon}^*$	Dimensionless strain rate
l	Length of element
m	Thermal softening constant
n	Hardening exponent
P_o	Reaction pressure
ρ	Density
σ_{eq}	Equivalent stress
σ_r	Radial stress
σ_t	Tangential Stress
σ^*	Triaxility
T	Working temperature
T_m	Melting temperature
T_o	Room temperature
*T**	Homologous temperature
Δt	Time step

4.3 Structural considerations

Throughout the life cycle of a motor, it will undergo numerous loads which can be split into two categories. These are the specified loads and induced loads (Fitzgerals and Hufferd, 1971). These loads are fixed by the mission requirements, and the propellant properties, respectively (Simo, 1987; Kumar and Rao, 2014). Specified loads are caused by effects such as environmental temperature, gravity, vibration, shock, transportation and handling, as well as ageing conditions and humidity (Fitzgerals and Hufferd, 1971). Induced loads are influenced by the propellant selection, manufacturing methods, cure shrinkage, chamber pressure, and the combined loads during a flight (Fitzgerals and Hufferd, 1971).

The loading conditions which are considered in the present research are the pressurisation loads. The chamber pressurisation is a result of the combustion process within the combustion chamber of the motor. This begins at the ignition of the motor and terminates at the end of the burn sequence, with compressive hydrostatic loading on the grain surface, as well as tensile hoop stresses (Fitzgerals and Hufferd, 1971). Ignition pressurisation can be significantly higher than that of the mean operating pressure, and this can cause grain failure before launch, however, prolonged exposure to higher temperatures and high pressures can result in mid-flight grain failure too. Chamber pressure is generally considered a static load with a magnitude equal to that of the initial maximum pressure measured from a static firing, or a theoretically modelled prediction (Ho, 2010). Depending on the propellant combination and ignition sequence, ignition pressurisation times can vary from 0.005 to 0.5 s (Douglass *et al.*, 1973). The speed of this transient pressure load can affect the grain's structural response, and thus, strain rate dependence must be investigated during the grain material characterisation.

In general, the fuel material is stronger but more brittle at lower temperatures such as 20°C than it is at temperatures as low as 30°C (Veale *et al.*, 2018). Low-temperature firing could be a concern due to the rigidity of the propellant, residual cure stresses, and the high ignition pressures. If a fuel grain was to remain intact after the pressurisation load, any resulting flaws and cracks might fail after exposure to a temperature increase and the in-flight inertial loading. When analysing the effects of in-flight combined loads, the effect of thermal softening should be considered (Fitzgerals and Hufferd, 1971). A number of paraffin structural enhancement techniques with the use of polymer additives have been researched by various institutions (Mengu and Kumar, 2018) which generally show that these additives reduce the regression rate of the fuel, often by increasing the melt viscosity, resulting in reduced fuel entrainment. Other

research has been conducted into the effect that structural discontinuities will have on the combustion performance of a motor (Andrianov *et al.*, 2019). The preliminary analysis shows that induced cracks do not lead to immediate failure of the grain but there is a clear regression inconsistency which can lead to chamber burn through if the burn time is long enough. Innovative structural matrices embedded within the grain are also being investigated in an attempt to minimise the inclusion of regression dampening materials. Initial tests indicate a reduced regression, yet the performance and structural properties are matrix material and geometry dependant (Hill *et al.*, 2019).

Paraffin wax is considered a brittle material, which has a very low ultimate tensile strength (UTS). This will likely reduce the fuels ability to withstand the pressurisation and inertial loads, without cracking, during flight. The structural performance of a fuel grain is dependent on a number of factors such as the size, length-to-diameter ratio and OD/ID ratio of the fuel grain. These design parameters of the fuel grain are often determined during the design phase to control the thrust, O\F ratio and mass flow rate of the motor (Karabeyoglu, Cantwell and Altman, 2001). Karabeyoglu (Karabeyoglu, 2011) has determined that the failure boundary is approached more rapidly with fuel grains with larger OD/ID ratios. In addition to the low strength of paraffin wax, the material has a low melting point and a large melting onset temperature range. This can be a problematic aspect to consider during analysis to ensure that the thermal penetration into the grain during combustion does not cause the fuel to prematurely melt or soften significantly.

Comprehensive material characterisations tests have been performed in an earlier publication of this work (Veale *et al.*, 2018). All test data used in this publication refer to this work. These tests were performed for pure paraffin wax (PW00) and paraffin wax with 40 wt% aluminium powder (PW40AL). This publication details the tensile and compression testing conducted at various strain rates and temperatures. These results show a distinct strain rate dependency of paraffin wax. Additionally, small temperature changes in the material result in a significantly weaker, more ductile material. This is a result of the long transition temperature before the material begins to melt, which initiate at temperatures as low as 30°C.

4.4 Material models

The strain-rate dependency of a material generally results in an increased yield stress at a lower strain at high strain rate. Generally, standard FEA packages make use of quasi-static material

properties when considering standard use failures, meaning that the internal forces of the material can be neglected. In the case of impact analysis, where there would be a rapid deformation of the material, such as an explosion, these internal forces significantly change the response of the material. Simulations on ignition pressurisation would be more appropriate if the strain rate dependency of the material can be accurately modelled.

Due to the low melting point, and low melting onset temperature, the thermal effects on the structural performance of paraffin wax are evident at temperatures as low as 30°C. Paraffin wax hybrid motors burn within a boundary layer formed between a melted fuel layer and the oxidiser stream. The liquid layer is constantly being stripped away throughout the burn and replenished with newly melted fuel. The thermal penetration into the fuel grain has been shown to be quite slow, considering the temperatures involved in combustion (Santi *et al.*, 2017). This is primarily due to the low thermal conductivity of the paraffin wax and the repeated formation of the insulating liquid layer. The tests conducted by Santi et al. (Santi *et al.*, 2017) were only considered for pure paraffin wax, while aluminised paraffin wax has a thermal conductivity coefficient nearing a factor of 3 higher (Veale *et al.*, 2018). While some early thermal simulations indicate that the expected thermal wave penetration into an aluminised grain is still not faster than the fuel regression, thus not causing slumping, this property should still be considered in the case of high ambient temperature launches.

The Johnson-Cook constitutive model (Johnson and Cook, 1983) was developed to determine an equivalent stress as a function of plastic strain, strain rate and temperature in metals. The use of this model is designed specifically for a range of metals but is known to have been used in some plastic applications within a verified tested range. The model is represented as follows:

$$\sigma_{eq} = \left[A + B\varepsilon_p^n\right]\left[1 + c\, ln\dot{\varepsilon}^*\right]\left[1 - T^{*m}\right] \qquad (1)$$

where *A, B, n, c*, and *m* are the empirically determined material constants, ε_p is the accumulated plastic strain, $\dot{\varepsilon}^*$ is the dimensionless strain rate and T^* is the homologous temperature.

Also,

$$\dot{\varepsilon}^* = \dot{\varepsilon}_p / \dot{\varepsilon}_0 \qquad (2)$$

$$T^* = (T - T_0)/(T_m - T_0) \qquad (3)$$

where $\dot{\varepsilon}_0$ is the user-defined reference strain rate, T is the working temperature, T_0 is the room temperature, and T_m is the melting temperature.

The five constants presented in the Johnson-Cook (J-C) equation (1) are to be determined empirically. The constant *A* is the yield stress of the material determined from a quasi-static tensile test. *B* and *n* are the hardening constants and are defined as the power fit curve of the true stress plastic strain curve after yield has occurred. The constant *c* represents the strain rate dependence of the material and *m* is the thermal softening constant.

There are several published methods to determine the constants necessary for the J-C constitutive model such as optical strain rate measurements (Stopel and Skibicki, 2016), ballistic impact (Burley *et al.*, 2018), Taylor anvil testing (M. Šlais, I. Dohnal and M. Forejt, 2012) and tensile testing (Banerjee *et al.*, 2015b; Dehgolan, Behzadi and Sola, 2016). In general, the agreement between the methods requires material testing to be conducted at both quasi-static strain-rates, high strain-rates, and elevated temperatures. The J-C model was originally developed for use on a specific range of materials such as copper, brass, iron, aluminium and steel. Often, FEA modelling for plastics makes use of a bilinear plastic material model which does not take into consideration the strain-rate and temperature dependency of the material. In certain cases, the J-C material model can be used on other materials such as polymers, with verification for each case (Louche *et al.*, 2009). To determine the J-C model constants, the true stress and strain curves from torsion and tensile tests at various strain rates and temperatures were modified with the Bridgeman correction and presented in equivalent tensile flow form. The Bridgman correction (Bridgman, 1952) is used to determine the equivalent stress of a round tensile specimen after necking occurs due to the tri-axial nature of the loading condition at that time. In the case of brittle materials, which demonstrate negligible necking, this correction is not necessary as it is a function of the necking diameter. Other researchers, such as Banerjee et al.(Banerjee *et al.*, 2014, 2015a), make use of only tensile testing to determine the constants required. This simplified approach for determining the constants is utilised in this work. The validity of this assumption will be verified through FEA modelling, as discussed later in this work.

In addition to the J-C material model, there is also the J-C failure model (Johnson and Cook, 1985). This is a modified version of the criterion proposed by Hancock and Mackenzie

(Hancock and Mackenzie, 1976) to include factors such as stress triaxiality, strain rate and temperature effects. This model defines material failure at the point where the accumulated damage (*D*) during plastic straining reaches a critical value. This is defined as follows:

$$D = \begin{cases} 0, when\ \varepsilon_p \leq \varepsilon_{p,d} \\ D_c/(\varepsilon_f - \varepsilon_{p,d}), when\ \varepsilon_p > \varepsilon_{p,d} \end{cases} \qquad (4)$$

where the fracture strain is ε_f, the damage threshold is $\varepsilon_{p,d}$ and the critical damage is D_c.

The J-C failure model define the fracture strain as:

$$\varepsilon_f = \left[D_1 + D_2{}^{D_3\sigma^*} \right] [1 + D_4 ln\dot{\varepsilon}^*][1 + D_5 T^*] \qquad (5)$$

where the D_1 is the strain at the initiation of necking for the quasi-static test, D_2 and D_3 define the variation in the failure strain in relation to the triaxiality (σ^*) of the material, D_4 is the strain rate dependent failure parameter, and D_5 defines the effect of temperature on the failure strain. For the purposes of this analysis, the triaxiality constants will be considered negligible (Hancock and Mackenzie, 1976) as the tensile testing conducted showed effectively no necking.

4.5 Determining the Johnson-Cook constants

The determination of the J-C material model constants required a range of tensile tests to be conducted at a range of strain rates and temperatures. In the case of paraffin wax, which is a brittle microcrystalline wax, the temperature range necessary for testing was quite small when compared to other materials which are typically described by the J-C material model. In the case of the quasi-static testing, the strain rate was selected where the acceleration effects on the load measuring devices were negligible, and where it was not necessary to consider the propagation of stress waves through the specimen.

The quasi-static testing was conducted at a strain rate of 2×10^{-2} s^{-1}, which was taken as the reference strain rate ($\dot{\varepsilon}_0$) for determining the other constants. The constant *A* was defined as the yield strength of the material at this reference strain-rate. In the case of paraffin wax, this is not a clearly defined point and was thus determined using a 0.1% offset yield due to the low elastic modulus and plastic strain. This low offset yield was applied due to the shape of the stress-

strain curve, and smooth transition into plastic deformation. The constants *B* and *n* were defined by the plastic region of the stress-strain curve. The stress-strain curve was trimmed to only reveal the plastic region, after the yield point. A power law trend line was fitted to these data on the basis of the least fit square approximation and the constants of the resulting equation in the form of $B\varepsilon_p^n$, were used to define the hardening constants.

The strain rate dependence constant (*c*) required testing at a variety of strain rates. In the case of this testing regime, the tests were conducted at the reference strain-rate of $2\text{x}10^{-2}\,\text{s}^{-1}$, as well as at $2\text{x}10^{-1}\,\text{s}^{-1}$ and $2\,\text{s}^{-1}$. The constant *c* was established by plotting the true stress at the yield strain for each strain rate, against $ln(\dot{\varepsilon}^*)$. The gradient of the linear fit that can be derived from these data was used to estimate the constant *c*. This plot can be seen in Figure 4 - 1.
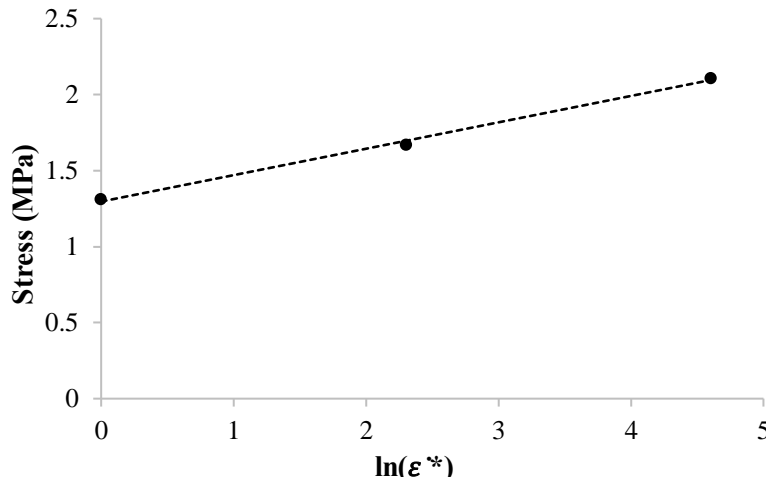
Figure 4 - 1: Definition of the J-C constant, *c*

Finally, the thermal softening constant, *m*, was determined by conducting tensile tests at a variety of elevated temperatures. Due to the low melting point of paraffin wax, these tests were only conducted at 30°C and 40°C. Equation 1 can be rearranged to give Equation 6, which shows a linear relationship between *ln(T*)* and $ln(K - \sigma_{eq})$, where *K* is the remaining constants from Equation 1. The constant *m*, is the gradient of the curve obtained when plotting $ln(K - \sigma_{eq})$ against *ln(T*)*. The stress values at a strain of 0.5% and at a strain rate of $2\text{x}10^{-1}\,\text{s}^{-1}$ for each temperature are substituted into this equation, along with the other constants which have already been defined to produce a best fit linear curve. This can be seen in Figure 4 - 2.

$$ln\big(K - \sigma_{eq}\big) = m\ln(T^*) + \ln K \qquad\qquad (6)$$
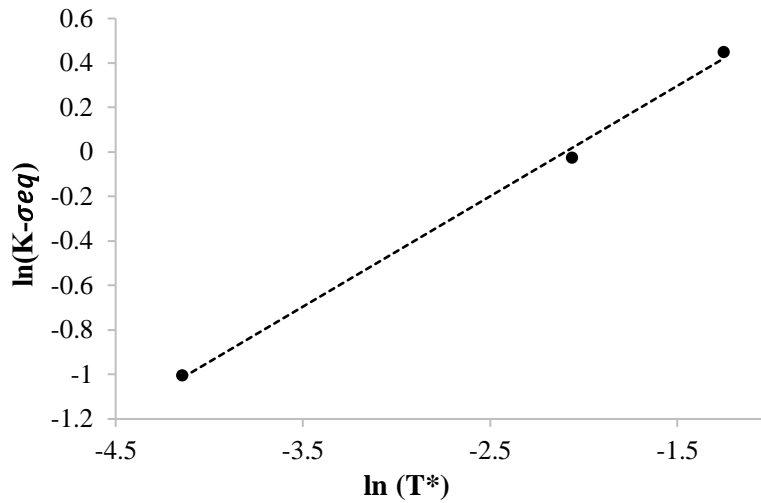
Figure 4 - 2: Definition of the J-C constant, *m*

All experimental tests used to find these material constants were conducted a minimum of 5 times with the average points utilised in this work. The experimental aspects can be found in a previous publication (Veale *et al.*, 2018). The J-C constants for both the pure and aluminised version of the paraffin wax were determined using the above method. These constants, defined in Table 4 - 1, were used as the material input criteria for the ANSYS (ANSYS, 2018b) explicit finite element model detailed later. The constants utilised in this model required verification prior to the application into the full grain. This was achieved by replicating the tensile tests in ANSYS at various temperatures and strain rates and comparing these results with the experimental results.

The constants required for the failure criteria are determined similarly to that of the material model. The constant D_1 is defined by the point in the quasi-static test where necking is initiated. In the case of paraffin wax, no necking is evident, and therefore, the plastic strain at failure is considered for this variable. For a similar reason, constants D_2 and D_3 are negligible. Constant D_4, which defines the strain-rate dependence failure, is defined by the gradient of a linear curve fitted to data for plastic strain at failure versus $ln(\dot{\varepsilon}^*)$ at different strain rates. Finally, the temperature-dependent failure is defined by the gradient of a linear curve fitted to data for plastic strain at failure versus T*. The simulated stress-strain data were validated against the experimental data, as described in section 4.6.

Table 4 - 1: Johnson-Cook constitutive model constants

Constant	PW00	PW40AL
A	1.3 MPa	1.47 MPa
B	21.3 MPa	13.169 MPa
n	0.7319	0.6344
c	0.175	0.1889
m	0.5827	0.3
D_1	0.00668	0.0078
D_2	0	0
D_3	1	1
D_4	-0.08	-0.12
D_5	18	10

4.6 Material model validation

The material constants, which were determined from the experimental data, were then validated through FEA modelling. The tensile test scenario was represented in a 1/8th symmetry model of a tensile test specimen using the ANSYS Mechanical Explicit Solver (AUTODYN). The size of the model could be reduced as a result of geometrical and boundary condition symmetry. The tensile specimen was discretised with a finer mesh in the active region (region of the extensometer), and a coarse mesh in the grip region. Due to the simplicity of the geometry, and loading, a full hex mesh could be applied to the model in order to reduce computational expense. First order hexahedral elements are susceptible to hour-glassing affects when experiencing large deflections, and thus hourglass dampening controls were required in this validation model to prevent unrealistic deformation of the elements. The hourglass dampening control utilised in this model was the Flanagan Belytschko method (Flanagan and Belytschko, 1981), with a stiffness coefficient of 0.03 and a viscous coefficient of 0.1.

Finite element models employing explicit solution regimes are computationally expensive, thus, the model duration is normally minimised, and utilised for impact or shock loading situations. In the case of modelling experimental tensile tests, the modelled duration, especially in the case of quasi-static testing, is significantly longer than what would normally be represented. The time taken to run a simulation is determined by the number, size and type of elements employed as well as the time step applied. In this case, the shockwave propagation within the material needs to be considered such that the resultant shockwave front is not able to travel further than the length of an element for each time step (ANSYS, 2018a). This ensures that the material's reaction to loading and deformation is considered. The time step size is

therefore calculated according to the ratio of the material speed of sound (C) and the length of the element (*l*), as described in equation (7) (ANSYS, 2018a).

$$\Delta t \leq \frac{l}{C} \tag{7}$$

where

$$C = \sqrt{\frac{E}{\rho}} \tag{8}$$

The meshed tensile test specimen model can be seen in Figure 4 - 3. The mesh is split into two parts, which are joined by connection nodes. These parts define the grip area and the test area between the grips. This allows the velocity load to be applied to the whole grip area. A 50 mm extensometer was used to measure the strain of the region of interest. A comparison of simulated stress-strain data and experimental data is presented in Figure 4 - 4, and provides an indication to the level of agreement between data sets.
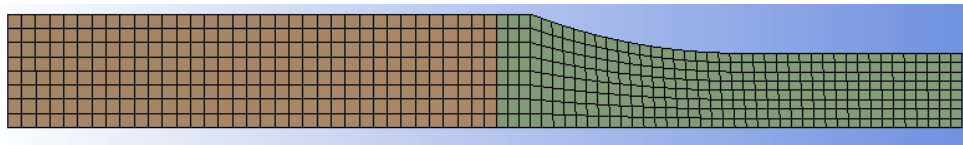
Figure 4 - 3: Meshed 1/8th model of tensile specimen

The plots in Figure 4 - 4 and Figure 4 - 5 show the difference between the empirical tensile data and the simulated data. The shapes of the stress-strain curved between the experimental and simulated results differ, with a discrepancy being particularly evident near the yield point, while the elastic modulus, plastic region, as well as the failure point, correlate closely. The reason behind this discrepancy is due to the development of the J-C model based on materials with more clearly defined transitions between the elastic and plastic regions, while the transition in paraffin wax is comparatively extended over a strain range. As described, the definition of the first three constants in the J-C constitutive model (*Eqn.1*) represent the yield point (A) , and the power law that defines the plastic region ($B\varepsilon_p^n$). The results presented indicate the plausibility of using the J-C model within the regime presented in the tensile tests, and may therefore be applied for the purpose of estimating the structural integrity of a paraffin wax fuel grain as the point of interest is the failure.
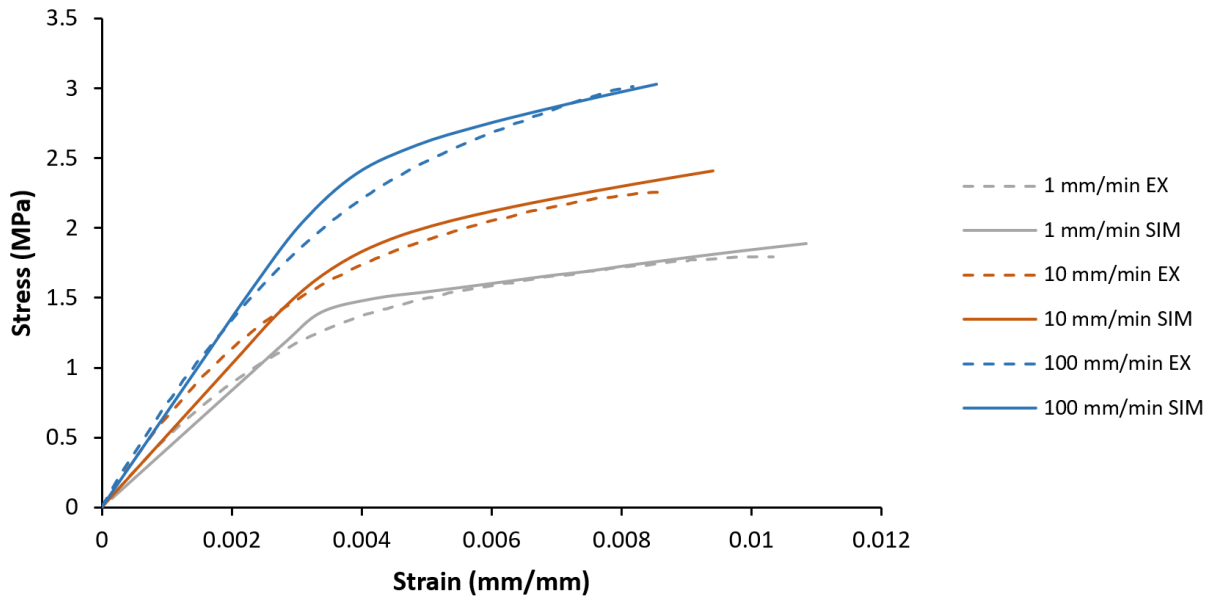
Figure 4 - 4: Graph of experimental (EX) vs. simulated (SIM) tensile tests at room temperature for pure wax
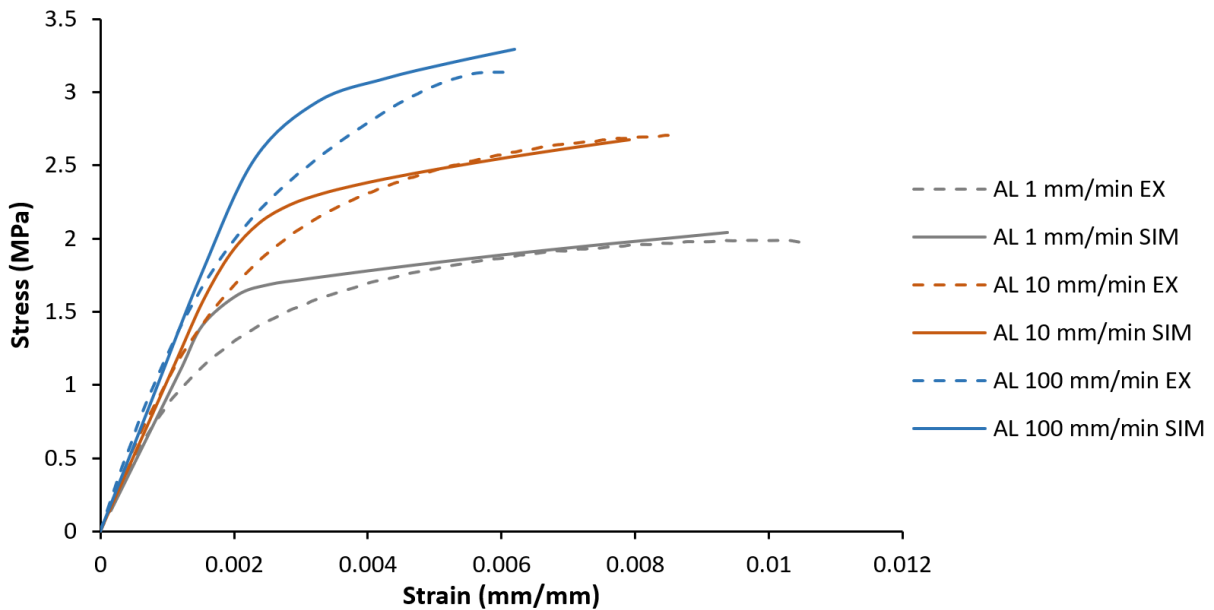
Figure 4 - 5: Graph of experimental (EX) vs simulated (SIM) tensile tests at room temperature for 40% aluminised wax

4.7 Fuel grain geometry

Design and test data of rocket motors is necessary to evaluate the use of the defined model parameters, and thus the authors based such inputs on design characteristics associated with sounding rockets of the University of KwaZulu-Natal's Phoenix Hybrid Sounding Rocket Program (Genevieve *et al.*, 2012, 2015; Leverone *et al.*, 2013, 2019; Balmogim *et al.*, 2015). These vehicles are at varying stages of development and are designed with a large variety of desired apogees and research outcomes. The primary propellant combinations for each of these vehicles are paraffin wax and nitrous oxide, while some make use of fuels containing aluminium additives. The vehicles considered for this analysis include the P-1A, a 10 km design apogee sounding rocket, the P-2A and the P-2A II, a 100 km design apogee sounding rocket, and the P-1B, a 15 km apogee design sounding rocket. The P-1A's pure wax hybrid rocket motor has been both static-fire tested, and flight tested. The P-1B's pure wax motor has been static-fire tested, and the P-2A and P-2A II motors remain as paper designs. The varying sizes of these vehicle designs offer a decent variety of loading conditions and resultant internal stresses to view the structural response of the material utilising the J-C material model. The geometrical properties of the above-mentioned vehicles can be seen in Table 4 - 2. The various geometrical and performance properties of these vehicles were determined using the internally developed Hybrid Rocket Performance Simulator (HYROPS). More information on the design process and the use of HYROPS can be found in the references (Leverone *et al.*, 2013; Balmogim *et al.*, 2015; Genevieve *et al.*, 2015).

Table 4 - 2: Phoenix Rocket fuel grain design properties

|	Composition	P-2A Pure Wax	P-2A II 40% Alu	P-1A Pure Wax	P-1B Pure Wax
Fuel grain	Outer Diameter (m)	0.365	0.365	0.151	0.148
	Port diameter (m)	0.254	0.254	0.069	0.06
	Length (m)	1.64	1.33	0.385	0.404
	OD/ID	1.44	1.44	2.1	2.46
Combustion Chamber	Design chamber pressure - max (bar)	42	42	40	40
	Ignition transient - modelled (s)	0.03	0.031	0.027	0.02
	Actual chamber pressure - max (bar)	-	-	33	34
	Ignition transient - actual (s)	-	-	0.3	0.66

The ratio of the outer diameter (*b*) to the inner diameter (*a*) (OD/ID ratio) has been used as a general design rule to reduce internal stresses of the grain as per Figure 4 - 6 with an understanding that the material approaches the failure boundary as the OD/ID ratio (or b/a as

depicted in the figure) increases (Majdalani, 2011). The radial distance, r/a, is the ratio of any point (r) within the grain thickness to the port diameter (a). In Figure 4 - 6, the simulated stress profile within an unspecified grain geometry is similar to that of a thick-walled pressure vessel with an internal pressure P_i, with some reaction given by the motor casing. The stress distribution over the thickness of the grain, without a reaction from the motor casing, is graphically presented in Figure 4 - 7(a). It can be seen that the tangential (or hoop) stresses in this schematic are positive, while the radial stresses are negative, with the maximum in both cases occurring closest to the port. When comparing this result to that presented in Figure 4 - 6, it can be seen that, in some cases, the hoop stresses become compressive as a reaction to the motor casing. The extent of this reaction force (P_o) will depend greatly on the material of the fuel and combustion chamber as well as the internal pressure. When there is a large material
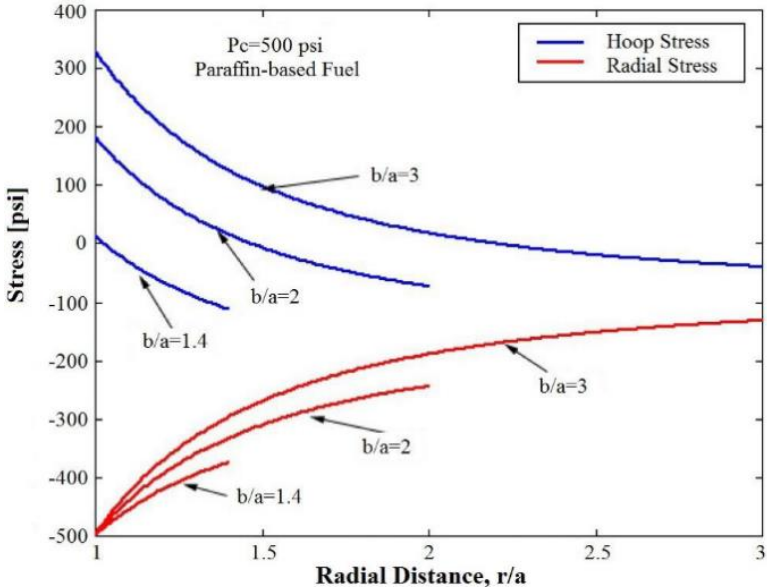
Figure 4 - 6: Fuel grain stress vs. radial distance for a single circular port grain.

(Majdalani, 2011)

stiffness difference between the grain and combustion chamber, it is estimated, based on multi-layered thick walled pressure vessels design calculations, that the stress distribution will look more similar to that presented in Figure 4 - 7(b), where both the tangential and radial stresses are compressive, while still exhibiting a similar trend. This means that a smaller OD/ID ratio may result in primarily compressive loads within the motor, reducing the likelihood of failure. It is also known that an increased fuel grain OD will further increase the maximum hoop stresses, and therefore, the OD\ID ratio should be considered in conjunction with the maximum OD of the grain.
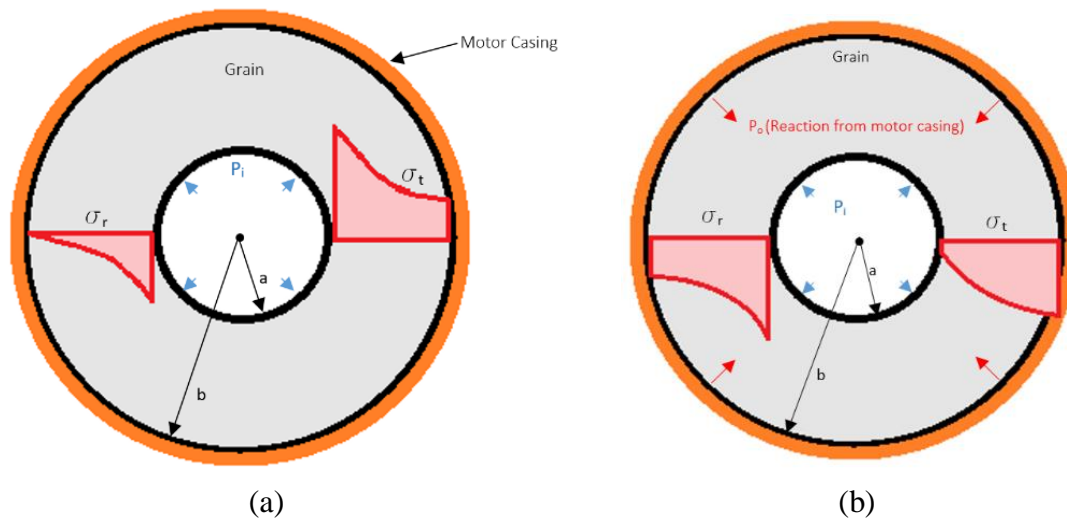
Figure 4 - 7: Radial and tangential stress profile characteristics through the grain thickness without (a) and with (b) reaction from motor casing

4.8 Model preparation

The simulations considered apply the J-C material and J-C failure models onto the paraffin wax fuel grain encased in an aluminium combustion chamber. The use of the J-C model was verified to account for the non-linear properties and strain-rate dependence of paraffin wax within the tested range. The modelling regimes, at this stage, only consider the ignition transient pressure loading, which in effect, allows the thermal effects, regression of the grain and the inertial loads to be neglected.

The motors listed above were modelled as full bodies, with only the grain, post- and pre-combustion chambers, and the motor casing present. An explicit model implemented in ANSYS Explicit (AUTODYN) was utilised due to the software's ability to model material responses to time dependant, high impact loads over very short time frames. In all the cases above, the combustion chamber was longer than the grain, as it would be in reality. The pre- and post-combustion chambers were included as their influence on the grain would need to be considered. The thermal liner was removed from the model at this early stage of the modelling regime, as the complex nature of composite materials would affect the interpretation and understanding of the grain response. It should, however, be included for any quantitative structural modelling after adequate material properties are obtained.

The fore-end of the motor housing was fully constrained in all degrees of freedom, while the aft-end was allowed freedom in the axial direction. This allows the chamber length to expand and contract axially, as it would be able to in reality, while restraining the ends in the radial direction due to the stiff bulkheads. The fuel grain and pre- and post-combustion chambers were set to move freely within the motor housing, however not able to pass the axial limit of the combustion chamber. This is a representative limit enforced by the bulkheads on either side of the motor. This constraint was applied as the parts are typically loosely fitted within the combustion chamber during manufacture and assembly. Of course, this constraint is based on the manufacturing method applied in these specific motors and may vary depending on the manufacturing and assembly methods used in other designs. An effective pressure load was applied as a step-wise, time dependent load to all internal surfaces of the combustion chamber. The pressure data applied to the model was determined from pressure transducers placed at the fore-end of the motor during experimental hot fire testing as well as the average chamber pressure modelled from HYROPS. The application of a constant pressure profile is an over simplification of the complex pressure distribution within an igniting hybrid rocket motor. The simplification allows us to analyse the resultant pressure profile and application of the J-C models before applying complexity. Body interactions between the grain, pre- and post-combustion chambers and the motor housing were activated to ensure that the varying material deformation and reaction forces were adequately accounted for. The load application was similar to that presented by Hsiao (Hsiao, 2013) in his work concerning solid propellant grains under ignition pressurisation.

A hex mesh, with mapped surfaces, was applied to all parts for computational simplicity, which means that hourglass dampening, similar to that described for the tensile test models, needed to be applied. Mesh size independency and quality were verified for each model before final simulation results were documented. A portion of the mesh used for the P-1A simulation can be seen in Figure 4 - 8. A variety of scenarios were simulated for each motor depending on what pressure data was available for each motor. These scenarios included actual pressure data from available hot-fire tests, the modelled pressure data based on the HYROPS software estimations (including an estimated pressure spike), and a reduced pressure profile where the chamber pressure does not exceed the design pressure (excluding the pressure spike). All pressure profiles are available in references (Genevieve *et al.*, 2012, 2015; Leverone *et al.*, 2013, 2019; Balmogim *et al.*, 2015). It is important to note that the pressure profiles and start-

up transients greatly affect the ability of paraffin wax fuel grains to withstand the loads applied, as the material is noticeably strain-rate dependent.
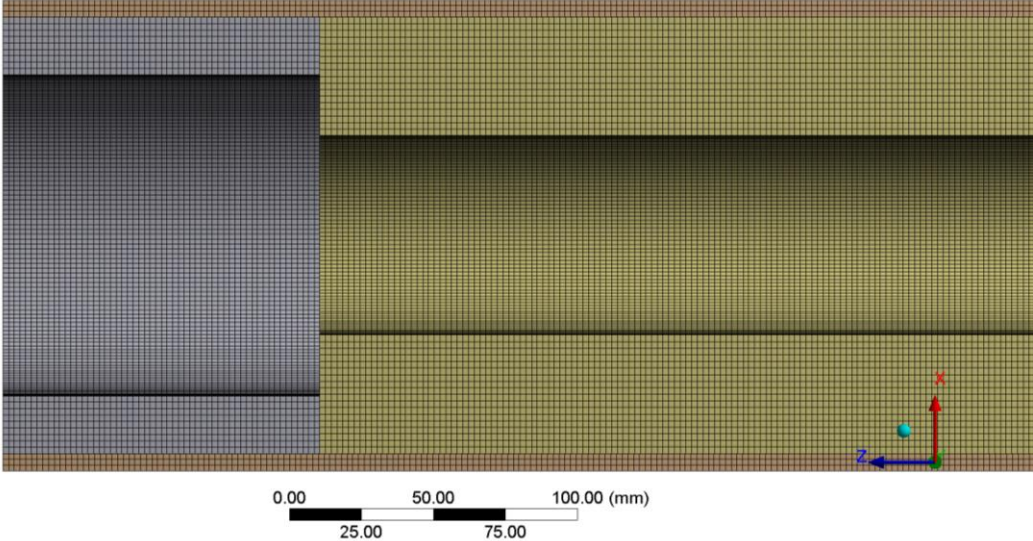
Figure 4 - 8: 4mm HEX mesh throughout P-1A motor

4.9 Case study

Two sets of analyses were considered in this study. The primary analyses considered the existing Phoenix sounding rocket motors and their susceptibility to failure given their modelled, and if available, tested ignition pressure profiles. The vast difference in the theoretically predicted and experimentally measured pressure profiles, as well as the difference in material response between the pure and aluminised waxes, affected the structural response of each grain.

Table 4 - 3 shows a summary of grain failure predictions in the respective simulations based on the J-C failure model. Due to the method of load application, if failure of the surface was to occur, and the subsequent elements began to erode, the loading profile will no longer be applied as intended, and thus the result will be at the point where failure occurs. This means that the simulation method utilised here can be used to predict if failure was to occur, but not its extent. Having said this, the prediction of failure initiation is an important exercise, which can lay the foundation for the development of a computationally intensive explosive model to more completely model the expected pressure application. In addition, it should be noted that based on the results discussed below, the maximum strain-rates for all the scenarios simulated fall

within the range of the test data, meaning that the 'slow' rate of applied load in hybrid ignition makes the use of the J-C model suitable.

Table 4 - 3: Summary of grain failures

Motor	Pressure profile	Result
P-1A	Actual – hot-fire test	Pass
	Modelled – with spike	Fail
	Modelled – without spike	Pass
P-1B	Actual – hot-fire test	Pass
	Modelled – with spike	Fail
	Modelled – without spike	Pass
P-2A	Modelled – without spike	Fail
P-2A II	Modelled – without spike	Fail

The aim of performing the secondary set of analyses was to investigate the effect that fuel grain geometry has on the stress profile within each of the motor's grains when subjected to the same pressure loading profile. This was achieved by applying the same pressure profile on each of the described grains, and by applying the same pressure profile to a grain of constant OD, but with a modified OD/ID ratio. In this case, secondary influencing bodies such as the pre- and post- combustion chambers were removed so that even pressure could be applied to all exposed grain surfaces, and to ensure there were no external influences when interpreting the stress profiles. The results obtained show the influences grain geometries have on the stress profile of the fuel grain, which would influence the design considerations at an early stage.

4.9.1 P-1A simulation

A series of images are presented in Figure 4 - 9 detailing the simulated Von Mises equivalent stress profiles within the pure wax grain of the P-1A motor, at the end of the ignition time during the hot-fire motor test. Due to the lower maximum pressure in this test, the resultant stresses are relatively low. A peak equivalent stress of 2.4 MPa is predicted near the aft end of the grain where the post-combustion chamber ring interacts with the fuel grain and casing. There was no evidence of any form of failure in this motor after this hot-fire test nor in this ignition simulation, lending validation to the proposed model.

In the modelled pressure loading scenario of the P-1A, the artificial pressure spike of 15% (47 bar) (Genevieve *et al.*, 2012) over the start-up transient of 0.027 s resulted in grain failure at 0.0243s. At this time, the material exceeded its maximum allowable stress at the effective strain

rate. The maximum equivalent stress at the moment before failure is 3.3 MPa. The simulation of the theoretical pressure transient without the artificial pressure spike did not result in grain failure but resulted in a maximum equivalent stress of 3.2 MPa. When comparing these two equivalent stresses, it can be seen that the simulation that did not exhibit failure reached an equivalent stress very close to that of the simulation that did fail. This reinforces concerns regarding the design pressure and the attributed risk associated with ignition spikes.

(a)

(b)

(c)
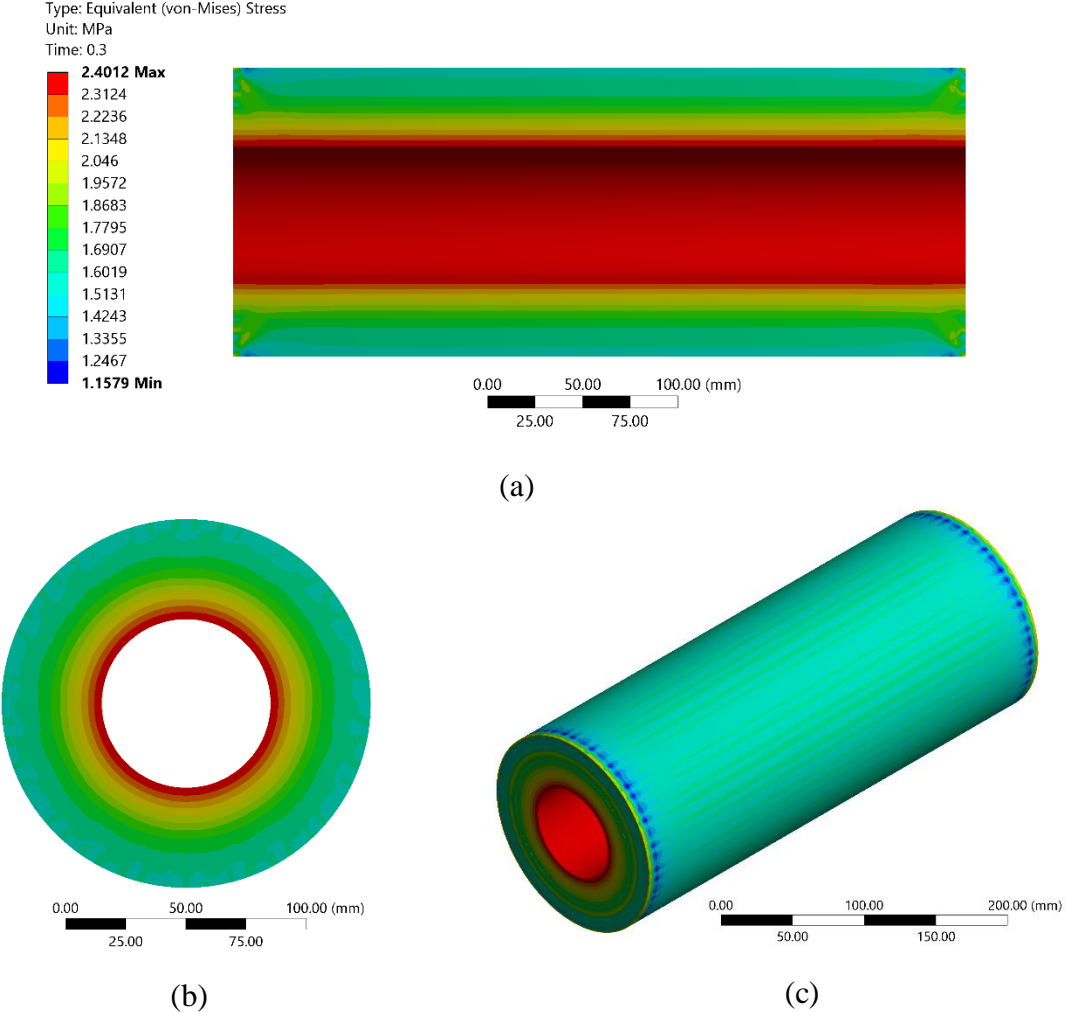
Figure 4 - 9: P-1A actual pressure profile – equivalent stress – (a) longitudinal cross section, (b) radial cross section, and (c) external isometric

As discussed, structural response predictions, after the initiation of failure occurs, are not likely to be accurate, as some nodes through which loads are transferred fail, and are removed from the active model, affecting the intended load application. While there are various ways to account for this, the purpose of this work is to determine the effectiveness of a simplified

analysis for the purposes to verifying a fuel grain design. It is, however, interesting to visualise where the grain failure is initiated. Figure 4 - 10 shows the initial predicted failure, and the propagation of the failure of the grain as determined by the J-C failure model which eliminates elements where the damage threshold is exceeded. The failure initiates at a few points at mid-length on the outer diameter of the grain and then propagates diagonally around the OD. At some time after this initial failure, as the pressure continues to increase, the grain fails on the surfaces in direct contact with the applied ignition pressure. At this time, it is apparent that the grain is failing as a direct response to the surface pressure on the port surface and the fore and aft ends.

(a)

(b)
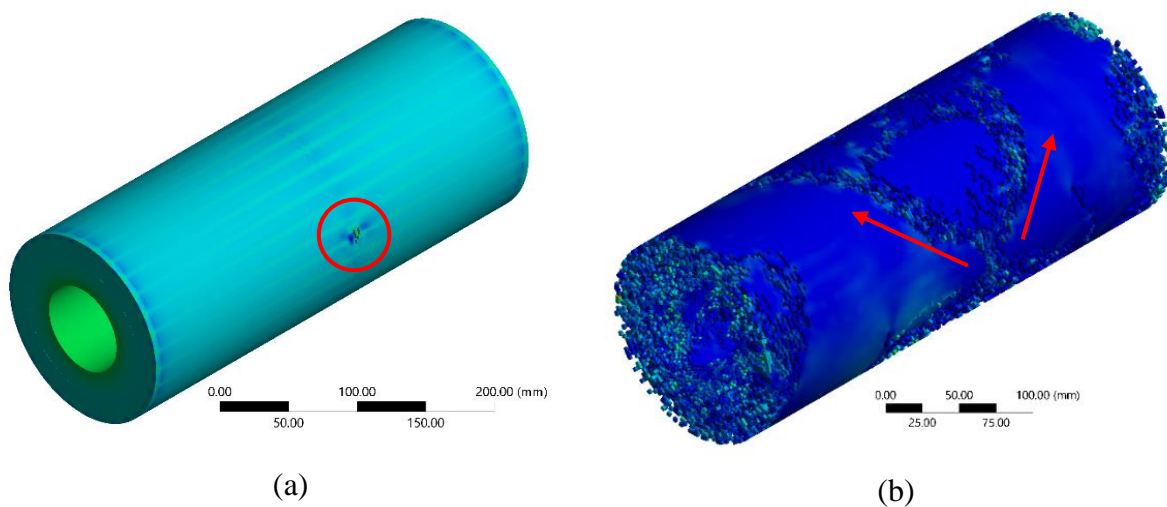
Figure 4 - 10: P-1A modelled (with peak pressure) (a) initiation of failure, (b) progression of failure

4.9.2 P-1B simulation

The P-1B motor grain was predicted to react similarly to that of the P-1A motor. This is attributed to the similar grain outer dimensions. The OD/ID ratio of the P-1B grain is only slightly more than that of the P-1A grain, which implies that this may result in a higher stress profile, however, the reduced OD will also act to reduce this stress profile slightly. Additionally, the actual hot-fire start-up transient time of the P-1B motor is more than double that of the P-1A motor, which will affect the material response due to its strain rate dependency. Figure 4 - 11 shows a cross-section of the equivalent stress profile for the P-1B grain under the actual loading conditions measured during its hot-fire test. A maximum equivalent stress of 2.5 MPa is predicted. The simulation with the pressure spike (43 bar) (Balmogim *et al.*, 2015) resulted in grain failure with a maximum equivalent stress of 3.05 MPa measured just prior to failure at

0.0165 s. When the modelled pressure scenario was simulated without the pressure spike, the grain did not fail and resulted in a maximum equivalent stress of 2.95 MPa at 0.02 s. These values are not directly comparable to the P-1A results due to the different pressure profiles.
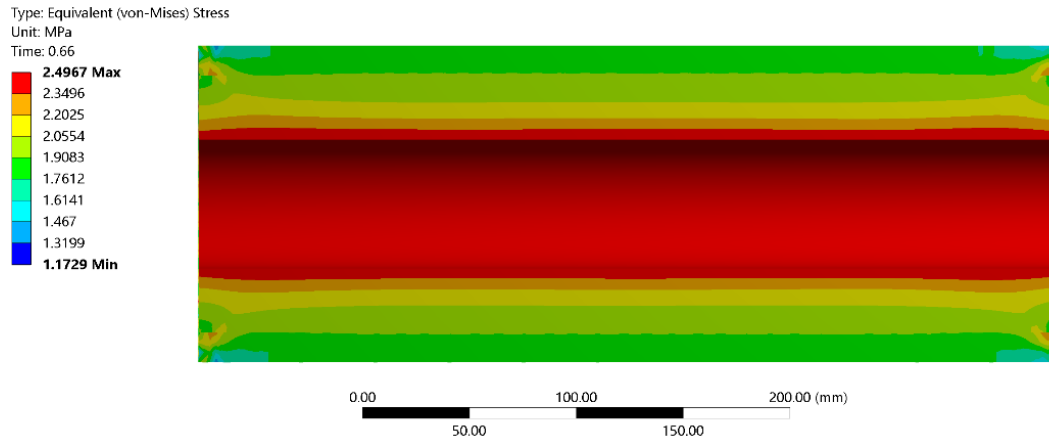
Figure 4 - 11: P-1B actual pressure profile - equivalent stress - side cross-section

4.9.3 P-2A simulation

The P-2A motor has a larger outer diameter when compared to the previous two motors. While the fuel thicknesses are similar, the tangential stresses within this motor are expected to be larger due to the increased diameter. On the other hand, however, the lower OD/ID ratio should counteract this effect. With the modelled loading condition determined during the design of the P-2A motor (Leverone *et al.*, 2013), with no ignition pressure spike, failure was predicted to occur by the associated simulation at 0.0086 s into the start-up transient.

The result presented in Figure 4 - 12 shows that the maximum equivalent stress prior to failure was predicted to be 3.38 MPa, which is significantly lower than the failure thresholds of the smaller motors. While the rate at which the load is applied does affect the vehicle's ability to withstand the stresses, the low toughness of this material indicates that the low OD/ID ratio of 1.44 is not enough to reduce the increased tangential stresses which are present due to the increase in diameter. This suggests that larger diameter grains should likely be strengthened with additives in order to resist premature failure.

Type: Equivalent (von-Mises) Stress
Unit: MPa
Time: 8.6004e-003

3.3756 Max
3.2245
3.0735
2.9224
2.7714
2.6203
2.4693
2.3182
2.1672
2.0161
1.8651
1.714
1.563
1.4119
1.2609 Min

0.00   350.00   700.00 (mm)
      175.00   525.00
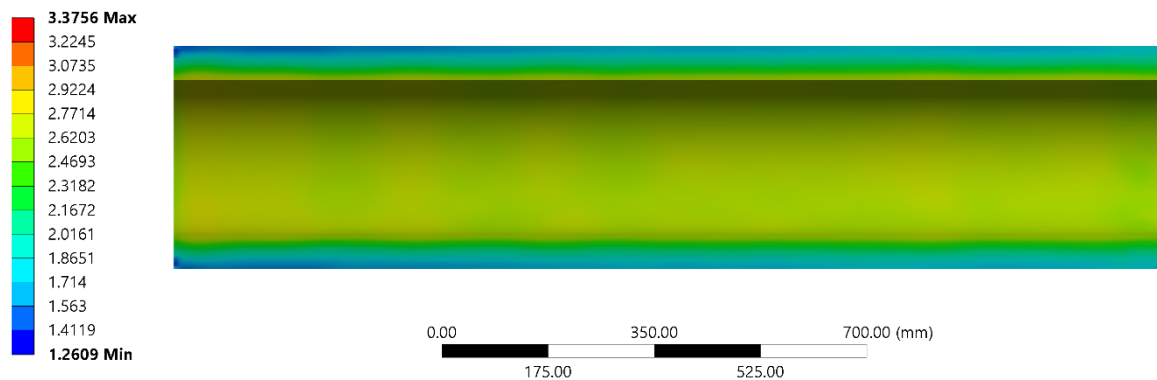
**Figure 4 - 12: P-2A modelled pressure profile (design pressure before failure) -
equivalent stress - side cross-section**

4.9.4 P-2A II simulation

The P-2A II (aluminised) motor has similar dimensions to that of the P-2A motor except that it
is shorter as a result of the increase in the density specific impulse, and lower optimal O/F ratio
of the fuel material. The material properties of the aluminised wax were considered in this
simulation. Based on the material testing described above, it is clear that the aluminised wax
considered in this study is notably more brittle than the pure wax. A simulation of the P-2A II
fuel grain's response to the modelled pressure profile, with no pressure spike, predicted the
initiation of failure at 0.00682 s at a peak equivalent stress of 2.99 MPa. The cross section of
the equivalent stress profile can be seen in Figure 4 - 13. At higher strain-rates the aluminised
wax is noticeably more brittle than the pure paraffin wax, having a higher strength with less
allowable deformation. The rapid pressure load therefore results in a rapidly increasing stress
throughout. This is evident in the image showing the point of grain failure, Figure 4 - 14, where
the wax grain is predicted to experience many internal failure initiations throughout its volume,
as opposed to the localised failure, crack propagation predicted in the pure wax grains. While
this image does not demonstrate the actual failure expected, it is interesting to note the predicted
differences between the failure profiles of pure wax and aluminized wax indicating an increased
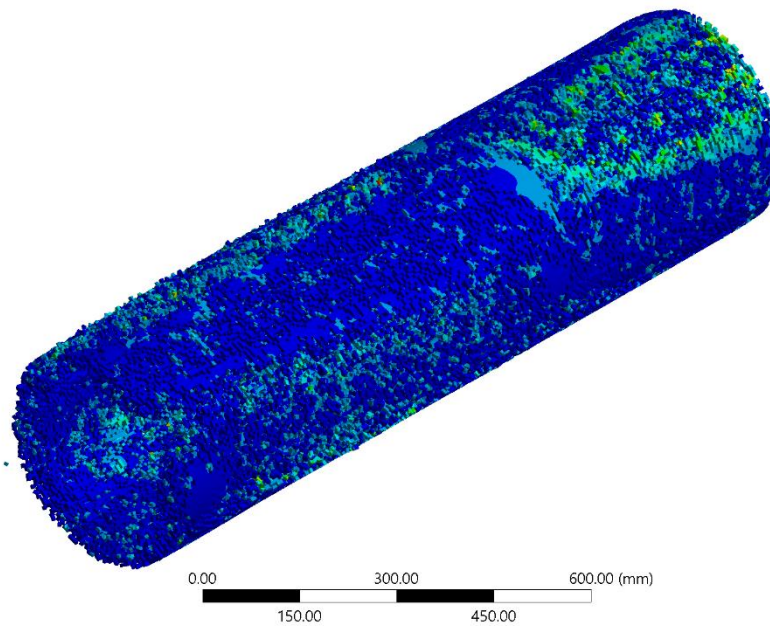brittleness of the aluminised grain.
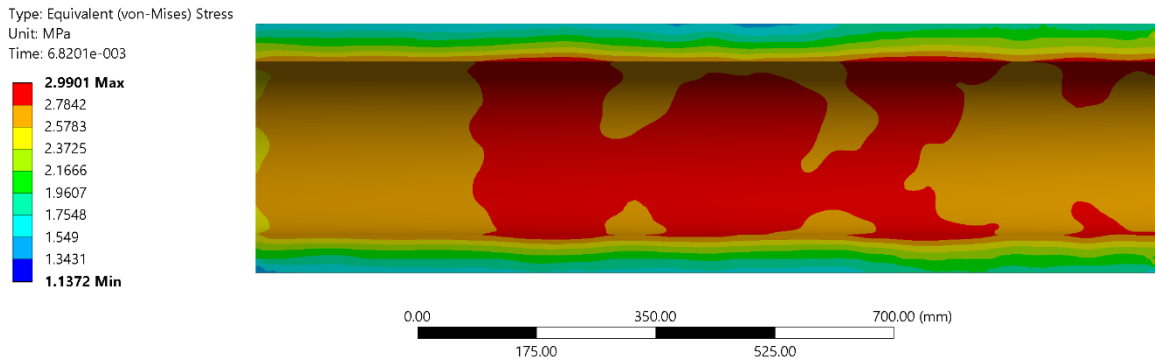
Figure 4 - 13: P-2A II modelled pressure profile (design pressure before failure) - equivalent stress - side cross-section

Figure 4 - 14: P-2A II modelled (design pressure) failure

4.9.5 Summary of results for existing motor designs

From the simulations presented above, it is difficult to define a direct correlation between loading and geometry due to the number of variables associated with failure. Table 4 - 4 lists the various peak stresses and strains for each motor at either the end of the simulation or just prior to failure. It is noted that all principal stresses are in compression. When considering the peak equivalent strains associated with each of the grains considered, it is clear that the higher

the OD/ID ratio, the higher the strain experienced at the end of the simulation. This correlation is not evident in respect of the tangential stresses which decrease as the OD/ID ratio is lowered, and increase as the OD is raised. It appears that the increasing OD has more of an effect on the stress profile changes in the OD/ID ratio.

Table 4 - 4: Summary of results

Motor	Pressure profile	Peak Equivalent stress (MPa)	Peak radial stress (MPa)	Peak tangential stress (MPa)	Peak longitudinal stress (MPa)	Peak Equivalent strain (mm/mm)
	Actual – Hot fire test	2.40	-3.22	-1.87	-4.12	0.0045
P-1A	Modelled – with spike*	3.30	-4.58	-3.15	-5.76	0.0059
	Modelled – without spike	3.18	-4.05	-2.32	-4.67	0.0050
	Actual – Hot fire test	2.50	-3.29	-1.66	-3.74	0.0053
P-1B	Modelled – with spike*	3.05	-4.08	-2.10	-4.91	0.0063
	Modelled – without spike	2.95	-3.91	-1.99	-4.72	0.0062
P-2A	Modelled – without spike*	3.38	-3.73	-1.77	-4.50	0.0047
P-2A II	Modelled – without spike*	2.99	-2.88	-1.14	-3.96	0.0027

* results taken in time step prior to failure

4.9.6 Effect of geometry on stress profile

It is clear from the above results that the radial and tangential stresses are, in fact, fully negative. However, to fully understand the estimated stress profile presented in Figure 4 - 7(b), these solutions cannot be directly utilised as numerous variables affect the result, including, primarily, the maximum pressure and the rate of loading. To have comparable results based solely on the geometry of the motor, a simplified loading scenario was simulated for each motor of different geometry by applying the same fictional loading condition to each motor. The maximum pressure simulated was 40 bar, reached at a start-up time of 0.02 s. The pre- and post-combustion chambers were removed so that the entire system was simplified and only predicted the direct response between the applied pressure and grain dimensions. However, the fore and aft end pressures were still applied. The radial and tangential stresses predicted for each scenario are plotted in Figure 4 - 15, showing the stress profiles through the thickness of each grain. A similar trend to that presented by Karabeyoglu (Karabeyoglu, 2011) was observed, except that all the predicted resultant stresses in this case are in compression. The maximum equivalent stress is predicted to be 2.72 MPa for P-1A grain, 3 MPa for the P1-B grain and 2.81MPa for the P-2A grain, while the associated maximum equivalent strain is predicted to be 0.004 mm/mm, 0.0052 mm/mm and 0.0043 mm/mm, respectively.
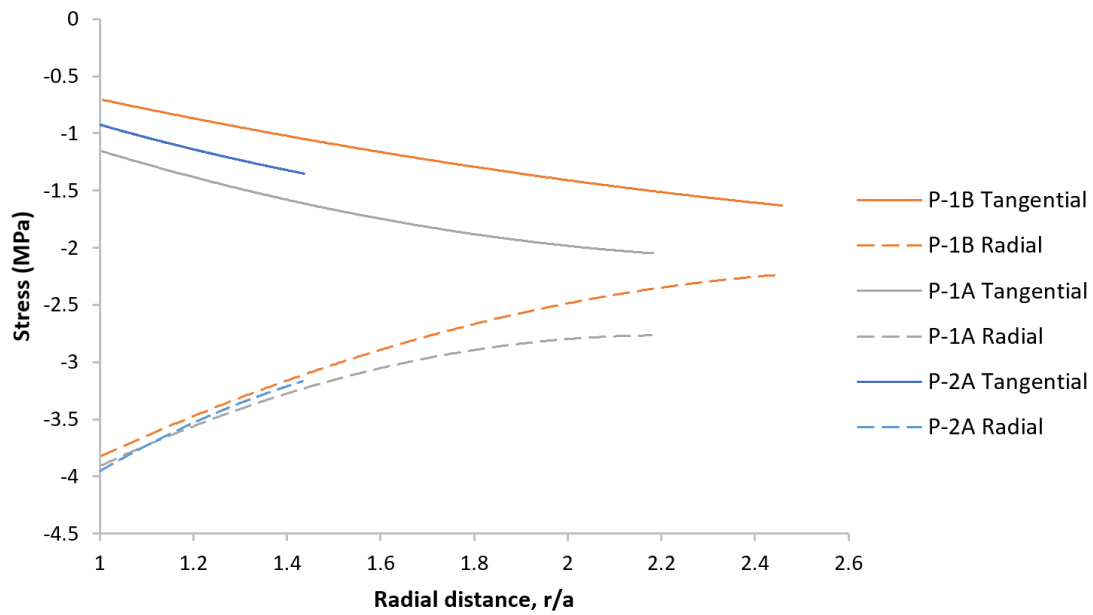
Figure 4 - 15: Tangential and radial stress vs radial distance for simulated grains

The work presented by Karabeyoglu (Karabeyoglu, 2011) in Figure 4 - 6 shows that for grains with the same OD, the grains with higher OD/ID ratio, have more positive tangential and radial stresses, while the stresses predicted in Figure 4 - 15 are not ordered in the same fashion. This is attributed to the effect of the different OD of each grain in the presented work, indicating that both the OD/ID ratio and the absolute OD have an effect on the stress profile within the fuel grain. The predicted stresses in this graph indicate that increasing outer diameter negatively affects the structural integrity of the grain design, and reducing the OD/ID ratio may not be sufficient to prevent failure.

To verify this consideration, an additional simulation was conducted on fictional versions of the P-1A fuel grain where the outer diameter remained the same, and the port diameter was modified to either reduce or increase the OD/ID ratio. The predicted tangential and radial stresses of these simulations can be seen in Figure 4 - 16. There is a distinct similarity to the result presented in Figure 4 - 6, also showing that the higher the OD/ID ratio, the closer the grain approaches failure. The change in the tangential stress profiles for each grain with varying ratios is quite large, while the effect of an increasing OD has an opposite effect.
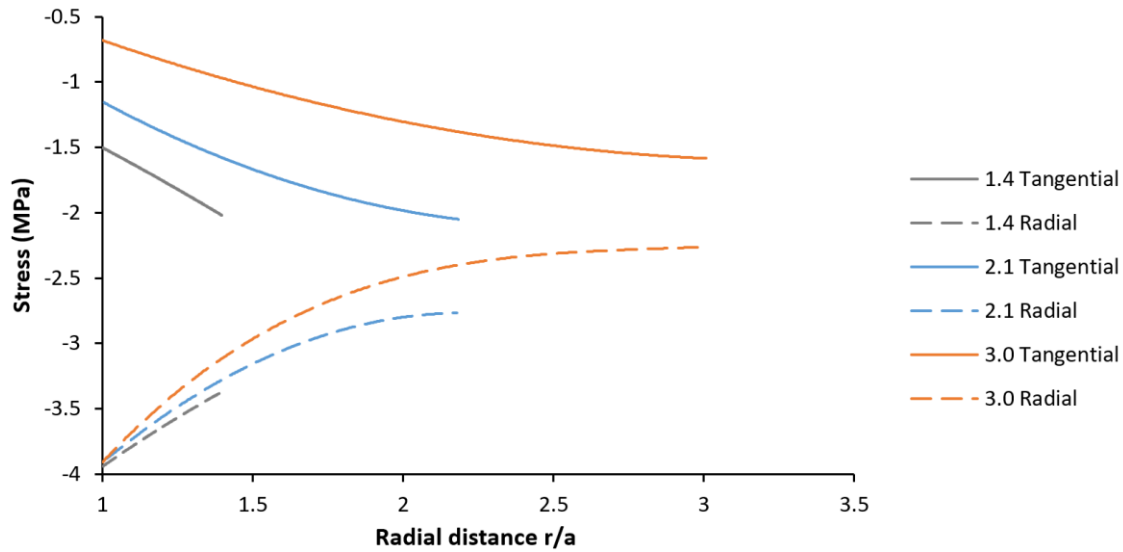
Figure 4 - 16: Tangential and radial stress vs radial distance for P-1A grain with various OD/ID ratios

4.10 Conclusion

While it is difficult to ascertain a direct correlation between the results obtained and the geometry of a motor grain given the current data set, these results do lead to the conclusion that that the J-C material and failure model and modelling method are suitable in the grain structural integrity validation during the initial design phases. Fuel grain dimensions, port size and the chamber pressure are determined through the mission objectives and design constraints. The usefulness of applying the J-C material and failure models to capture the strain rate dependency of a material that is not metallic, such as paraffin wax, is limited. However, the data and testing presented in this work show that within the range specified, these models can be utilised for determining the grain material response and in particular the failure point.

Previous fuel grain stress estimations have considered the fuel grain to be a constrained, thick-walled pressure vessel, with a different material encapsulating it and restricting its deformation, resulting in compressive stress profiles. In the models presented in this paper, the addition of a fore- and aft-end loading condition is necessary for an accurate determination of the stress profile. While it could be said that the pressure loading imposed on the fuel grain should not be applied evenly to all wetted surfaces, as the chamber pressure tends to decrease from the fore- to aft-end, this effect was neglected at this early stage in the analysis. Unsymmetrical loading would add significant complexity for a very small increase in accuracy with the interpretation

of the resultant stresses and applicability of the J-C material models at this early stage of development. This being said, the next phase of analysis and simulation should allow for this attribute to be included. When analysing the principal radial, tangential and longitudinal stresses in each design case there is no distinct response pattern, as the same loading condition is not applied to each associated geometry. These results do, however, highlight how these simulation methods offer more insight into the grain response to unintentional pressure spikes, or geometric attributes.

A hypothetical set of analyses was conducted with the same pressure profile applied to each geometry to visualise the direct effect that the geometry has on the stress profile. It is clear from these results that, while the OD/ID ratio does have an effect on the point of failure, the maximum OD of the motor is likely to have a larger effect.

The estimated tangential and radial stress profiles presented in this work show a similar trend to what would be expected in a thick-walled pressure vessel. The tangential stress profile is, however, in compression due to the constraining force imposed by the combustion chamber, which has vastly different material properties. This constraining force will depend on the material and geometric characteristics of the combustion chamber and any thermal liner, if present.

The results presented here aim to validate a procedure for determining the structural response of paraffin wax hybrid rocket motor fuel grains by means of simulations utilising the J-C material and failure models within a verified range of testing. While it is impossible to determine the validity of each grain simulation without extensive testing, the implication from the stress profile shows the plausibility of utilising the J-C models for more grain analyses. Full validation of these results can only be achieved with extensive motor testing, which is beyond the scope of this paper, however, it should be noted that the simulations which utilised data from actual hot-fire tests did not predict failure, and no failure was discovered after the tests. Additionally, should the presented modelling methods be utilized, not only for the initial design stages but additionally for the final design verification, the ignition pressure profile should be applied with an expanding gas model or explosive model to more realistically apply the loads inside the combustion chamber after failure occurs. This will allow the pressure profile to be applied to the exposed grain surface independent of surface failure, and where complex pressure gradients throughout the grain length can be applied more realistically. Further studies into this

topic should tackle the material characterisation of a wider range of mechanically strengthened paraffin wax grains, and the improvements in geometrical properties that can be obtained with these structural enhancements with their associated effects on rocket motor performance.

CHAPTER 5: CONCLUSIONS AND RECOMMENDATIONS

5.1 Original objectives

At the commencement of this research, an area of paraffin wax hybrid rocket fuel technology lacking in development was identified to be the structural performance of paraffin wax hybrid fuels. The lack of existing research and development in this area limited the functional use of these motors in a wider range of applications. In addressing this topic, a set of objectives were generated to bridge the knowledge gap in the fuel development. The primary aim of the research was the development of a fuel characterisation and FEA fuel grain modelling methodology for paraffin wax hybrid motors. The research objectives set were as follows:

1. Investigate the current paraffin wax-based hybrid rocket state-of-the-art, and identify the deficiencies associated with fuel grain structural assessment. This investigation should include structural and performance-enhancing additives and the effect these have on the performance of the motor.
2. Develop an experimental testing regime to fully characterise paraffin wax fuel as an input to a structural FEA model.
3. Verify the use of material constitutive and failure models for structural response modelling considering the specific characteristics of paraffin wax.
4. Develop a computationally efficient structural response model to represent the ignition pressurisation loading condition associated with a set of hybrid rocket motor designs.
5. Apply the findings from the above studies to propose recommendations for future work and development.

The following section details the contributions made in addressing each of these objectives.

5.2 Key contributions of the thesis

Objective 1 was addressed by means of a review article, published in Volume 141 of *Acta Astronautica,* and presented as Chapter 2 of this thesis. This review addressed the scope of current investigation methods into the use of paraffin wax as a hybrid fuel while considering performance metrics such as regression rate and the ultimate tensile strength. The review also investigated resources that included fuel additives which were hypothesised to either increase structural properties and/or regression rate.

In terms of regression rate, the review article was able to draw together a multitude of experimental testing regimes of paraffin wax-based fuels and compare them with one another. There are noticeable differences in the regression rate reported by some of the sources, implying that the experimental technique differences were important to note for each source. Specifically, there were measurably different results presented when considering annular grains versus slab grains, or with respect to the regression rate measurement technique applied. That is, if the regression rate was measured instantaneously, or as a time-averaged result at the end of the burn.

A primary influencing factor which lacked consistency across the range of the various experimental methods is the grade of paraffin wax used. The length of the carbon chain of the wax molecule has an influence on the formation of the crystal structure of the paraffin wax in solid form, as well as the melting temperature and viscosity of the melt layer. It was often difficult to ascertain what type of paraffin wax was used in each experiment, even though the results appeared to be heavily influenced by this factor. Often this attribute was overlooked, and candidate fuels were generally lumped into one category.

This review also investigated paraffin wax-based fuels with additives, which were either included for structural or performance enhancement purposes. In general, metallic additives were added for performance enhancement, while polymeric or polymer-like additives were added to improve the structural properties. The collation of these results presents a unified source of information as to the effects various additives have on the regression rate of paraffin wax. The combustion testing of doped fuel grains often do not include information on the now modified structural performance. Once again, the grade of paraffin wax and the applied testing techniques were noted as influencing factors.

The use of additives in paraffin wax, which as described, has the advantage of being a liquefying fuel within the liquid viscosity range which allows for droplet entrainment, is noted to change the viscous properties, thus affecting the aforementioned advantage. In the case of structural enhancing polymers, the viscosity of the melt layer is increased and the extent of entrainment is decreased, negatively affecting the regression performance of the fuel. The use of some metallised additives, such as aluminium, increases the performance of the fuel by raising its energy density; however, these performance advantages were reported to be heavily dependent on the grade, particle size and processing method of the aluminium used.

The review additionally assessed the relationship between fuels and regression characteristics and the corresponding structural properties. While extensive details concerning regression rate testing methodologies are provided, the provision of details concerning structural testing methodologies is limited. In most cases, the structural tests were performed only to ascertain the difference between the pure wax and the doped wax, and not specifically to determine a working set of results for any form of material characterisation.

In general, structural enhancement additives functioned as expected, by increasing structural performance. In particular, the use of aluminium additives resulted in a noticeable increase in the UTS of the material, albeit with a reduced strain. The complex loading conditions which would be present inside a hybrid motor suggest that existing results are of limited value in determining the structural feasibility of these fuels for launch applications.

The outcome of the review paper presented in Chapter 2 indicated that there is a limitation to the structural consideration of paraffin wax, with only a handful of studies having specifically considered structural properties. The review detailed the extent of existing paraffin wax combustion testing methods, however noted the lack of consistency in contributing factors such as measurement techniques and fuel grades. Additionally, it highlighted the lack of investigation into the complexity of material structural properties, such as strain-rate and temperature dependency that would usually be considered for this type of material, especially under the loading conditions expected.

Objective 2 was addressed in the paper published in Volume 151 of *Acta Astronautica* and presented as Chapter 3 of this thesis. The full characterisation of the paraffin wax-based hybrid fuels under consideration was initiated by defining the principal properties which would affect the structural performance. Experimental testing was limited to the fuel types used within the Phoenix Hybrid Sounding Rocket Program, which were the pure and 40% aluminised SASOL 0907 paraffin wax, and considered aspects such as the mechanical properties, thermal softening and the melting onset temperature of paraffin wax – the temperature at which it is assumed that the material is unable to effectively take a load.

This temperature is especially important to consider when making use of metallised additives. While paraffin wax itself is fairly insulative, the addition of metallised additives will typically

result in an enhancement of heat transfer into the wax during combustion, thus increasing the temperature of the solid wax beneath the fuel surface and potentially improving ductility. Material samples were tested using Differential Scanning Calorimetry, which identified the melting onset temperature as 40 °C. This was set as the temperature beyond which structural tests would not be performed.

The melting onset temperature identified was remarkably low, which prompted concerns about the consequences of excessive thermal penetration into the grain body during combustion, especially for metallised grains. The conductivity of the wax grains, both with and without aluminium, were tested using thermal imagining measurement techniques (TIMTower) to determine their thermal conductivity and modelled in a transient thermal analysis to determine if the thermal propagation rate exceeds the regression rate of the fuel. This was a simplified analysis, which could be considered as a worst-case scenario because the insulative liquid layer which is formed by this fuel type, was assumed not to be present. The results indicated that the fuel grains considered experience some thermal penetration but without the speed of the 40 °C thermal wave exceeding the theoretical regression rate. However, the aluminised grain was shown to have a thermal conductivity approximately three times higher than that of pure wax, resulting in the thermal wave propagation nearing the theoretical regression rate.

Structural testing in the form of tensile and compressive tests indicated that paraffin wax, in both pure and aluminised forms, shows a strong strain-rate and temperature dependency. The range of testing conducted ensured that there were both quasi-static results, and high strain-rate results. The highest strain-rate was determined by the expected ignition transient within a combustion chamber, which is defined to be relatively slow in the case of paraffin wax and nitrous oxide when compared to other combustible materials.

The outcome of these tests showed that a high strain rate is associated with a higher material UTS, but a reduction in the allowable strain. In the case of aluminised paraffin wax, the UTS was higher and the allowable strain was lower, in all cases. This implies that the addition of aluminium makes the material stronger in tension and compression, but more brittle. It is also important to note the shape of the stress-strain plots. These plots do not show a clear yield point, but rather indicate a transition over time from the elastic to plastic regions, with a general, continuously increasing stress until failure. This indicates that no necking or cross-sectional area reduction is present in the samples during testing.

Furthermore, the tests, performed at different temperatures, indicate a rapid reduction in the UTS of paraffin wax with even slight temperature increases. The material was shown to rapidly soften to the point that it is not able to effectively resist a load, although a much larger strain before failure was observed.

It is clear from the testing performed that the material presents complex failure properties well within the range of loading conditions expected within a hybrid rocket motor. Characterisation of these material properties is, therefore, necessary to accurately model the structural performance of these fuels for the desired application.

Objectives 3 and 4 were addressed in Chapter 4 of the thesis, which is presented in the form of a publication which is currently under review. Objective 3, which is aimed at determining and verifying the use of material constitutive and failure models for structural response modelling, makes up the first half of this passage of work. It would appear that the structural performance of paraffin waxes has never been analysed to the extent presented in Chapter 4, nor does it seem that structural property characterisation has been conducted in as much detailed as in Chapter 3.

This offered a unique opportunity to model and analyse the realistic structural response of a paraffin wax hybrid rocket fuel grain during motor ignition. Before any analysis could be performed, adequate material constitutive and failure models had to be identified and verified. Research into various material models which could capture the strain-rate dependency and temperature dependencies of paraffin wax led to the use of the modified Johnson-Cook material and failure models, which are able to consider both the temperature dependency and the strain-rate dependency of a material. This model is ordinarily used for metals, and some plastics, and therefore a model verification was necessary.

After the model inputs were determined from the experimental testing presented in Chapter 3, the tensile tests that generated the structural data were simulated. The modelled stress-strain curves were extracted and compared to the experimental scenarios. The resultant stress-strain curves and failure points closely matched those of the experimental tests at the various strain rates and were considered acceptable for use in the structural response modelling of a paraffin wax fuel grain during motor ignition.

Objective 4 was addressed in the second half of the publication presented in Chapter 4. This aspect of the work made use of the now verified material models to analyse a simplified structural response of fuel grains associated with existing motor designs within the Phoenix Program. This work made use of information from the design, combustion modelling and hot-fire testing of hybrid rocket motors designed within the Phoenix Hybrid Sounding Rocket Program. The variety of data sources available offered an opportunity to compare the simulation results obtained when using actual combustion data from hot-fire tests versus modelled theoretical combustion data.

There was a clear discrepancy between the simulated ignition transient and the actual ignition transient, as well as the associated peak chamber pressures. In most cases, the hot-fire test data indicated that the motors did not reach their design chamber pressures, nor did the predicted ignition chamber pressure spike occur. In the case of the modelled pressure profiles applied as the loading conditions, the motors were more susceptible to failure if the pressure spiked above the design chamber pressure. However, failure indication was also influenced by the geometry of the fuel grains.

A structural and failure analysis method was defined, where key input criteria were taken from the published work of Chapter 3. Figure 5 - 1 summarises into flow diagram form, the process followed to perform the structural response and failure analysis used for paraffin wax fuel grains. The model is defined by addressing input data such as the geometry, part interactions, loading conditions and finite element meshing properties. The material structural response requires input information from material testing data, and the definition of a material constitutive model. The work presented in this thesis made use of the Johnson-Cook material constitutive model which considers complex material response information for explicit analyses.

To further analyse the structural response of the fuel grain, a failure criteria is also included in the simulations. The input information for this includes material failure properties obtained from destructive testing. The failure properties are used to define the failure criteria. In the case of this research, the failure criteria were obtained on the basis of the Johnson-Cook failure model, which defines a damage threshold based on the loads experienced and the material properties defined. The simulated output offers insight into the subsequent grain response and potential for failure in-flight.
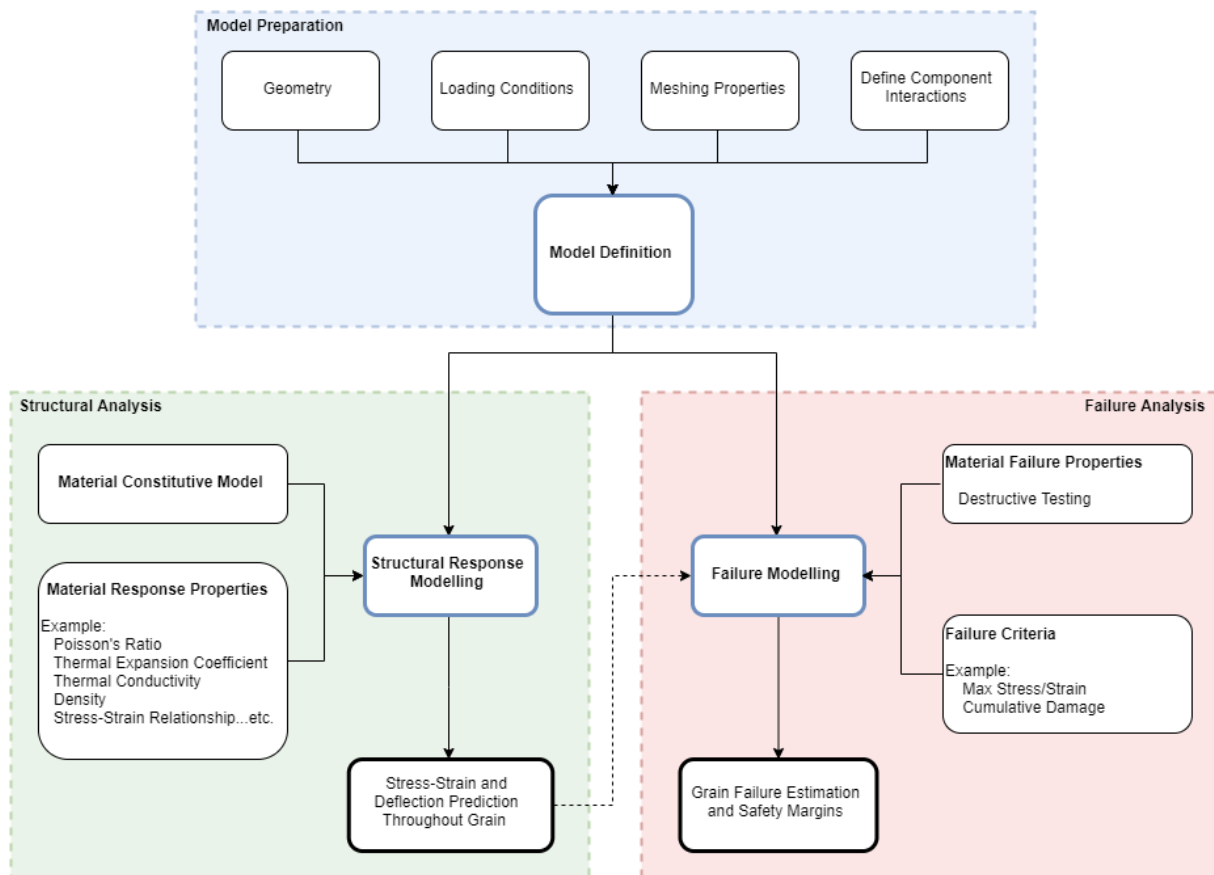
Figure 5 - 1: Process of fuel grain structural and failure analysis

The initial analysis then led to the development of a direct structural response comparison between geometric variables such as the outer diameter and the outer to inner diameter ratio for a constant pressure versus time profile. It was found that an increasing outer diameter and an increasing OD/ID ratio both have a negative effect on the grain's ability to manage the load without failure. This is as a result of the compressive radial and tangential stresses within the grain. It is also noted from the results that an increase in outer diameter has a larger effect on the potential failure than that of the OD/ID ratio. This suggests that larger grains, such as that of the Phoenix-2A sounding rocket, will likely require structural compensation in the form of additives, structural matrices or reduced chamber pressure.

5.3 Recommendations for future research

A substantial amount of experimentation and analysis is required to fully verify the structural and regression performance of a paraffin wax fuel grain in a hybrid rocket motor, some of it iterative. While the research presented here focuses on a particular range of use cases, it details

a clear path for researches to follow when considering the use of a paraffin wax-based fuel. There are limitations to the work presented, and several areas would benefit from expansion in order to derive a more conclusive structural response analysis.

The structural testing regime was developed specifically to derive the material properties required to perform the ignition transient structural response simulations. It is possible to expand the testing regime to include other material properties for specific analyses, should they be deemed important. For example, should a mission require long term grain storage or transportation, material properties relating to the slump characteristics of the material could be derived via creep testing.

The modelling work presented should be considered to be an initial assessment, on the grounds of the simplicity of the modelling regime employed. Explicit structural analyses are computationally expensive, and any additional components or more refined meshing in specific areas would significantly increase the simulation run-time. This is not feasible in the conceptualisation phase of vehicle design; however, the second phase of analysis should be considered after the broad specification of a motor geometry is frozen.

A more complex analysis should consider aspects such as the change in chamber pressure over the length of the motor, as well as the strength of bonding between the internal chamber components. These additions to the model would improve the representation of the interaction between internal components and may lead to alterations in certain design aspects, such as the inclusion of strain relief components within the motor design. This would also require a number of motor test firings to define certain working parameters, such as the chamber pressure, as well as structural bond tests between the material of bonded surfaces, if any.

The described modelling only considered an explicit modelling technique representing a short-duration transient at ignition. This was assumed to represent the worst-case loading condition scenario for a hybrid rocket motor fuel grain due to the ignition pressure spike generally anticipated in these motors. It cannot be overlooked that the in-flight loading conditions, i.e. the loading that occurs after stable combustion commences, may initiate failure in the fuel grain, and further analysis should consider this aspect of the fuel grain operation. During this modelling phase, special attention should be given to the regression of the grain as well as thermal penetration effects.

An aspect which was beyond the scope of this work, but would greatly benefit the accuracy of the modelled results would be the development of an analytical method to generate a more accurate ignition period pressure profile. In all cases where both actual and theoretical chamber pressure data are present, the theoretical pressure profile peaks at a much higher level than that of the experimental data, and in a much shorter time. This results in inaccuracies in the predictions made by the structural response model, due to its strain rate dependencies. Noting that the structural responses generally predicted failure with the theoretical models, and not with the experimental models indicates that there could be an unnecessary design rigidity applied to a motor grain in terms of failure prevention.

References

Andrianov, A. *et al.* (2019) 'Experimental Study of Severity Level of Structural Discontinuities in Paraffin Grains of Hybrid Propellant Rocket', *Acta Astronautica*, 162, pp. 256–265. doi: 10.1016/j.actaastro.2019.06.015.

ANSYS (2018a) *Academic Research Mechanical, Release 19.1, Help System, Explicit Dynamics Theory Guide. ANSYS, Inc*.

ANSYS (2018b) 'Academic Research Mechanical, Release 19.1'.

ASTM International (2014) *ASTM D 638 Standard test Method for Tensile Properties of Plastics*, *ASTM Standards*. doi: 10.1520/D0638-10.1.

ASTM International (2015) *ASTM D 695 Standard Test Method for Compressive Properties of Rigid Plastics*, *ASTM Standards*. doi: 10.1520/D0695-10.2.

Balmogim, U. *et al.* (2015) 'Preliminary Design of the Phoenix-1B Hybrid Rocket', in *51st AIAA/SAE/ASEE Joint Propulsion Conference, 27 - 29 July*. doi: doi:10.2514/6.2015-4048.

Banerjee, A. *et al.* (2014) 'An Experimental Determination of Johnson Cook Material and Failure Model Constants for Armour Steel', *Applied Mechanics and Materials*, 592–594, pp. 990–995. doi: 10.4028/www.scientific.net/AMM.592-594.990.

Banerjee, A. *et al.* (2015a) 'Determination of Johnson cook material and failure model constants and numerical modelling of Charpy impact test of armour steel', *Materials Science and Engineering A*. Elsevier, 640, pp. 200–209. doi: 10.1016/j.msea.2015.05.073.

Banerjee, A. *et al.* (2015b) 'Determination of Johnson Cook Material and Failure Model Constants and Numerical Modelling of Charpy Impact Test of Armour Steel', *Materials Science and Engineering A*. Elsevier, 640, pp. 200–209. doi: 10.1016/j.msea.2015.05.073.

Bridgman, P. W. (1952) *Studies in Large Plastic Flow and Fracture*. New York: McGraw-Hill.

Burley, M. *et al.* (2018) 'Johnson-Cook Parameter Evaluation from Ballistic Impact Data via Iterative FEM Modelling', *International Journal of Impact Engineering*. Elsevier, 112(October 2017), pp. 180–192. doi: 10.1016/j.ijimpeng.2017.10.012.

Cai, G. *et al.* (2016) 'Effect of grain port length–diameter ratio on combustion performance in hybrid rocket motors', *Acta Astronautica*. Elsevier, 128, pp. 83–90. doi: 10.1016/j.actaastro.2016.07.002.

Calabro, M. *et al.* (2007) 'Advanced Hybrid Solid Fuels', in *58th International Astronautical Congress*.

Cantwell, B. J. (2007) *AA283 Aircraft and Rocket Propulsion - Course Notes*.

Cantwell, B., Karabeyoglu, A. and Altman, D. (2010) 'Recent Advances in Hybrid Propulsion', *International Journal of Energetic Materials and Chemical Propulsion*, 4(4), pp. 305–326. doi: 10.1615/IntJEnergeticMaterialsChemProp.v9.i4.20.

Cardoso, K. P. *et al.* (2017) 'Preparation of Paraffin-Based Solid Combustible for Hybrid Propulsion Rocket Motor', *Journal of Propulsion and Power*, 33(2), pp. 448–455. doi: 10.2514/1.B36197.

Carmicino, C., Scaramuzzino, F. and Russo Sorge, A. (2014) 'Trade-off between paraffin-based and aluminium-loaded HTPB fuels to improve performance of hybrid rocket fed with N2O', *Aerospace Science and Technology*. Elsevier Masson SAS, 37, pp. 81–92. doi: 10.1016/j.ast.2014.05.010.

Chandler, A. *et al.* (2010) 'A Two-Stage, Single Port Hybrid Propulsion System for a Mars Ascent Vehicle', in *46th AIAA/ASME/SAE/ASEE Joint Propulsion Conference & Exhibit*. Reston, Virigina: American Institute of Aeronautics and Astronautics. doi: 10.2514/6.2010-6635.

Chandler, A. (2012) *An Investigation of Liquefying Hybrid Rocket Fuels With Applications To Solar System Exploration*. Stanford University.

Chandler, A. A. *et al.* (2011) 'Feasibility of a single port Hybrid Propulsion system for a Mars Ascent Vehicle', *Acta Astronautica*. Elsevier, 69(11–12), pp. 1066–1072. doi: 10.1016/j.actaastro.2011.07.004.

Chiaverini, M. J. *et al.* (2000) 'Regression Rate Behavior of Hybrid Rocket Solid Fuels', *Journal of Propulsion and Power*, 16(1), pp. 125–132. doi: 10.2514/2.5541.

Chowdhury, S. M. (2012) *Design and performance simulation of a hybrid sounding rocket*. University of KwaZulu-Natal.

Dean, D. L. (1995) *Hybrid Fuel Formulation and Technology Development*.

Dehgolan, F. R., Behzadi, M. and Sola, J. F. (2016) 'Obtaining Constants of Johnson-Cook Material Model Using a Combined Experimental, Numerical Simulation and Optimization Method', *World Academy of Science, Engineering and Technology International Journal of Mechanical and Mechatronics Engineering I*, 10(9), pp. 1615–1622.

DeLuca, L. T. *et al.* (2011) 'Time-Resolved Burning of Solid Fuels for Hybrid Rocket Propulsion', *Progress in Propulsion Physics*, 2, pp. 405–426.

Desain, J. D. *et al.* (2009) 'Tensile Tests of Paraffin Wax for Hybrid Rocket Fuel Grains', in *45th AIAA/ASME/SAE/ASEE Joint Propulsion Conference & Exhibit*. doi: 10.2514/6.2009-5115.

Doran, E. *et al.* (2007) 'Nitrous Oxide Hybrid Rocket Motor Fuel Regression Rate Characterization', in *43rd AIAA/ASME/SAE/ASEE Joint Propulsion Conference*, pp. 1–12. doi: 10.2514/6.2007-5352.

Douglass, H. W. *et al.* (1973) *Solid Propellant Grain Structural Integrity Analysis (NASA-SP-8073)*. doi: NASA SP-8073.

Evans, B. *et al.* (2004) 'Characterization of Nano-Sized Energetic Particle Enhancement of Solid-Fuel Burning Rates in an X-Ray Transparent Hybrid Rocket Engine', in *40th AIAA/ASME/SAE/ASEE Joint Propulsion Conference and Exhibit*.

Evans, B. *et al.* (2009) 'Hybrid Rocket Investigations at Penn State University's High Pressure Combustion Laboratory: Overview and Recent Results', in *45th AIAA/ASME/SAE/ASEE Joint Propulsion Conference*, pp. 1–22. Available at: http://arc.aiaa.org/doi/pdf/10.2514/6.2009-5349.

Fitzgerals, J. E. and Hufferd, W. L. (1971) *Handbook for the Engineering Structural Analysis of Solid Propellants*.

Flanagan, D. P. and Belytschko, T. (1981) 'A Uniform Strain Hexahedron and Quadrilateral with Orthogonal Hourglass Control', *International Journal for Numerical Methods in Engineering*, 17, pp. 679–706. doi: dx.doi.org/10.1002/nme.1620170504.

Freund, M. *et al.* (1983) *Paraffin Products*. Edited by G. . Mozes. Elsevier.

Galfetti, L. *et al.* (2013) 'Experimental Investigation of Paraffin-Based Fuels for Hybrid Rocket Propulsion', *Progress in Propulsion Physics*, 4, pp. 59–74. doi: 10.1051/eucass/201304059.

Gany, A. and Netzer, N. W. (1986) 'Combustion Studies of Metallized Fuels for Solid-fuel Ramjets', *Journal of Propulsion and Power*, 2(5), pp. 423–427. doi: 10.2514/3.22924.

Gariani, G., Maggi, F. and Galfetti, L. (2011) 'Numerical simulation of HTPB combustion in a 2D hybrid slab combustor', *Acta Astronautica*. Elsevier, 69(5–6), pp. 289–296. doi: 10.1016/j.actaastro.2011.03.015.

Genevieve, B. *et al.* (2012) 'The Phoenix Hybrid Sounding Rocket Program: A Progress Report 2012', in *48th AIAA/ASME/SAE/ASEE Joint Propulsion Conference & Exhibit*. doi: doi:10.2514/6.2012-4312.

Genevieve, B. *et al.* (2015) 'Flight Test of the Phoenix-1A Hybrid Rocket', in *51st AIAA/SAE/ASEE Joint Propulsion Conference*. Reston, Virginia: American Institute of Aeronautics and Astronautics. doi: 10.2514/6.2015-4047.

Genevieve, B., Pitot de la Beaujardiere, J. P. and Brooks, M. (2017) 'A computational tool for predicting hybrid rocket motor performance', *R&D Journal of the South African Institute of Mechanical Engineers*, 33, pp. 56–65.

George, P. *et al.* (1998) 'Fuel Regression Rate Enhancements Studies in HTPB/GOX Hybrid Rocket Motors', in *34th AIAA/ASME/SAE/ASEE Joint Propulsion Conference & Exhibit*.

Gondouin, B. (1993) 'Structural Analysis of Propellant Grains', in Davenas, A. (ed.) *Solid Rocket Propulsion Technology*. Pergamon Press, pp. 215–301.

Gordon, W. E. (1962) *The Relative Importance of Density, Specific Impulse and Other Propellant Properties in the Frame of Long-Term research Goals*.

Guendugov, V. M., Smirnov, N. N. and Tyurenkova, V. V. (2013) 'Solving the problem of diffusion combustion of a droplet with allowance for several independent reactions', *Combustion, Explosion, and Shock Waves*, 49(6), pp. 648–656. doi: 10.1134/S0010508213060026.

Hancock, J. . and Mackenzie, A. . (1976) 'On the Mechanisms of Ductile Failure in High-Strength Steels Subjected to Multi-Axial Stress-States', *Journal of the Mechanics and Physics of Solids*, 24(2–3), pp. 147–160. doi: 10.1016/0022-5096(76)90024-7.

Hill, C. *et al.* (2019) 'Modification of Paraffin-based Hybrid Rocket Fuels Using Structural Lattices', in *AIAA Propulsion and Energy 2019 Forum*. Reston, Virginia: American Institute of Aeronautics and Astronautics. doi: 10.2514/6.2019-4191.

Ho, S. Y. (2010) 'Solid-Fueled Rocket Structural Integrity Analysis', in Ho, S.-Y. (ed.) *Structural Failure Analysis and Prediction Methods for Aerospace Vehicles and Structures*. Bentham Science Publishers. doi: 10.2174/97816080502461100101.

Hsiao, R. C. (2013) 'Structural Analysis of Solid Propellant Grain using Explicit Dynamics Method for Ignition Pressurization', in *49th AIAA/ASME/SAE/ASEE Joint Propulsion*

Conference, 14 - 17 July. Reston, Virginia: American Institute of Aeronautics and Astronautics, pp. 1–8. doi: 10.2514/6.2013-3959.

Humble, R. W., Henry, G. N. and Larson, W. J. (1995) *Space Propulsion Analysis and Design*. United States of America: McGraw-Hill.

Jens, E. T., Cantwell, B. J. and Hubbard, G. S. (2016) 'Hybrid rocket propulsion systems for outer planet exploration missions', *Acta Astronautica*. Elsevier, 128, pp. 119–130. doi: 10.1016/j.actaastro.2016.06.036.

Johnson, G. and Cook, W. (1983) 'A Constitutive Model and Data for Metals Subjected to Large Strains, High Strain Rates and High Temperatures', in *Proceedings of the 7th International Symposium on Ballistics*. The Hague, Netherlands, pp. 541–547.

Johnson, G. R. and Cook, W. H. (1985) 'Fracture Characteristics of Three Metals Subjected to Various Strains, Strain Rates, Temperatures and Pressures', *Engineering Fracture Mechanics*, 21(I), pp. 31–48.

Karabeyoglu, A. *et al.* (2004) 'Scale-Up Tests of High Regression Rate Paraffin-Based Hybrid Rocket Fuels', *Journal of Propulsion and Power*, 20(6), pp. 1037–1045. doi: 10.2514/1.3340.

Karabeyoglu, A. (2011) 'Chapter X2.1: Hybrid Rockets Propulsion Design Issues', in *Lecture notes distributed in AIAA Hybrid Rocket Propulsion Course at the 47th AIAA/ASME/SAE/ASEE Joint Propulsion Conference & Exhibit San Diego, CA, United States of America, 4-5 August*.

Karabeyoglu, A. *et al.* (2011) 'High Performance Hybrid Upper Stage Motor', in *47th AIAA/ASME/SAE/ASEE Joint Propulsion Conference and Exhibit 2011*, pp. 1–24. doi: 10.2514/6.2011-6025.

Karabeyoglu, A. and Arkun, U. (2014) 'Evaluation of Fuel Additives for Hybrid Rockets and SFRJ Systems', *50th AIAA/ASME/SAE/ASEE Joint Propulsion Conference*, pp. 1–41. doi: 10.2514/6.2014-3647.

Karabeyoglu, M. A. (1998) *Transient Combustion in Hybrid Rockets*. Stanford University.

Karabeyoglu, M. A. *et al.* (2003) 'Scale-up Tests of High Regression Rate Liquefying Hybrid Rocket Fuels', in *41st Aerospace Sciences Meeting and Exhibit*, pp. 1–19. doi: 10.2514/6.2003-1162.

Karabeyoglu, M. A. (2014) 'Nitrous Oxide and Oxygen Mixtures (Nytrox) as Oxidizers for Rocket Propulsion Applications', *Journal of Propulsion and Power*, 30(3), pp. 696–706. doi: 10.2514/1.B34768.

Karabeyoglu, M. A. (2017) 'Performance Additives for Hybrid Rockets', in De Luca, L. T. et al. (eds) *Chemical Rocket Propulsion: A Comprehensive Survey of Energetic Materials*. Springer International Publishing (Springer Aerospace Technology), pp. 139–164. doi: 10.1007/978-3-319-27748-6.

Karabeyoglu, M. A., Cantwell, B. J. and Altman, D. (2001) 'Development and Testing of Paraffin-Based Hybrid Rocket Fuels', in *37th AIAA/ASME/SAE/ASEE Joint Propulsion Conference & Exhibit*, pp. 1–24. doi: 10.2514/6.2001-4503.

Karabeyoglu, M. A., Cantwell, B. J. and Zilliac, G. (2005) 'Development of a Scalable Space-Time Averaged Regression Rate Expression for Hybrid Rockets', in *41st AIAA/ASME/SAE/ASEE Joint Propulsion Conference & Exhibit*, pp. 1–21.

Karabeyoglu, M. A., Cantwell, B. J. and Zilliac, G. (2007) 'Development of Scalable Space-Time Averaged Regression Rate Expressions for Hybrid Rockets', *Journal of Propulsion and Power*, 23(4), pp. 737–747. doi: 10.2514/1.19226.

Kelley, F. N. (1969) 'Solid Propellant Mechanical Properties Testing, Failure Criteria, and Aging', *Advan. Chem. Ser.*, No. 88, pp. 188–243.

Kim, S. *et al.* (2010) 'Effect of Paraffin-LDPE Blended Fuel in Hybrid Rocket Motor', in *46th AIAA/ASME/SAE/ASEE Joint Propulsion Conference*, pp. 1–16.

Kim, S. *et al.* (2015) 'Evaluation of Paraffin–Polyethylene Blends as Novel Solid Fuel for Hybrid Rockets', *Journal of Propulsion and Power*, 31(6), pp. 1750–1760. doi: 10.2514/1.B35565.

Kobald, M. *et al.* (2014) 'Evaluation of Paraffin-based Fuels for Hybrid Rocket Engines', in *50th AIAA/ASME/SAE/ASEE Joint Propulsion Conference*, pp. 1–14. doi: 10.2514/6.2014-3646.

Kobald, M. *et al.* (2016) 'Rheological, Optical, and Ballistic Investigations of Paraffin-based Fuels for Hybrid Rocket Propulsion Using a Two-dimensional Slab-burner', *Progress in Propulsion Physics*, 8, pp. 263–282. doi: 10.1051/eucass/201608263.

Kobald, M., Ciezki, H. and Schlechtriem, S. (2013) 'Optical Investigation of the Combustion Process in Paraffin-based Hybrid Rocket Fuels', *49th AIAA/ASME/SAE/ASEE Joint Propulsion Conference*, pp. 1–15. doi: doi:10.2514/6.2013-3894.

Kobald, M., Verri, I. and Schlechtriem, S. (2015) 'Theoretical and Experimental Analysis of Liquid Layer Instability in Hybrid Rocket Engines', *CEAS Space Journal*, 7(1), pp. 11–22. doi: 10.1007/s12567-015-0076-2.

Kumar, N. and Rao, V. V. (2014) 'Dynamic Analysis of Solid Propellant Grain for Launch Load', *MIT International Journal of Mechanical Engineering*, 4(2), pp. 79–84.

Kumar, R. and Ramakrishna, P. A. (2013) 'Issues Related to the Measurement of Regression Rate of Fast-Burning Hybrid Fuels', *Journal of Propulsion and Power*, 29(5), pp. 1114–1121. doi: 10.2514/1.B34757.

Kumar, R. and Ramakrishna, P. A. (2014) 'Measurement of regression rate in hybrid rocket using combustion chamber pressure', *Acta Astronautica*. Elsevier, 103, pp. 226–234. doi: 10.1016/j.actaastro.2014.06.044.

Larson, D. B. *et al.* (2015) 'Formulation, Casting, and Evaluation of Paraffin-Based Solid Fuels Containing Energetic and Novel Additives for Hybrid Rockets', *International Journal of Energetic Materials and Chemical Propulsion*, 14(6), pp. 453–478. doi: 10.1615/IntJEnergeticMaterialsChemProp.2015005757.

Lestrade, J. (2012) *Modélisation de la Régression des Combustibles Liquéfiables Dans un Moteur Hybride*. Université de Toulouses.

Lestrade, J. Y., Anthoine, J. and Lavergne, G. (2011) 'Liquefying Fuel in Hybrid Propulsion : First Step Towards a 1D Model', in *4th European Conference for Aerospace Sciences (EUCASS)*, pp. 1–8.

Lestrade, J. Y., Anthoine, J. and Lavergne, G. (2015) 'Liquefying fuel regression rate modeling in hybrid propulsion', *Aerospace Science and Technology*. Elsevier Masson SAS, 42, pp. 80–87. doi: 10.1016/j.nucengdes.2007.10.005.

Leverone, F. K. *et al.* (2013) 'Performance Modeling of the Phoenix-2A Hybrid Sounding Rocket using the HYROPS Software', in *49th AIAA/ASME/SAE/ASEE Joint Propulsion Conference and Exhibit*. doi: doi:10.2514/6.2013-4133.

Leverone, F. K. (2013) *Performance Modelling and Simulation of a 100 Km Hybrid Sounding Rocket*. Univeristy of KwaZulu-Natal.

Leverone, F. K. *et al.* (2019) 'Performance Sensitivity Study on a Blowdown Nitrous Oxide Paraffin Wax Hybrid Sounding Rocket', *Acta Astronautica*, 160, pp. 230–239. doi: 10.1016/j.actaastro.2019.04.043.

Li, C., Cai, G. and Tian, H. (2016) 'Numerical analysis of combustion characteristics of hybrid rocket motor with multi-section swirl injection', *Acta Astronautica*. Elsevier, 123, pp. 26–36. doi: 10.1016/j.actaastro.2016.02.023.

Li, X. *et al.* (2014) 'Experimental investigation of fuel regression rate in a HTPB based lab-scale hybrid rocket motor', *Acta Astronautica*. Elsevier, 105(1), pp. 95–100. doi: 10.1016/j.actaastro.2014.08.028.

Lips, H. R. (1976) 'Metal Combustion in High Performance Hybrid Rocket Propulsion Systems', in *AIAA/SAE 12th Propulsion Conference*.

Lips, H. R. (1977a) 'Experimental Investigation on Hybrid Rocket Engines Using Highly Aluminized Fuels', *Journal of Spacecraft and Rockets*, 14(9), pp. 539–545. doi: 10.2514/3.57234.

Lips, H. R. (1977b) 'Heterogeneous Combustion of Highly Aluminized Hybrid Fuels', *AIAA Journal*, 15(6), pp. 777–778. doi: 10.2514/3.60710.

Lohner, K. *et al.* (2006) 'Fuel Regression Rate Characterization Using a Laboratory Scale Nitrous Oxide Hybrid Propulsion System', in *42nd AIAA/ASME/SAE/ASEE Joint Propulsion Conference*. doi: 10.2514/6.2006-4671.

Louche, H. *et al.* (2009) 'An Experimental and Modeling Study of the Thermomechanical Behavior of an ABS Polymer Structural Component During an Impact Test', *International Journal of Impact Engineering*, 36(6), pp. 847–861. doi: 10.1016/j.ijimpeng.2008.09.007.

M. Šlais, I. Dohnal and M. Forejt (2012) 'Determination of Johnson-Cook Equation Parameters', *Acta Metallurgica Slovaca*, 18(2), pp. 125–132.

Maharaj, C. *et al.* (2016) 'Development of a 75 mm hybrid rocket motor to test metal additives', in *52nd AIAA/SAE/ASEE Joint Propulsion Conference, 2016*.

Maharaj, C. S. (2018) *Performance Characterisation of Metal Additives in Paraffin Wax Hybrid Rocket Fuel Grains*. University of KwaZulu-Natal.

Majdalani, J. (2011) 'Hybrid Rocket Propulsion', in *AIAA Professional Development Course*. San Diego.

Maruyama, S. *et al.* (2011) 'Study on Mechanical Characteristic of Paraffin-Based Fuel', in *47th AIAA/ASME/SAE/ASEE Joint Propulsion Conference and Exhibit*, pp. 1–9. doi: 10.2514/6.2011-5678.

Marxman, G. A. (1965) 'Combustion in the Turbulent Boundary Layer on a Vaporizing Surface', in *Symposium (International) on Combustion*, pp. 1337–1346. doi: 10.1016/S0082-0784(65)80268-5.

Marxman, G. and Gilbert, M. (1963) 'Turbulent Boundary Layer Combustion in the Hybrid Rocket', in *Symposium (International) on Combustion*, pp. 371–383. doi: 10.1016/S0082-0784(63)80046-6.

Mazzetti, A., Merotto, L. and Pinarello, G. (2016) 'Paraffin-based hybrid rocket engines applications: A review and a market perspective', *Acta Astronautica*, 126, pp. 286–297. doi: 10.1016/j.actaastro.2016.04.036.

McCulley, J., Bath, A. and Whitmore, S. (2012) 'Design and Testing of FDM Manufactured Paraffin-ABS Hybrid Rocket Motors', in *48th AIAA/ASME/SAE/ASEE Joint Propulsion Conference & Exhibit*. Reston, Virigina: American Institute of Aeronautics and Astronautics. doi: 10.2514/6.2012-3962.

McKinney, B. C. and Kniffen, R. J. (1994) 'Hybrid Rocket Motor Solid Fuel Grain'. United States.

Mengu, D. and Kumar, R. (2018) 'Development of EVA-SEBS Based Wax Fuel for Hybrid Rocket Applications', *Acta Astronautica*, 152, pp. 325–334. doi: 10.1016/j.actaastro.2018.08.034.

Merotto, L. *et al.* (2011) 'Characterization of a Family of Paraffin-based Solid Fuels', in *4th European Conference for Aerospace Sciences (Eucass)*, p. 11. Available at: https://www.researchgate.net/publication/275231392_Characterization_of_a_family_of_paraffin-based_solid_fuels.

Nakagawa, I. and Hikone, S. (2009) 'Study on the Regression Rate of Paraffin-Based Hybrid Rocket Fuels', *Journal of Propulsion and Power*, 27(6), pp. 1276–1279. doi: 10.2514/1.B34206.

Natan, B. and Gany, A. (1993a) 'Combustion Characteristics of a Boron-Fueled Solid Fuel Ramjet with Aft-Burner', 9(5).

Natan, B. and Gany, A. (1993b) 'Effects of Bypass Air on Boron Combustion in Solid Fuel Ramjets', *Journal of Propulsion and Power*, 9(1), pp. 155–157. doi: 10.2514/3.11499.

Pal, Y. and Kumar, V. R. (2017) 'Physical and Ballistic Characterization of Aluminum-Loaded Paraffin Hybrid Rocket Fuels', *Energy & Fuels*, 31(9), pp. 10133–10143. doi: 10.1021/acs.energyfuels.7b01636.

Pal, Y. and Ravikumar, V. (2019) 'Mechanical Characterization of Paraffin-Based Hybrid Rocket Fuels', *Materials Today: Proceedings*, 16, pp. 939–948. doi: 10.1016/j.matpr.2019.05.180.

Paravan, C., Galfetti, L. and Maggi, F. (2017) 'A Critical Analysis of Paraffin-based Fuel Formulations for Hybrid Rocket Propulsion', *53rd AIAA/SAE/ASEE Joint Propulsion Conference*, (July). doi: 10.2514/6.2017-4830.

Pastrone, D. (2012) 'Approaches to Low Fuel Regression Rate in Hybrid Rocket Engines', *International Journal of Aerospace Engineering*, 2012(ii). doi: 10.1155/2012/649753.

Pei, X. and Hou, L. (2014) 'Numerical investigation on cavity structure of solid-fuel scramjet combustor', *Acta Astronautica*. Elsevier, 105(2), pp. 463–475. doi: 10.1016/j.actaastro.2014.09.009.

Pelletier, N. (2009) *Etude des Phénomènes de Combustion dans un Propulseur Hybride : Modélisation et Analyse Expérimentale de la Régression des Combustibles Liquéfiables*. Université de Toulouses.

Piscitelli, F. *et al.* (2015) 'Microcrystalline paraffin wax as fuel for Hybrid Rocket Engine', in *6th European conference for Aeronautics and Space Sciences*.

Risha, G. A. *et al.* (2001) 'Combustion of HTPB-Based Solid Fuels Containing Nano-sized Energetic Powder in a Hybrid Rocket Motor', in *37th AIAA/ASME/SAE/ASEE Joint Propulsion Conference & Exhibit*, pp. 0–11.

Risha, G. A. *et al.* (2002) 'Performance Comparison of HTPB-Based Solid Fuels Containing Nano-Sized Energetic Powder in a Cylindrical Hybrid Rocket Motor', in *38th AIAA/ASME/SAE/ASEE Joint Propulsion Conference & Exhibit 7-10 July 2002, Indianapolis, Indiana*. doi: 10.2514/6.2002-3576.

Risha, G. A. *et al.* (2007) 'Metals, Energetic Additives, and Special Binders Used in Solid Fuels for Hybrid Rockets', in Chiaverini, M. J. and Kuo, K. K. (eds) *Fundamentals of Hybrid Rocket Combustion and Propulsion*. Reston: AIAA, pp. 413–456.

Ryu, S. *et al.* (2016) 'Tensile and Compressive Strength Characteristics of Aluminized Paraffin Wax Fuel for Various Particle Size and Contents', *Journal of the Korean Society of Propulsion Engineers*, 20(5), pp. 70–76. doi: 10.6108/KSPE.2016.20.5.070.

Saccone, G. *et al.* (2015) 'Manufacturing Processes of Paraffin Grains as Fuel for Hybrid Rocket Engines', *51st AIAA/ASME/SAE/ASEE Joint Propulsion Conference*, pp. 27–29. doi: 10.2514/6.2015-4039.

Santi, M. *et al.* (2017) 'Development and Testing of a Long Burning Time Lab-scale Paraffin-based Hybrid Rocket Motor', *53rd AIAA/SAE/ASEE Joint Propulsion Conference*, (July), pp. 1–16. doi: 10.2514/6.2017-4829.

Santos, L. M. C. *et al.* (2004) 'Experimental Investigation of a Paraffin Based Hybrid Rocket', in *10th Brazilian Congress of Thermal Sciences and Engineering*.

Santos, L. M. C. *et al.* (2005) 'Regression Rate Studies of a Paraffin-Based Hybrid', in.

Santos, L. M. C. *et al.* (2006) 'Experimental Investigation of a Paraffin Based Hybrid Rocket', *Thermal Engineering*, 5(1), pp. 8–12.

Sasol Wax GmbH (2010) *SASOL Wax 0907 MSDS*.

Scaramuzzino, F. *et al.* (2013) 'Fuel Regression-Rate Characterization on a Lab-Scale Hybrid Rocket Burning N2O and Paraffin-Based Propellants', in *49th AIAA/ASME/SAE/ASEE Joint Propulsion Conference and Exhibit*, pp. 1–15.

Schultz, R. G. (2013) *Hybrid Rocket Motor (HRM) Test Stand : An Investigation of the Effects of Additives*. The University of Arizona. Available at: http://hdl.handle.net/10150/297738.

Simo, J. C. (1987) 'On a Fully Three-dimensional Finite-strain Viscoelastic Damage Model: Formulation and Computational Aspects', *Computer Methods in Applied Mechanics and Engineering*, 60(2), pp. 153–173. doi: 10.1016/0045-7825(87)90107-1.

Sinha, Y. K., Sridhar, B. T. N. and Kishnakumar, R. (2016) 'Study of Thermo-Mechanical Properties of HTPB–Paraffin Solid Fuel', *Arabian Journal for Science and Engineering*, 41(11), pp. 4683–4690. doi: 10.1007/s13369-016-2230-3.

Smirnov, N. N. (1985) 'Heat and mass transfer in a multi-component chemically reactive gas above a liquid fuel layer', *International Journal of Heat and Mass Transfer*, 28(5), pp. 929–938. doi: 10.1016/0017-9310(85)90274-1.

Smirnov, N. N., Tyurenkova, V. V. and Smirnova, M. N. (2015) 'Laminar diffusion flame propagation over thermally destructing material', *Acta Astronautica*. Elsevier, 109, pp. 217–224. doi: 10.1016/j.actaastro.2014.09.016.

Smoot, L. D. and Price, C. F. (1966) 'Regression Rates of Metalized Hybrid Fuel Systems', *AIAA Journal*, 4(5), pp. 910–915.

Stopel, M. and Skibicki, D. (2016) 'Determination of Johnson-Cook Model Constants by Measurement of Strain Rate by Optical Method', in *Fatigue Failure and Fracture Mechanics, AIP Conference Proceedings*. American Institute of Physics. doi: 10.1063/1.4965956.

Strand, L. D. *et al.* (1992) 'Hybrid Rocket Fuel Combustion and Regression Rate Study', in *28th AIAA/ASME/SAE/ASEE Joint Propulsion Conference*.

Strand, L. D., Ray, R. L. and Cohen, N. S. (1993) 'Hybrid Rocket Combustion Study Jet', in *29th AIAA/ASME/SAE/ASEE Joint Propulsion Conference*. doi: 10.2514/6.1993-2412.

Sun, X. *et al.* (2016) 'Regression rate behaviors of HTPB-based propellant combinations for hybrid rocket motor', *Acta Astronautica*. Elsevier, 119, pp. 137–146. doi: 10.1016/j.actaastro.2015.11.015.

Sutton, G. and Biblarz, O. (2001) *Rocket Propulsion Elements*, *Rocket propulsion elements*. John Wiley & Sons, INC. doi: 10.1017/CBO9781107415324.004.

Swami, R. D. and Gany, A. (2003) 'Analysis and testing of similarity and scale effects in hybrid rocket motors', *Acta Astronautica*, 52(8), pp. 619–628. doi: 10.1016/S0094-5765(02)00126-1.

Thomas, J. C. *et al.* (2015) 'Enhancement of Regression Rates in Hybrid Rockets with HTPB Fuel Grains by Metallic Additives', in *51st AIAA/ASME/SAE/ASEE Joint Propulsion Conference*, pp. 1–16. doi: 10.2514/6.2015-4041.

Tyurenkova, V. V. (2012) 'Non-equilibrium diffusion combustion of a fuel droplet', *Acta Astronautica*. Elsevier, 75, pp. 78–84. doi: 10.1016/j.actaastro.2012.01.010.

Tyurenkova, V. V., Smirnov, N. N. and Guendugov, V. M. (2013) 'Analytical solution for a single droplet diffusion combustion problem accounting for several chain reaction stages', *Acta Astronautica*. Elsevier, 83, pp. 208–215. doi: 10.1016/j.actaastro.2012.09.008.

Tyurenkova, V. V. and Smirnova, M. N. (2016) 'Material combustion in oxidant flows: Self-similar solutions', *Acta Astronautica*. Elsevier, 120, pp. 129–137. doi: 10.1016/j.actaastro.2015.11.033.

Veale, K. L. *et al.* (2017) 'A Review of the Performance and Structural Considerations of Paraffin Wax Hybrid Rocket Fuels with Additives', *Acta Astronautica*. Elsevier Ltd, 141(October), pp. 196–208. doi: 10.1016/j.actaastro.2017.10.012.

Veale, K. L. *et al.* (2018) 'The Structural Properties of Paraffin Wax Based Hybrid Rocket Fuels with Aluminium Particles', *Acta Astronautica*. Elsevier Ltd, 151(June), pp. 864–873. doi: 10.1016/j.actaastro.2018.07.042.

Veale, K. L., Brooks, M. J. and Pitot de la Beaujardiere, J.-F. P. (2015) 'Structural Performance of Large Scale Paraffin Wax Based Fuel Grains', in *51st AIAA/SAE/ASEE Joint Propulsion Conference, 27 - 29 July*, pp. 1–8. doi: 10.2514/6.2015-3942.

Vickland, C. W. (1967) *Experimental Investigation of Prepackaged Hybrid Propulsion Systems*.

Wang, J., Severtson, S. J. and Stein, A. (2006) 'Significant and Concurrent Enhancement of Stiffness, Strength, and Toughness for Paraffin Wax Through Organoclay Addition', *Advanced Materials*, 18(12), pp. 1585–1588. doi: 10.1002/adma.200502615.

Weinstein, A. and Gany, A. (2013) 'Testing and Modeling Liquefying Fuel Combustion in Hybrid Propulsion', *Progress in Propulsion Physics*. Les Ulis, France: EDP Sciences, 4, pp. 99–112. doi: 10.1051/eucass/201304099.

Zalewski, R. and Wolszakiewicz, T. (2011) 'Analysis of uniaxial tensile tests for homogeneous solid propellants under various loading conditions', *Central European Journal of Energetic Materials*, 8(4), pp. 223–231.

Zaseck, C. *et al.* (2012) 'Paraffin Fuel and Additive Combustion in an Opposed Flow Burner Configuration', in *48th AIAA/ASME/SAE/ASEE Joint Propulsion Conference & Exhibit*. Reston, Virigina: American Institute of Aeronautics and Astronautics. doi: 10.2514/6.2012-3963.

Zilliac, G. *et al.* (2014) 'Peregrine Hybrid Rocket Motor Development', in *50th AIAA/ASME/SAE/ASEE Joint Propulsion Conference*. Reston, Virginia: American Institute of Aeronautics and Astronautics. doi: 10.2514/6.2014-3870.